



TITLE:

Lepton-number asymmetry generation via
multiscalar field evolution in
supersymmetric electroweak models(
Dissertation_全文)

AUTHOR(S):

Senami, Masato

CITATION:

Senami, Masato. Lepton-number asymmetry generation via multiscalar field evolution in supersymmetric electroweak models. 京都大学, 2004, 博士(工学)

ISSUE DATE:

2004-03-23

URL:

<https://doi.org/10.14989/doctor.k10822>

RIGHT:

**Lepton-number asymmetry generation
via multiscalar field evolution
in supersymmetric electroweak models**

Masato Senami

2003

Contents

1	Introduction	5
2	Review of baryogenesis	9
2.1	Baryogenesis	9
2.2	Leptogenesis	12
2.3	Affleck-Dine mechanism	16
3	Higgs triplet model	22
3.1	Model	23
3.2	Flat Directions	25
3.3	Leptogenesis with heavy Higgs triplets	26
3.3.1	(i) $t \ll M_{\Delta}^{-1}$	27
3.3.2	(ii) $t \sim M_{\Delta}^{-1}$	30
3.3.3	(iii) $t \gg M_{\Delta}^{-1}$	31
3.3.4	Numerical analysis	31
3.4	Leptogenesis with Higgs triplets in TeV region	36
3.4.1	Thermal effects	37
3.4.2	Case (i): asymmetry fixing with $M_{\Delta} > H_{\text{th}}$	38
3.4.3	Case (ii): asymmetry fixing with $M_{\Delta} < H_{\text{th}}$	42
3.5	Summary	46
4	Right-handed neutrino model	47
4.1	Model	47
4.2	multiscalar leptogenesis	49
4.2.1	Large coupling : $h_{\nu} \gtrsim \sqrt{H_{\text{inf}}/M}$	50
4.2.2	Small coupling : $h_{\nu} \lesssim \sqrt{H_{\text{inf}}/M}$	54

4.3	Numerical analysis	59
4.4	Summary	62
5	Nonrenormalizable superpotential term	63
5.1	Model	63
5.2	Flat Manifold Leptogenesis	65
5.2.1	$H = H_{\text{inf}}$	66
5.2.2	$H_{\text{osc}} < H < H_{\text{inf}}$	67
5.2.3	$m_{3/2} \ll H \lesssim H_{\text{osc}}$	70
5.3	Thermal Effects	71
5.4	Numerical Analysis	72
5.5	Summary	80
6	Phenomenological signature	82
6.1	Higgs Triplet model	82
6.1.1	Lepton flavor violation	82
6.1.2	Lepton flavor violating processes	87
6.1.3	Muon anomalous magnetic moment	95
6.1.4	Muonium to antimuonium conversion	95
6.2	Right-handed neutrino model	97
6.2.1	Lepton flavor violation	98
6.2.2	$\mu \rightarrow e\gamma$ and $\tau \rightarrow \mu\gamma$	101
6.3	summary	105
7	Conclusion	107
	Acknowledgements	109
	References	110

Chapter 1

Introduction

The experiment of atmospheric neutrinos by the Super-Kamiokande collaboration indicates a convincing evidence for the neutrino masses and mixings [1]. After the discovery of the atmospheric neutrino oscillation, the existence of neutrino masses and mixings is further convinced by many neutrino observations including the solar and atmospheric neutrino experiments by Super-Kamiokande [2] and SNO [3], the reactor anti-neutrino disappearance experiment by KamLand [4], and the long-baseline experiment of accelerator-produced neutrinos by K2K [5]. The neutrino masses, however, can not be explained in the standard model, which is quite successful for describing the interactions among elementary particles, quarks, leptons and gauge bosons, in terms of the gauge symmetry $SU(3)_C \times SU(2)_L \times U(1)_Y$. An extension of the standard model to the supersymmetric one [6] with R -parity conservation can not even provide a solution for the neutrino masses. The nonzero neutrino masses should hence be regarded as an evidence of new physics beyond the standard model either nonsupersymmetric or supersymmetric.

The natural explanation of the small neutrino masses are usually made by the so-called seesaw mechanism with heavy right-handed neutrinos [7]. Since the right-handed neutrinos are electroweak $SU(2)_L \times U(1)_Y$ singlet, they may have large Majorana masses consistent with the gauge symmetry of standard model. By integrating out these heavy right-handed neutrinos, the effective operator for the small Majorana masses of the ordinary neutrinos is generated through the Yukawa coupling of right-handed neutrinos to the left-handed leptons and Higgs fields of electroweak doublet. This operator providing the small neutrino masses is also generated through the exchange of heavy electroweak Higgs triplet fields [8]. The masses of the Higgs triplets can be in TeV region particularly under

the lepton-number L and R -parity conservations which hold very well in a natural manner [9]. It may even be considered in the framework of unified theory that the lepton-number violating operators such as desired for the small neutrino masses are generated through the exchange of some exotic particles with huge masses of Planck scale [10].

Another signature requiring the extension of standard model is the origin of the baryon number asymmetry in our universe. The successful big-bang nucleosynthesis requires some amount of baryon number asymmetry in order to produce light nuclei, D, ^3He , ^4He and ^7Li , at the temperature $T = 0.07 - 1$ MeV, or the time $t = 1 - 200$ sec in the early universe [11, 12]. In addition, the recent measurements of the cosmic microwave background anisotropy by MAXIMA[13], BOOMERanG[14], DASI[15] and WMAP[16] indicate the strong evidence of the baryon number asymmetry in the early universe. The inflation is an outstanding solution of the flatness, monopole (unwanted cosmological relics) and horizon problems in the universe. If the baryon number asymmetry exists before the inflation, it would have been diluted extremely by the inflation. Therefore, the baryon-number asymmetry generation, *baryogenesis*, must occur after the inflation. For the production of the baryon number asymmetry after the inflation, three conditions are required, as noted by Sakharov; (i) baryon number B violation, (ii) C and CP violation and (iii) nonequilibrium of the B -violating interaction.

In the standard model, there is a $B + L$ violating electroweak anomalous process mediated by the quasi particle state called sphaleron. This sphaleron process conserving $B - L$ is in thermal equilibrium at high temperature above the electroweak scale [17]. Hence, for the successful baryogenesis the $B - L$ asymmetry should be generated before the electroweak phase transition, unless the baryon number asymmetry is generated later. Particularly, if the lepton-number asymmetry generation, *leptogenesis*, occur before the electroweak phase transition, it can be transferred significantly to the baryon-number asymmetry through the sphaleron process. [18].

It is broadly considered that the ordinary neutrinos are Majorana particles, which means that the lepton number is not conserved strictly in nature. The lepton number violating interactions are also relevant for the leptogenesis. Hence, the leptogenesis in the early universe is a very interesting issue in the extensions of standard model with lepton number violation for generating the neutrino masses. The nonequilibrium decays of the right-handed neutrinos produced by thermal scattering processes are considered

for leptogenesis in the seesaw model of neutrino masses [18, 19]. The delayed decays of right-handed neutrinos can satisfy the nonequilibrium condition, and their Yukawa couplings provides the CP violation. In order that this right-handed decay scenario for leptogenesis works successfully without fine tuning, the mass of the lightest right-handed neutrino is required to be larger than 10^{10-11} GeV [20]. For the thermal production of right-handed neutrinos the reheating temperature of the universe after the supercooling by inflation should be higher than the right-handed neutrino masses. On the other hand, in the supersymmetric models the reheating temperature T_R is constrained as $T_R \lesssim 10^8 - 10^{10}$ GeV to avoid the gravitino overproduction, which would have otherwise spoiled the successful big-bang nucleosynthesis [21, 22, 23]. Then, the high reheating temperature to produce the right-handed neutrinos with mass $\sim 10^{10}$ GeV seems to be in conflict with the constraint from the gravitino problem. The leptogenesis through the CP violating decays of heavy Higgs triplets suffers from the same problem [24]. Therefore, in the supersymmetric extensions of standard models, which may be derived from the unified theory such as superstring theory, the baryogenesis and leptogenesis through the heavy particle decays are confronted with this difficulty.

It is promising that there is another mechanism for baryogenesis and leptogenesis in the supersymmetric models, which is called the Affleck-Dine mechanism [25, 26]. In this mechanism, a coherent evolution of scalar field takes place with a large initial value after the inflation along a flat direction inherent in supersymmetric models. The rotation in the complex configuration space of scalar field is induced by a CP violating potential term, and hence some charge asymmetries such as baryon-number and lepton-number can be generated. The Affleck-Dine mechanism has been investigated intensively in one-dimensional flat direction cases. It is, however, noted that in supersymmetric electroweak models there are usually some multi-dimensional flat configuration manifolds for the scalar potential. Then, it is expected that the baryon and/or lepton number asymmetries may be generated via multiscalar field evolution on such a flat manifold. We call the lepton-number asymmetry generation by this mechanism as *flat manifold leptogenesis*.

In this thesis, we study in detail the flat manifold leptogenesis in three supersymmetric electroweak models providing the neutrino masses; (1) Higgs triplet model, (2) right-handed neutrino model and (3) nonrenormalizable superpotential term model. Then, we investigate the phenomenological implications of these leptogenesis models. In the future

collider experiments, the signatures of these leptogenesis models may be discovered. This thesis is based on the studies in Refs. [9, 10, 27, 28, 29].

The remaining parts of this thesis are presented as follows. Chapter. 2 is devoted to a review of leptogenesis. We briefly mention the observed evidences for the baryon number asymmetry in the universe and the essential features of baryogenesis. Then, we discuss the leptogenesis for baryogenesis through the electroweak sphaleron process. We describe the leptogenesis through the right-handed neutrino decays, and then the Affleck-Dine mechanism in the supersymmetric standard model considering the effects of thermal plasma produce by the inflaton decays. In Chapter 3, we investigate the flat manifold leptogenesis in the Higgs triplet model. The neutrino mass generation is described through the exchange of Higgs triplet. Then, the flat directions relevant for leptogenesis are discussed, and the lepton-number asymmetry generation is investigated by solving the equation of motions for multiscalar fields in the case of heavy Higgs triplets and that of TeV region Higgs triplets, respectively. In Chapter 4, we investigate the flat manifold leptogenesis in the supersymmetric seesaw model for the neutrino masses. The scalar fields participating in the leptogenesis are identified, and their evolution is investigated to show the efficient generation of lepton-number asymmetry. In Chapter 5, we investigate the supersymmetric standard model for leptogenesis with nonrenormalizable superpotential term providing the neutrino masses. The flat manifold leptogenesis is investigated following the respective epochs starting with the inflation, and the resultant lepton number asymmetry is estimated specifically related to the lightest neutrino mass. Then, the reasonable range of model parameters is identified for the sufficient leptogenesis. In Chapter 6, we investigate the phenomenological effects of the leptogenesis models. In the Higgs triplet model, the relation between lepton flavor violation and the neutrino mass matrix is considered, and the renormalization effects on the lepton flavor violating couplings are calculated. Then, the lepton flavor violating charged lepton decays are examined. Similar analysis is also presented for the right-handed neutrino model by considering the condition for leptogenesis.

Chapter 2

Review of baryogenesis

In this chapter, we review essential aspects of baryogenesis. It is first explained why the existence of baryon number asymmetry is required for the present universe including ourselves. Then, the essential ingredients for baryogenesis are presented. The gravitino problem is also mentioned, which may be relevant for baryogenesis. As one of promising scenarios for baryogenesis, leptogenesis is introduced; if the lepton number asymmetry is generated, it is partially converted to the baryon number asymmetry. Then, the Affleck-Dine leptogenesis is especially described in detail, and the thermal effects are considered, which may suppress the asymmetry generation in the one-dimensional Affleck-Dine mechanism.

2.1 Baryogenesis

There are convincing reasons for the existence of baryon number asymmetry in the early universe from the big-bang nucleosynthesis and cosmic microwave background anisotropy. In the big-bang nucleosynthesis, light nuclei, D, ^3He , ^4He and ^7Li were generated [12]. The theoretical prediction of the abundances of these light nuclei agrees with the observational data of their primordial abundances, if the baryon number asymmetry of

$$\eta \equiv \frac{n_B}{n_\gamma} = (2.6 - 6.2) \times 10^{-10} \quad (2.1)$$

was present at the temperature $T \sim 1\text{MeV}$ of the universe [11].

The baryon number asymmetry is also required for explaining the ratio of the height of the first peak to that of the second peak of the cosmic microwave background multipole data [30]. The cosmic microwave background radiation was fixed at the temperature $T \simeq$

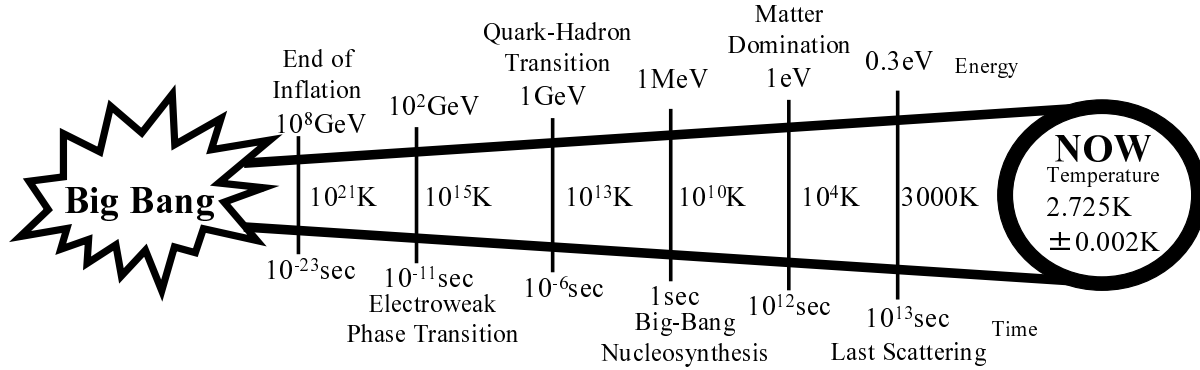


Figure 2.1: The brief thermal history of our universe is shown.

0.3eV in the epoch of last scattering, as shown in Fig. 2.1. The best fit parameters of the baryon number asymmetry by using the recent report on cosmic microwave background radiation of WMAP [16] combined with CBI [31], ACBAR [32], 2dFGRS [33] and Lyman- α [34] data is obtained as

$$\eta = (5.9 - 6.4) \times 10^{-10}. \quad (2.2)$$

This range of baryon number asymmetry required from the cosmic microwave background is really consistent with that from the big-bang nucleosynthesis.

It is believed to solve the horizon and flatness problems that the universe underwent the inflationary epoch with huge expansion. Then, the initial baryon number asymmetry, even if it existed, is diluted away through the inflation. Therefore, the baryon number asymmetry should be generated after the inflation. The three essential conditions for baryogenesis are presented by Sakharov; (i) baryon number violation, (ii) C and CP violation and (iii) nonequilibrium condition. The first condition is obvious to generate the baryon number asymmetry. The second condition provides the asymmetry between particle and antiparticle. Even if some baryon number violating interaction exists, without C and CP violation it produces baryons and antibaryons at the same rate. Hence, C and CP violation is also required to generate the baryon number asymmetry. If the third condition is not realized, the baryon number nonconserving process and the inverse process occur at the same rate. Hence, baryon number violating interaction can not generate the asymmetry in thermal equilibrium. The Sakharov's three conditions are summarized as

follows for a certain baryon number violating interaction $A \rightarrow B + C$:

- Baryon number violation

$$A \rightarrow B + C$$

- C and CP violation

$$\begin{aligned} A \rightarrow B + C & : \Delta Q_B = 1 \\ \bar{A} \rightarrow \bar{B} + \bar{C} & : \Delta Q_B = -1 \end{aligned} \quad R(A \rightarrow B + C) \neq R(\bar{A} \rightarrow \bar{B} + \bar{C})$$

- Nonequilibrium

$$\begin{aligned} A \rightarrow B + C & : \Delta Q_B = 1 \\ B + C \rightarrow A & : \Delta Q_B = -1 \end{aligned} \quad R(A \rightarrow B + C) > R(B + C \rightarrow A)$$

Here, the baryon number Q_B is assigned as $Q_B(A) = Q_B(C) = 0$ and $Q_B(B) = 1$.

The baryogenesis scenario was originally proposed in grand unified theories (GUT's) [35], where the baryon number asymmetry is generated through the CP and B -violating nonequilibrium decays of heavy particles. However, this baryon number asymmetry may not survive through the electroweak phase transition, unless the net $B - L$ asymmetry is generated. This is because the $B + L$ asymmetry is erased completely by the sphaleron process [17], which is $(B - L)$ -conserving but $(B + L)$ -violating, as discussed in the next section.

Another serious problem should be mentioned for realizing the baryogenesis in supersymmetric GUT's. The reheating temperature after the inflation is required to be high enough to produce the heavy particles with masses of GUT scale $M_G \sim 10^{16}$ GeV. However, in the supersymmetric theories the reheating temperature is constrained as

$$T_R \lesssim 10^8 - 10^{10} \text{ GeV} \quad (2.3)$$

to avoid the gravitino problem [21, 22, 23]. The decay of gravitinos occurs at a very late time $t \sim m_{3/2}^3/M_P^2 > t_{\text{BBN}}$ where $m_{3/2} \sim 10^3 \text{ GeV}$ is the gravitino mass, $M_P \simeq 2.4 \times 10^{18} \text{ GeV}$ is the reduced Planck mass, and $t_{\text{BBN}} \sim 1 \text{ sec}$ is the time of nucleosynthesis. The high energy photons from the late decay of gravitinos after the nucleosynthesis dissociate the light nuclei produced by nucleosynthesis. Hence, the abundance of gravitinos produced in the reheating should be suppressed enough for the successful nucleosynthesis. The gravitino abundance is estimated to be proportional to the reheating temperature, placing the above severe constraint.

This problem may be evaded if the gravitino is stable kinematically as the lightest supersymmetric particle. In this case of stable gravitino, however, the condition $m_{3/2} < 1$ keV is required in order that the gravitinos do not overclose the universe [36]. It is not easy to provide this light gravitino mass in a wide class of supersymmetric theories. Hence, the GUT baryogenesis in the supersymmetric theories may not be so attractive.

It is also considered to generate the baryon number asymmetry at the epoch of electroweak phase transition at the temperature $\sim 10^2$ GeV, the so-called electroweak baryogenesis [37]. In this scenario the sphaleron process is used as the baryon number violation. The nonequilibrium condition is provided by the first order phase transition associated with the electroweak gauge symmetry breaking. The first order electroweak phase transition, however, requires the Higgs mass m_H to be lower than 90 GeV in the standard model, which is now excluded by the experimental bound $m_H > 114.4$ GeV by the experiment of LEP [11]. The CP violation in the Cabbibo-Kobayashi-Maskawa mixing of quarks [38] is either shown to be ineffective for baryogenesis. In supersymmetric standard model these problems can be overcome but in a very restricted parameter region. This region for electroweak baryogenesis in the supersymmetric standard model might be excluded by the future accelerator experiments.

2.2 Leptogenesis

The leptogenesis is attractive to explain the origin of baryon number asymmetry in our universe, since the lepton number asymmetry, if it is generated, is partially converted to the baryon number asymmetry through the sphaleron process conserving $B - L$. We here describe the baryogenesis from leptogenesis through the sphaleron process. The baryon and lepton numbers are conserved at classical level in the standard model. They may, however, be violated by the quantum effect due to the rich structure of vacuum in the non-Abelian gauge symmetry, i.e., the θ -vacuum [12]. The tunneling transition between different θ -vacua is accompanied by the change of $B + L$ charge. The rate of this sphaleron process with $B + L$ violation is too small at zero temperature to make any effect, being proportional to $\exp(-4\pi/\alpha_W) \sim 10^{-160}$ with $\alpha_W = g^2/(4\pi) \sim 1/30$. The situation changes drastically at finite temperatures. In fact it is shown that the sphaleron process is no longer suppressed above the critical temperature of electroweak phase transition.

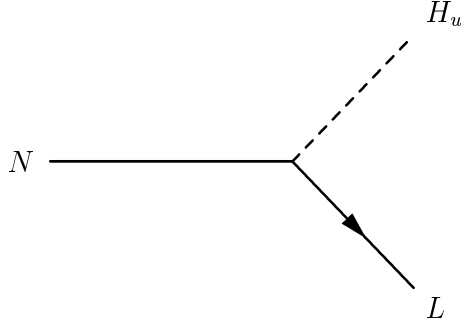


Figure 2.2: The tree diagram of the right-handed neutrino decay is shown.

On the other hand, at the very high temperature $T > 10^{12}$ GeV the expansion of the universe is faster than the sphaleron process. Hence, the $(B + L)$ -violating sphaleron process enters in thermal equilibrium at the temperatures $10^2 \text{ GeV} \lesssim T \lesssim 10^{12} \text{ GeV}$. Then, if a net $B - L$ number asymmetry is not generated before the electroweak phase transition, the baryon number asymmetry is erased by the sphaleron process. In other words, if the lepton number asymmetry n_L is present before electroweak phase transition, it is partially converted to baryon number asymmetry n_B through the sphaleron process. The chemical equilibrium between leptons and baryons determines the baryon-to-lepton ratio as $n_B/n_L \simeq -0.35$ [39] in the MSSM (minimal supersymmetric standard model). Therefore, the leptogenesis is a very attractive solution to baryogenesis.

The leptogenesis is usually considered from the decay of thermally produced right-handed neutrinos [18]. Since the right-handed neutrinos are electroweak gauge singlet, they may acquire the lepton number violating Majorana masses. Then, the right-handed neutrinos can decay into the final states of (s)lepton and anti-(s)lepton with different lepton numbers Q_L :

$$N \rightarrow L + H_u, \tilde{L} + \tilde{H}_u (\Delta Q_L = 0), \quad (2.4)$$

$$N \rightarrow \bar{L} + H_u^*, \tilde{L}^* + \tilde{H}_u (\Delta Q_L = -2). \quad (2.5)$$

The difference between the rates of these lepton number conserving and violating decays is produced through the interference of decay amplitudes of the tree (Fig. 2.2) and loop diagrams (Figs. 2.3 and 2.4), if the CP violating phase is included in the Yukawa coupling of right-handed neutrinos and ordinary leptons. Hence, the generated lepton number asymmetry is related the CP violating phase in the Yukawa coupling. The CP asymmetry

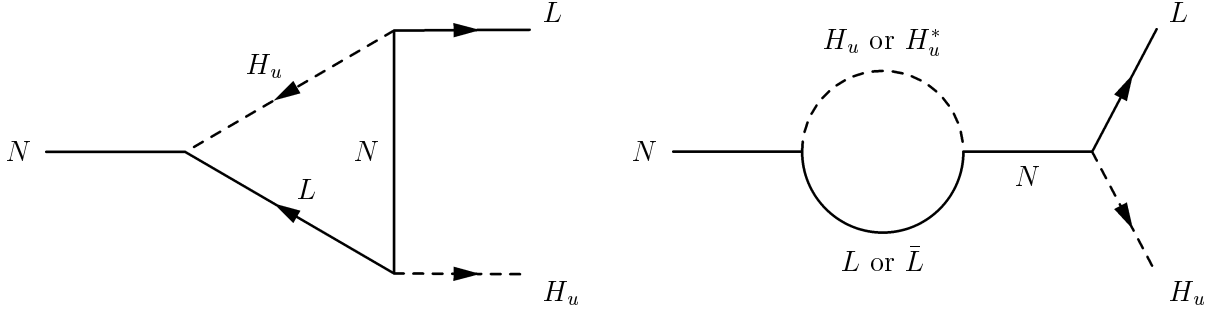


Figure 2.3: The nonsupersymmetric diagrams contributing to the CP violation in the right-handed neutrino decay.

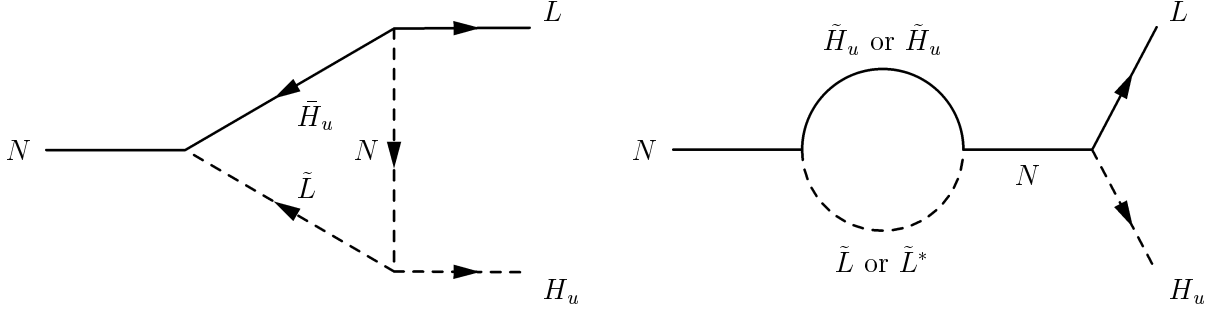


Figure 2.4: The supersymmetric diagrams contributing to CP violation in the right-handed neutrino decay.

$\epsilon_{N \rightarrow L}$ produced per one right-handed neutrino decay to lepton or antilepton is given by

$$\epsilon_{N \rightarrow L} \equiv \frac{\Gamma(N \rightarrow L) - \Gamma(N \rightarrow \bar{L})}{\Gamma(N \rightarrow L) + \Gamma(N \rightarrow \bar{L})}, \quad (2.6)$$

and the $\epsilon_{N \rightarrow \tilde{L}}$ from the decay to slepton or antislepton is given similarly. The CP asymmetry produced per one right-handed sneutrino decay is also given by

$$\epsilon_{\tilde{N} \rightarrow L} \equiv \frac{\Gamma(\tilde{N}^* \rightarrow L) - \Gamma(\tilde{N} \rightarrow \bar{L})}{\Gamma(\tilde{N}^* \rightarrow L) + \Gamma(\tilde{N} \rightarrow \bar{L})}, \quad (2.7)$$

and similarly for the asymmetry $\epsilon_{\tilde{N} \rightarrow \tilde{L}}$. These CP asymmetries are shown to be the same [40],

$$\epsilon_{N \rightarrow L} = \epsilon_{N \rightarrow \tilde{L}} = \epsilon_{\tilde{N} \rightarrow L} = \epsilon_{\tilde{N} \rightarrow \tilde{L}} \equiv \epsilon. \quad (2.8)$$

This CP asymmetry is evaluated [40] as

$$\epsilon = -\frac{1}{8\pi(h^\dagger h)_{11}} \sum_{i=2,3} \text{Im} \left[(h^\dagger h)_{1i}^2 \right] [f_1(x_i) + f_2(x_i)]. \quad (2.9)$$

where h is the Yukawa coupling of the right-handed neutrinos, and $x_i \equiv (M_i/M_1)^2$ with the right-handed neutrino masses M_i ($i = 1, 2, 3$). The functions $f_{1,2}(x)$ are given by

$$f_1(x) = \sqrt{x} \left(\frac{x+1}{x} \right), \quad (2.10)$$

$$f_2(x) = \frac{2\sqrt{2}}{x-1}, \quad (2.11)$$

where f_1 and f_2 represent the vertex and wave-function contributions (the left and right diagrams in Figs. 2.3 and 2.4), respectively.

The right-handed neutrinos decay in the epoch with Hubble parameter $H \sim \Gamma_N \sim h^2 M_1/(8\pi)$. The decay of the lightest right-handed neutrinos is important for leptogenesis, since the heavier ones soon decay to the lightest one. The abundance of lightest right-handed neutrinos is estimated as

$$\frac{n_{N_1}}{n_\gamma} \sim 1, \quad (2.12)$$

where n_{N_1} and n_γ are the number densities of the lightest right-handed neutrino and photon, respectively. Then, the lepton-to-entropy ratio is given by

$$\frac{n_L}{s} \sim \frac{\kappa \epsilon n_{N_1}}{g_* n_\gamma} \sim \frac{\kappa \epsilon}{g_*}, \quad (2.13)$$

where $g_* \sim 230$ is the degree of freedom of light particles in the MSSM, and $\kappa \lesssim 1$ is the suppression factor representing the wash-out effect. The precise value of κ is obtained by solving the Boltzmann equations.

The CP asymmetry ϵ is estimated [41] as

$$\epsilon \lesssim \frac{3}{8\pi} \frac{M_1}{\langle H_u \rangle^2} (m_3 - m_1) \quad (2.14)$$

$$\lesssim 10^{-6} \left(\frac{M_1}{10^9 \text{GeV}} \right) \left(\frac{m_3}{0.05 \text{eV}} \right), \quad (2.15)$$

where m_i ($i = 1, 2, 3$) are the ordinary neutrino masses. Then, the baryon-to-entropy ratio is bounded as

$$\frac{n_B}{s} \simeq 0.35 \frac{n_L}{s} \lesssim 10^{-10} \left(\frac{M_1}{10^9 \text{GeV}} \right) \left(\frac{m_3}{0.05 \text{eV}} \right) \left(\frac{\kappa}{0.1} \right). \quad (2.16)$$

Hence, the baryon number asymmetry of the universe may be generated with $M_1 \sim 10^9 - 10^{10}$ GeV. On the other hand, the reheating temperature is constrained as $T_R \lesssim$

$10^8 - 10^{10}$ GeV. The mass of the lightest right-handed neutrino should be less than the reheating temperature for the thermal production of right-handed neutrinos. Therefore, the leptogenesis through the right-handed neutrino decay appears to be very restrictive in supersymmetric models.

2.3 Affleck-Dine mechanism

The Affleck-Dine mechanism [25, 26] may be more promising for baryogenesis and leptogenesis in supersymmetric models, while the leptogenesis through the right-handed neutrino decay suffers from the gravitino problem. In supersymmetric models, there are many flat directions which contains scalar fields such as squarks and/or sleptons fields with baryon and/or lepton numbers. The renormalizable terms in the scalar potential disappear along the flat directions. Hence, during the inflation the scalar fields develop large expectation values. The number asymmetry of a scalar field ϕ is given by

$$n_\phi \equiv N_\phi - \bar{N}_\phi = i \left(\dot{\phi}^* \phi - \phi^* \dot{\phi} \right) = \dot{\theta} |\phi|^2, \quad (2.17)$$

where N_ϕ and \bar{N}_ϕ represent the particle and anti-particle numbers, respectively, and θ is the phase of ϕ . If the scalar field ϕ with $B - L$ charge begins to rotate in its phase θ on the complex configuration plane, the nonzero particle number asymmetry of ϕ , i.e., the $B - L$ number asymmetry is generated.

We describe in detail the rotational motion of ϕ by considering the $\tilde{L}H_u$ direction in the MSSM [42]. The one-dimensional Affleck-Dine mechanism for leptogenesis along this direction has been considered intensively in literature [43, 44, 45]. It is interesting in this case that the lepton number asymmetry is given in terms of the lightest neutrino mass m_{ν_1} . We will investigate the flat manifold leptogenesis in the following chapters by extending this mechanism.

The scalar field ϕ along the $\tilde{L}H_u$ flat direction is identified as

$$\tilde{L}_1 = \begin{pmatrix} \phi/\sqrt{2} \\ 0 \end{pmatrix}, \quad H_u = \begin{pmatrix} 0 \\ \phi/\sqrt{2} \end{pmatrix}, \quad (2.18)$$

where we consider the first generation of sneutrino since the lightest neutrino has the flattest potential. This $\tilde{L}H_u$ flat direction is lifted by the effective nonrenormalizable superpotential term for generating the neutrino masses,

$$W = \frac{\kappa}{2M} L H_u L H_u = \frac{m_\nu}{2\langle H_u \rangle^2} L H_u L H_u, \quad (2.19)$$

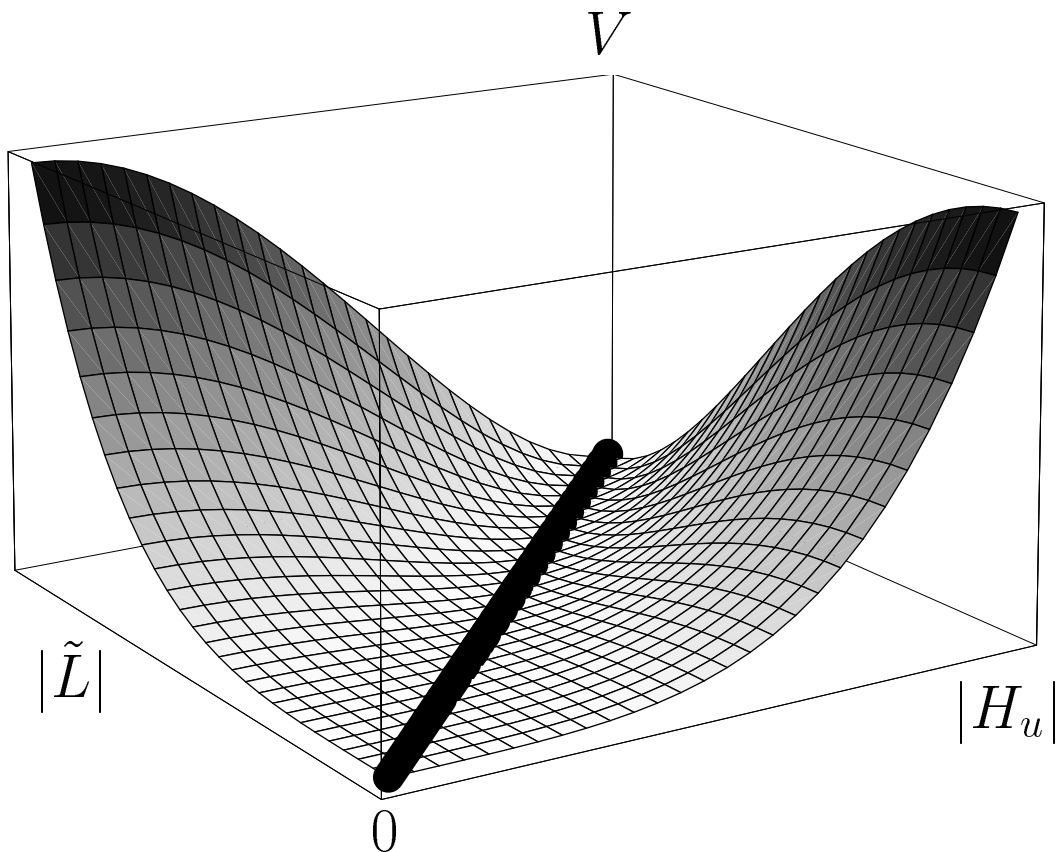


Figure 2.5: The scalar potential of \tilde{L}^0 and H_u^0 is shown. Thick line represents the flat direction, $|\tilde{L}^0| = |H_u^0|$, which is taken as D flat configuration. The potential apart from the flat direction is dominated by the D -term.

where M represents some large mass scale, e.g., the Planck mass. The superpotential (2.19) is given effectively for ϕ by

$$W = \frac{\kappa}{8M} \phi^4, \quad (2.20)$$

and the scalar potential is given by

$$V = (m_0^2 - cH^2)|\phi|^2 + \left[\frac{1}{8M} (Am_0 + aH) \kappa \phi^4 + \text{H.c.} \right] + \frac{|\kappa|^2 |\phi|^6}{4M^2}, \quad (2.21)$$

where m_0 is soft supersymmetry breaking mass. Here, we assume the hidden sector supersymmetry breaking providing $m_0 \sim 10^3$ GeV. The nonzero density of the inflaton in the early universe provides the soft supersymmetry breaking terms with the Hubble parameters H [26] in addition to the low energy ones with mass scale m_0 . In some

supergravity models, the Hubble induced mass term of ϕ may become negative ($c > 0$). The A and a terms do not conserve the lepton number, and the mismatch between these terms drives the phase rotation of ϕ . Then, with this plat potential the scalar field ϕ evolves governed by the equation of motion,

$$\ddot{\phi} + 3H\dot{\phi} + \frac{\partial V}{\partial \phi} = 0. \quad (2.22)$$

We examine in the following the evolution of ϕ in the respective epochs of the early universe, showing how the lepton number asymmetry is generated.

During the inflation, the Hubble parameter takes almost a constant value $H_{\text{inf}} \gg m_0$. Since the origin of the scalar potential (2.21) is unstable for $c > 0$, the ϕ field quickly settles into one of the minima of the scalar potential with $H = H_{\text{inf}}$:

$$\phi_0 = e^{i\theta_0} r_0 \sqrt{H_{\text{inf}}(M/\kappa)}, \quad (2.23)$$

where $r_0 \sim 1$, and

$$\theta \simeq \frac{-\arg a + (2n+1)\pi}{4} \quad (n = 0, \dots, 3). \quad (2.24)$$

After the inflation (before the reheating is completed), the coherent oscillation of the inflaton dominates the energy density of the universe, and the universe is in the matter dominated epoch with the Hubble parameter varying in time as $H = 2/(3t)$. Then, with this decreasing H the ϕ field is tracking the instantaneous minima,

$$\phi = e^{i\theta_0} r \sqrt{H(M/\kappa)} \quad (2.25)$$

with $r \sim 1$, decreasing its magnitude. Since the a term dominates in phase dependence, $\theta = \theta_0$ is fixed in this epoch.

The Hubble parameter eventually decreases after the inflation, and when it becomes as

$$H \lesssim m_0, \quad (2.26)$$

all the terms of the scalar potential (2.21) have comparable in magnitude, including A and a terms. In this epoch the m_0 mass term dominates over the Hubble induced negative mass term, so that the ϕ field begins to oscillate coherently with initial amplitude $|\phi| \sim \sqrt{m_0(M/\kappa)}$. The desired CP violation arises from the difference between $\arg a$ and

$\arg A$, and the A term becomes important for determining the variation of phase θ . Since $\arg A \neq \arg a$ without fine tuning, the rotation of ϕ field in the complex configuration plane is driven by the A term with nonzero and almost constant $\dot{\theta} \sim \epsilon$. As a result, the lepton number asymmetry generated at $H \lesssim m_0$, which is estimated as

$$n_L = \frac{\epsilon}{2} H^2 (M/\kappa), \quad (2.27)$$

where the factor $1/2 = (1+0)/2$ represents the effective lepton charge of the scalar field ϕ corresponding to the flat direction of \tilde{L} ($Q_L = 1$) and H_u ($Q_L = 0$).

The lepton number asymmetry is diluted as $n_L \propto H^2$ in the later time. Then, the reheating is completed with $H \ll m_0$, and the lepton-to-entropy ratio is obtained as

$$\frac{n_L}{s} \simeq \frac{\epsilon (M/\kappa) T_R}{2 \cdot 3M_{\text{P}}^2}, \quad (2.28)$$

where the entropy density is given by $s \simeq 3H^2 M_{\text{P}}^2 / T_R$. Then, by considering Eq. (2.19), the lepton number asymmetry is given in terms of the neutrino mass,

$$\frac{n_L}{s} \sim 10^{-10} \left(\frac{m_\nu}{10^{-5} \text{eV}} \right)^{-1} \left(\frac{T_R}{10^8 \text{GeV}} \right). \quad (2.29)$$

As a result, the sufficient lepton number asymmetry appears to be generated in the scenario.

This mechanism is, however, drastically changed by including the thermal effects which are provided from the plasma of the inflaton decay products [46, 47] should be included. Before the reheating is completed, the inflatons continue to decay producing light particles, though the decay rate is slow compared to the expansion rate H of the universe. The decay products form the thermal plasma with the energy density,

$$\rho_{\text{p}} = (\Gamma_{\text{I}}/H) \rho_{\text{I}}, \quad (2.30)$$

where the energy density of the coherent oscillation of inflaton is given by

$$\rho_{\text{I}} = 3H^2 M_{\text{P}}^2, \quad (2.31)$$

and the decay rate of inflaton is estimated in terms of the reheating temperature T_R as $\Gamma_{\text{I}} \simeq (\pi^2 g_*/30)^{1/2} T_R^2 / M_{\text{P}}$. Then, the temperature of thermal plasma is given by

$$T_{\text{p}} \simeq \rho_{\text{p}}^{1/4} \sim (T_R^2 H M_{\text{P}})^{1/4}. \quad (2.32)$$

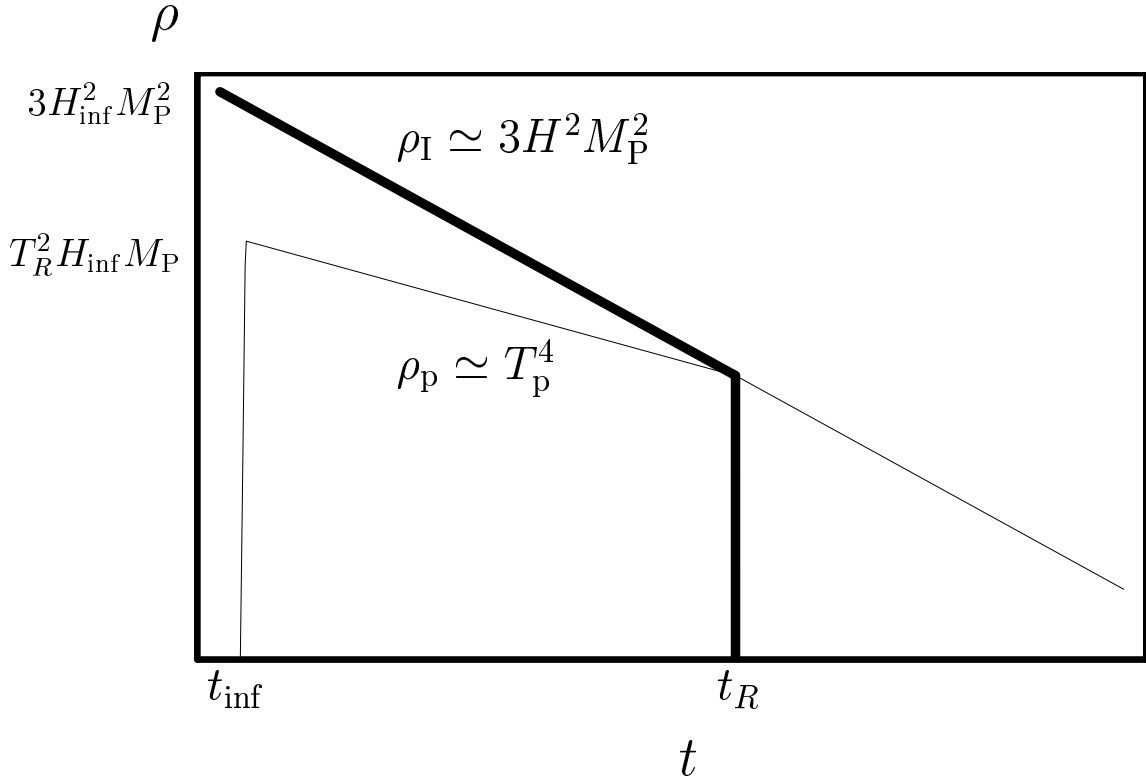


Figure 2.6: The time variation of inflaton energy density ρ_I and thermal plasma energy density ρ_p is shown. The inflaton energy density disappears exponentially at $t = t_R$, and the reheating is completed.

The time variation of the energy densities of inflaton and thermal plasma is illustrated in Fig. 2.6. The inflaton energy density disappears exponentially at $t = t_R$, and the reheating is completed.

The scalar field ϕ acquires a thermal mass term from the plasma consisting of quarks, leptons and gauge bosons as

$$V_{\text{th1}} \simeq \sum_a y_a^2 T_p^2 |\phi|^2 \quad (2.33)$$

for the couplings satisfying the condition $y_a |\phi| < T_p$. The particles coupling to ϕ acquire effective masses as

$$m_a = y_a |\phi|. \quad (2.34)$$

Then, if the particles are light enough as $m_a < T_p$, they enter the thermal plasma providing the effective mass term for the ϕ field. It is found that this thermal mass term V_{th1} begins

to dominate over the Hubble induced mass terms for the Hubble parameter

$$H_{\text{th1}} \sim \min \left[\frac{T_R^2 M_P}{y_a^4 (M/\kappa)^2} (y_a^4 T_R^2 M_P)^{1/3} \right]. \quad (2.35)$$

In practice, the Yukawa coupling of up quark is small enough for inducing the thermal mass term satisfying the condition $y_a |\phi| < T_p$ [44].

The thermal-log term also provides significant effect on the evolution of ϕ field and hence the leptogenesis [47]. The top quark decouples from the thermal plasma due to its large effective mass. This makes a change in the temperature dependence of the strong gauge coupling through renormalization as

$$\delta g_3(T) \simeq \frac{g_3(M_G)}{32\pi^2} \ln \left(\frac{y_t^2 |\phi|^2}{T^2} \right), \quad (2.36)$$

where M_G is a large scale such as GUT scale. The gluons and gluinos in the plasma without acquiring the effective masses from ϕ produce the thermal free energy at two loop level, $\delta V \propto g_3(T)^2 T^4$. Then, the above modification of the strong gauge coupling includes thermal-log term,

$$V_{\text{th2}} \simeq a \alpha_3(T)^2 T^4 \ln \left(\frac{|\phi|^2}{T^2} \right), \quad (2.37)$$

where $a \sim 1$ and $\alpha_3 = g_3^2/4\pi$. This thermal-log term also begins to dominate the Hubble induced mass term for the Hubble parameter

$$H_{\text{th2}} \simeq \alpha_3 T_R \sqrt{\frac{M_P}{M/\kappa}} \quad (2.38)$$

If the ϕ field begins to oscillate for

$$H \sim H_{\text{th}} = \max[H_{\text{th1}}, H_{\text{th2}}] > m_0, \quad (2.39)$$

the generated lepton number asymmetry is suppressed significantly by the factor m_0/H_{th} ,

$$\frac{n_L}{s} \simeq \frac{\epsilon}{2} \frac{(M/\kappa) T_R}{3 M_P^2} \frac{m_0}{H_{\text{th}}}. \quad (2.40)$$

Therefore, it is found that by including these thermal effects the generated lepton number asymmetry is almost independent of the reheating temperature T_R [45]. Then, in order to obtain the sufficient leptogenesis the lightest neutrino mass is required to extremely small as

$$m_{\nu_1} = 10^{-10} - 10^{-8} \text{eV} \quad (2.41)$$

with $10^5 \text{GeV} \lesssim T_R \lesssim 10^{12} \text{GeV}$.

Chapter 3

Higgs triplet model

In this chapter, we study an extension of the supersymmetric standard model including a pair of electroweak Higgs triplet Δ and $\bar{\Delta}$. The neutrinos acquire Majorana masses mediated by these Higgs triplet fields. The successful leptogenesis for baryogenesis can be realized after the inflation through the Affleck-Dine mechanism on a flat manifold consisting of Δ , $\bar{\Delta}$, \tilde{e}^c (anti-slepton), even if the Higgs triplet mass M_Δ is much larger than the gravitino mass $m_{3/2} \sim 10^3 \text{GeV}$. Specifically, due to the effects of the potential terms provided with the superpotential terms $M_\Delta \bar{\Delta} \Delta$, $(\lambda_{\not{L}}/2M) \bar{\Delta} \bar{\Delta} e^c e^c$, $(\lambda_\Delta/2M) \bar{\Delta} \Delta \bar{\Delta} \Delta$ ($\lambda_{\not{L}}/\lambda_\Delta \sim 0.3 - 3$), the phases of Δ , $\bar{\Delta}$, \tilde{e}^c are rotated at the time with the Hubble parameter $H \sim M_\Delta$, producing generally the asymmetry with fraction $\epsilon_L \sim 0.1$. If M_Δ is large enough, this early leptogenesis can be completed before the negative thermal-log term dominates over the scalar potential. This scenario is possible even for $M_\Delta \sim 1 \text{TeV}$ of Higgs triplets in TeV region if the reheating temperature is relatively low, $T_R \sim 10^5 \text{GeV}$, and the mass scale of the nonrenormalizable terms is high enough, $M/\lambda \sim 10^{23} \text{GeV}$. On the other hand, the negative thermal-log term may be dominant for $M_\Delta \sim 1 \text{TeV}$. Then, the lepton number asymmetry is amplified for some period by the thermal-log effect, and fixed later by the rotation of antislepton field. Even with this amplification, the resultant lepton-to-entropy ratio can be appropriate for some reasonable values of T_R and M/λ .

3.1 Model

We investigate an extension of the minimal supersymmetric standard model by introducing a pair of Higgs triplet superfields,

$$\Delta = \begin{pmatrix} \Delta^+/\sqrt{2} & \Delta^{++} \\ \Delta^0 & -\Delta^+/\sqrt{2} \end{pmatrix}, \quad \bar{\Delta} = \begin{pmatrix} \bar{\Delta}^-/\sqrt{2} & \bar{\Delta}^0 \\ \bar{\Delta}^{--} & -\bar{\Delta}^-/\sqrt{2} \end{pmatrix}. \quad (3.1)$$

The lepton doublets $L_i = (\nu_i, l_i)$, anti-lepton singlets l_i^c ($i = e, \mu, \tau$) and the Higgs doublets H_u, H_d are given as usual. The generic lepton number conserving superpotential for the leptons and Higgs fields is given by

$$W_0 = h_{ij} L_i H_d l_j^c + \mu H_u H_d + \frac{1}{\sqrt{2}} f_{ij} L_i \Delta L_j + M_\Delta \bar{\Delta} \Delta. \quad (3.2)$$

We consider the case of one lepton generation for definiteness in the following, though the essential results are even valid for the case that more than one generations participate in leptogenesis. The lepton numbers are assigned to the Higgs triplets as

$$Q_L(\Delta) = -2, \quad Q_L(\bar{\Delta}) = 2. \quad (3.3)$$

The lepton number violating terms may also be included in the superpotential as

$$W_{LV} = \xi_1 \bar{\Delta} H_u H_u + \xi_2 \Delta H_d H_d. \quad (3.4)$$

The Higgs triplets develop nonzero vacuum expectation values (VEV's) due to the effects of W_{LV} as

$$\langle \Delta^0 \rangle = -c_1 \frac{\xi_1 \langle H_u \rangle^2}{M_\Delta}, \quad \langle \bar{\Delta}^0 \rangle = -c_2 \frac{\xi_2 \langle H_d \rangle^2}{M_\Delta}. \quad (3.5)$$

The factors $c_1, c_2 \sim 1$ (with $\xi_1 \sim \xi_2$) are determined precisely by minimizing the scalar potential including the soft supersymmetry breaking terms with the mass scale $m_0 \sim 10^3 \text{ GeV}$. If the Higgs triplets are very heavy with $M_\Delta \gg m_0$, the soft supersymmetry breaking terms are negligible and $c_1, c_2 = 1$ is realized. It should here be noted that these VEV's are induced by the ξ_1 and ξ_2 couplings explicitly violating the lepton number conservation. Hence, the so-called triplet Majoron does not appear from the Δ and $\bar{\Delta}$ fields, which rather acquire masses $\simeq M_\Delta$. The slepton fields $\tilde{L}_i, \tilde{l}_i^c$ do not develop VEV's since the R -parity is still preserved by the VEV's of Higgs triplets.

The neutrino mass matrix is provided by the VEV of the Higgs triplet as

$$M_\nu = f\sqrt{2}\langle\Delta^0\rangle, \quad (3.6)$$

which is diagonalized with a unitary matrix U as

$$U^T M_\nu U = \text{diag}(m_1, m_2, m_3). \quad (3.7)$$

The charged lepton mass matrix is also given as

$$M_l = h\langle H_d \rangle = \text{diag}(m_e, m_\mu, m_\tau). \quad (3.8)$$

Here, the flavor structure of leptons is described at M_W by the f coupling with the diagonal h coupling. This neutrino mass matrix should reproduce the masses m_i and mixing angles θ_{ij} inferred from the data of neutrino experiments [2, 3, 4, 48]. The constraint on the magnitude of f coupling is then placed from $m_i \lesssim 10^{-1}\text{eV}$ roughly as

$$|f| \lesssim 10^{-1} \left(\frac{\xi}{10^{-2}} \right)^{-1} \left(\frac{M_\Delta}{10^{11}\text{GeV}} \right) = 10^{-1} \left(\frac{\xi}{10^{-10}} \right)^{-1} \left(\frac{M_\Delta}{10^3\text{GeV}} \right), \quad (3.9)$$

where the upper bound of the neutrino mass is given by WMAP [16] ,

$$m_\nu < 0.23\text{eV}. \quad (3.10)$$

If the Higgs triplet masses are very heavy with $M_\Delta \sim 10^{11}$ GeV, this condition may be realized for reasonable values of $\xi_1, \xi_2 \sim \xi \sim 10^{-2}$.

The Higgs triplets, on the other hand, may exist in the TeV region with $M_\Delta \sim 10^3\text{GeV}$. Then, it is required that $\xi_1, \xi_2 \sim \xi \sim 10^{-10}$ for the neutrino masses. These tiny lepton number violating couplings ξ_1, ξ_2 inducing the VEV's of Higgs triplets may be explained naturally as follows [27, 28]. Suppose that the lepton number/ R -parity violation originates in the Planck scale physics. Then, it may be provided with certain higher-order effective superpotential terms as

$$W'_{\text{LV}} = \xi'_1 \frac{\bar{S} H_u \bar{\Delta} H_u}{M_{\text{P}}} + \xi'_2 \frac{S H_d \Delta H_d}{M_{\text{P}}} \quad (3.11)$$

with the reduced Planck mass $M_{\text{P}} = m_{\text{P}}/\sqrt{8\pi} = 2.4 \times 10^{18}\text{GeV}$. Here, some singlet superfields S and \bar{S} of R -parity odd with $Q_L = 1, -1$, respectively are also considered.

The lepton number/ R -parity violating terms SH_uH_d and $S\Delta\bar{\Delta}$ are hence excluded. These singlet fields may have the lepton number/ R -parity preserving superpotential terms,

$$W_S = M_S S\bar{S} + \lambda_S \frac{SS\bar{S}\bar{S}}{M_P}, \quad (3.12)$$

where the Higgs singlet mass is assumed to be $M_S \sim 10^3 \text{ GeV}$ as well as the Higgs triplet mass $M_\Delta \sim 10^3 \text{ GeV}$. Without cubic terms for the Higgs singlets, they are considered as flatons [49], and may develop large VEV's with vanishing F -terms $|F_S|, |F_{\bar{S}}| \approx 0$ as

$$\langle S \rangle \sim \langle \bar{S} \rangle \sim \sqrt{M_S M_P} \sim 10^{10} \text{ GeV}. \quad (3.13)$$

Then, the lepton number violating couplings ξ_1 and ξ_2 are derived effectively as

$$\xi_1 = \xi'_1(\langle \bar{S} \rangle / M_P), \xi_2 = \xi'_2(\langle S \rangle / M_P) \quad (3.14)$$

with the tiny factor desired for ξ in Eq. (3.9),

$$\langle S \rangle / M_P, \langle \bar{S} \rangle / M_P \sim \sqrt{M_S / M_P} \sim 10^{-8}. \quad (3.15)$$

3.2 Flat Directions

We assume that the Higgs triplet mass is negligible at the end of inflation,

$$M_\Delta \ll H_{\text{inf}}. \quad (3.16)$$

Then, the Higgs triplet fields are allowed to enter into certain flat directions until the Hubble parameter H decreases to M_Δ . (This situation is similar to the μ term in the case of $\tilde{L}H_u$ flat direction.) The F -terms are actually given (except for the contributions of W_{LG}) as

$$\begin{aligned} F_L &= hH_d e^c + \sqrt{2}f\Delta L, \\ F_{e^c} &= hLH_d, \\ F_{H_u} &= \mu H_d, \\ F_{H_d} &= hLe^c + \mu H_u, \\ F_\Delta &= M_\Delta \bar{\Delta} + \frac{1}{\sqrt{2}}fLL, \\ F_{\bar{\Delta}} &= M_\Delta \Delta. \end{aligned} \quad (3.17)$$

These terms represent the flat directions, $\bar{\Delta}\bar{\Delta}\tilde{e}^c\tilde{e}^c$ ($Q_L = 2$) and $\bar{\Delta}\Delta$ ($Q_L = 0$), respectively. The nonrenormalizable terms relevant for leptogenesis is given by,

$$W_{\text{LG}} = \frac{\lambda_{\cancel{L}}}{2M}\bar{\Delta}\bar{\Delta}e^ce^c + e^{i\delta}\frac{\lambda_{\Delta}}{2M}\bar{\Delta}\Delta\bar{\Delta}\Delta, \quad (3.18)$$

where M represents some very large mass scale such as the grand unification or Planck scale. Then, if these directions are comparably flat with

$$0.3 \lesssim \lambda_{\cancel{L}}/\lambda_{\Delta} \lesssim 3, \quad (3.19)$$

the coherent evolution of the scalar fields, say AD-flatons [10, 25, 26, 49], may take place on the complex two-dimensional flat manifold spanned by these directions, starting with large initial values after the inflation. This flat manifold is specified by the D -flat condition,

$$|\Delta^+|^2 - |\bar{\Delta}^-|^2 + |\tilde{e}^c|^2 = 0, \quad (3.20)$$

and the other fields are negligibly small.

3.3 Leptogenesis with heavy Higgs triplets

We now examine the lepton-number asymmetry generation on the flat manifold in the Higgs triplet model. In this section, we first consider the case of heavy Higgs triplets with $M_{\Delta} \gg m_0$ [27]. In this case, thermal effects may be neglected. The relevant flat manifold is specified in Eq. (3.20). The scalar potential for the AD-flatons Δ^+ , $\bar{\Delta}^-$, \tilde{e}^c is given by

$$\begin{aligned} V = & (C_1 m_{3/2}^2 - c_1 H^2) |\Delta|^2 + (C_2 m_{3/2}^2 - c_2 H^2) |\bar{\Delta}|^2 + (C_3 m_{3/2}^2 - c_3 H^2) |\tilde{e}^c|^2 \\ & + \left| M_{\Delta} \Delta + \frac{\lambda_{\cancel{L}}}{M} \bar{\Delta} \tilde{e}^c \tilde{e}^c + e^{i\delta} \frac{\lambda_{\Delta}}{M} \bar{\Delta} \Delta \Delta \right|^2 \\ & + \left| M_{\Delta} \bar{\Delta} + e^{i\delta} \frac{\lambda_{\Delta}}{M} \bar{\Delta} \bar{\Delta} \Delta \right|^2 + \left| \frac{\lambda_{\cancel{L}}}{M} \bar{\Delta} \bar{\Delta} \tilde{e}^c \right|^2 \\ & + [(b_{\Delta} H + B_{\Delta} m_0) M_{\Delta} \bar{\Delta} \Delta + \text{h.c.}] \\ & + \left[\frac{1}{2M} (a_{\cancel{L}} H + A_{\cancel{L}} m_0) \lambda_{\cancel{L}} \bar{\Delta} \bar{\Delta} \tilde{e}^c \tilde{e}^c + \text{h.c.} \right] \\ & + \left[\frac{1}{2M} (a_{\Delta} H + A_{\Delta} m_0) \lambda_{\Delta} \bar{\Delta} \Delta \bar{\Delta} \Delta + \text{h.c.} \right] \\ & + g_1^2 (|\Delta|^2 - |\bar{\Delta}|^2 + |\tilde{e}^c|^2)^2, \end{aligned} \quad (3.21)$$

($\Delta \equiv \Delta^+$ and $\bar{\Delta} \equiv \bar{\Delta}^-$ henceforth for simplicity of notation). The last term with $U(1)_Y$ gauge coupling g_1 is included to realize the D -flat condition (3.20) for the large enough $|\Delta|$, $|\bar{\Delta}|$, $|\tilde{e}^c|$. The nonzero energy density in the early universe provides the soft supersymmetry breaking terms with the Hubble parameter H in addition to the low-energy ones with the gravitino mass $m_{3/2}$ [26]. We consider the case that at least one c_a is positive. In the following, the evolution of the AD-flatons is described in the respective epochs for evaluating the lepton number asymmetry. It will really be confirmed later by solving the equations of motion numerically with the initial values specified by the potential minimum in the inflation epoch.

3.3.1 (i) $t \ll M_\Delta^{-1}$

During the inflation the Hubble parameter takes almost a constant value H_{inf} , and the AD-flatons quickly settle into one of the minima of the scalar potential V with $H = H_{\text{inf}}$:

$$\phi_a^{(0)} = e^{i\theta_a^{(0)}} r_a^{(0)} \sqrt{H_{\text{inf}}(M/\lambda)}, \quad (3.22)$$

where $\phi_a = \Delta, \bar{\Delta}, \tilde{e}^c$, and λ represents the mean value of $\lambda_{\tilde{L}}$ and λ_Δ . These minima are determined depending on the values of the parameters in the scalar potential. Specifically, the $\lambda_{\tilde{L}}\text{-}\lambda_\Delta$ cross term, $a_{\tilde{L}}$ term and a_Δ term, which are significant for $H \gg M_\Delta, m_{3/2}$, have different dependences on the phases θ_a of AD-flatons. Then, some valleys are formed on the flat manifold so as to minimize the sum of these three terms depending generally on $|\phi_a|$, and the potential minima are located along them. Actually, we find the minima with

$$r_a^{(0)} \sim 0.1 - 1 \leftarrow \lambda_{\tilde{L}} \sim \lambda_\Delta, \quad c_a \sim 1. \quad (3.23)$$

(It should be mentioned for completeness that if $\lambda_{\tilde{L}}$ and λ_Δ are rather different from each other, the minimum is formed along one of the flat directions with $r_\Delta^{(0)} = 0$ or $r_{\tilde{e}^c}^{(0)} = 0$. We do not consider such cases here.) As for the initial phases, up to the physically irrelevant arbitrary phase of $U(1)_{\text{em}}$ gauge transformation they are specified in terms of the $U(1)_{\text{em}}$ invariant combinations as

$$\theta_\Delta^{(0)} + \theta_{\bar{\Delta}}^{(0)}, \quad \theta_{\tilde{e}^c}^{(0)} + \theta_{\tilde{\Delta}}^{(0)}. \quad (3.24)$$

The dependence of $\theta_a^{(0)}$ on the parameters $c_a, \lambda_{\tilde{L}}, \lambda_\Delta, a_{\tilde{L}}, a_\Delta$ is really complicated in contrast to the one-dimensional Affleck-Dine scenario, unless the fine-tuning, $\arg(a_{\tilde{L}}) -$

$\arg(a_\Delta) = \pi \bmod 2\pi$, is made so as to align simultaneously the three phase-dependent potential terms.

After the inflation the inflaton oscillates coherently, and it dominates the energy density of the universe. In this epoch of $t \ll M_\Delta^{-1} < m_{3/2}^{-1}$ ($H \gg M_\Delta > m_{3/2}$), the AD-flatons are moving toward the origin with the initial conditions at $t = t_0 \sim H_{\text{inf}}^{-1}$ just after the inflation,

$$\phi_a(t_0) = \phi_a^{(0)}, \quad \dot{\phi}_a(t_0) = 0. \quad (3.25)$$

The evolution of the AD-flatons are governed by the equations of motion,

$$\ddot{\phi}_a + 3H\dot{\phi}_a + \frac{\partial V}{\partial \phi_a^*} = 0. \quad (3.26)$$

The Hubble parameter varies in time as $H = (2/3)t^{-1}$ in the matter-dominated universe. The AD-flatons may be represented suitably in terms of the dimensionless fields χ_a [26] as

$$\phi_a = \chi_a \sqrt{H(M/\lambda)} \equiv e^{i\theta_a} r_a \sqrt{H(M/\lambda)}. \quad (3.27)$$

where we define $\bar{\phi} \equiv \sqrt{H(M/\lambda)}$. Then, the equations of motion (3.26) are rewritten with $z = \ln(t/t_0)$ as

$$\frac{d^2 \chi_a}{dz^2} + \frac{\partial U}{\partial \chi_a^*} = 0, \quad (3.28)$$

and the initial conditions from Eq. (3.25) are given as

$$\chi_a(0) = e^{i\theta_a^{(0)}} r_a^{(0)}, \quad \frac{d\chi_a}{dz}(0) = \frac{1}{2}\chi_a(0). \quad (3.29)$$

The dimensionless effective potential U is given by

$$U(\chi_a, M_\Delta/H, m_{3/2}/H) = \frac{4}{9H^3(M/\lambda)} V(\phi_a, H, M_\Delta, m_{3/2}) - \frac{1}{4}|\chi_a|^2. \quad (3.30)$$

The second term is due to the time variation of the factor $\bar{\phi}$ in Eq. (3.27), which apparently provides the change of the mass terms in U ,

$$c_a \rightarrow c_a + \frac{9}{16}. \quad (3.31)$$

It should be noticed in Eq. (3.28) that the first-order z -derivative is absent due to the parameterization of $\phi_a \propto H^{1/2} \propto t^{-1/2}$ in Eq. (3.27). In this epoch with $H \gg M_\Delta, m_{3/2}$, the effective potential U is almost independent of the mass parameters $M_\Delta, m_{3/2}$:

$$U(\chi_a, M_\Delta/H, m_{3/2}/H) = U_1(\chi_a) + O(M_\Delta/H, m_{3/2}/H). \quad (3.32)$$

The motion of the phases θ_a of AD-flatons is described in this epoch as follows. The initial conditions at $t = t_0$ ($z = 0$) are given from Eq. (3.29) as

$$\theta_a(0) = \theta_a^{(0)}, \quad \frac{d\theta_a}{dz}(0) = 0. \quad (3.33)$$

On the other hand, the asymptotic trajectory of the AD-flatons is found by the conditions $\partial U_1 / \partial \chi_a^* = 0$ in this epoch with $H \gg M_\Delta, m_{3/2}$ as

$$\theta_a = \theta_a^{(1)}. \quad (3.34)$$

It is remarkable for the multi-dimensional motion of the AD-flatons with $\lambda_{\not{L}} \sim \lambda_\Delta$ that the direction of this trajectory is somewhat different from the initial direction, i.e.,

$$\theta_a^{(1)} \neq \theta_a^{(0)}. \quad (3.35)$$

This is because the apparent change of the mass terms in Eq. (3.31) due to the redshift induces the new balance among the $\lambda_{\not{L}}\text{-}\lambda_\Delta$ cross term, $a_{\not{L}}$ term and a_Δ term in $U_1(\chi_a)$, which have different dependences on θ_a . (If the fine-tuning is made as $\arg(a_{\not{L}}) - \arg(a_\Delta) = \pi \bmod 2\pi$, the initial balance is maintained independently of $|\chi_a|$ so as to realize $\theta_a^{(0)} = \theta_a^{(1)}$.) Without the $d\chi_a/dz$ (friction) term in Eq. (3.28), the phases of AD-flatons θ_a slowly fluctuate around $\theta_a^{(1)}$ starting from $\theta_a^{(0)}$ as a function of $z = \ln(t/t_0)$ in the epoch $H_{\text{inf}}^{-1} \sim t_0 \leq t < M_\Delta^{-1}$. That is, in the motion on the multi-dimensional flat manifold the AD-flatons no longer track exactly behind the decreasing instantaneous minimum of scalar potential V . This is a salient contrast to the usual Affleck-Dine mechanism on the one-dimensional flat direction, where the phase of one AD-flaton is kept constant until it begins to oscillate by the low-energy supersymmetry breaking mass term or the thermal mass term. In this way, even in this very early epoch the lepton number asymmetry really appears due to this phase fluctuation of the AD-flatons on the multi-dimensional flat manifold.

The lepton number asymmetry is evaluated by combining the contributions of the AD-flatons as

$$n_L = 2\Delta n_{\bar{\Delta}} - 2\Delta n_{\Delta} - \Delta n_{\bar{e}^c}, \quad (3.36)$$

where the particle number asymmetry (particle number – anti-particle number) is calculated with the homogeneous coherent scalar field $\phi_a(t)$ by

$$\Delta n_a \equiv n_a - \bar{n}_a = i(\phi_a^* \dot{\phi}_a - \dot{\phi}_a^* \phi_a). \quad (3.37)$$

The resultant lepton number asymmetry is given as

$$n_L(t) = \epsilon_L(t)(3/2)H^2(M/\lambda) \quad (3.38)$$

in terms of the parameter $\epsilon_L(t)$ representing the fraction of the lepton number asymmetry

$$\epsilon_L(t) = \sum_a Q_L(a)\epsilon_a(t) \quad (3.39)$$

with the respective fractions of particle number asymmetries

$$\epsilon_a(t) = i \left(\chi_a^* \frac{d\chi_a}{dz} - \frac{d\chi_a^*}{dz} \chi_a \right) = -2r_a^2 \frac{d\theta_a}{dz}. \quad (3.40)$$

Since the phases of AD-flatons are fluctuating in this early epoch, as mentioned so far, the lepton number asymmetry is oscillating in time as $|\epsilon_L(t)| \sim |d\theta_a/dz| \lesssim |\theta_a^{(0)} - \theta_a^{(1)}| \sim 0.01 - 0.1$ ($r_a \sim 0.1 - 1$) numerically for the reasonable parameter values.

3.3.2 (ii) $t \sim M_\Delta^{-1}$

The Hubble parameter eventually decreases after the inflation, and when it becomes as

$$H \sim M_\Delta \quad (t \sim M_\Delta^{-1}), \quad (3.41)$$

the AD-flatons start to oscillate due to the Higgs triplet mass terms $M_\Delta^2(|\Delta|^2 + |\bar{\Delta}|^2)$. The significant torque is also applied to the AD-flatons by the phase-dependent potential terms which are provided with the superpotential terms $\bar{\Delta}\Delta$, $\bar{\Delta}\bar{\Delta}e^ce^c$, $\bar{\Delta}\Delta\bar{\Delta}\Delta$. Then, in this epoch the AD-flatons are rotating around the origin, and the lepton number asymmetry soon approaches certain nonzero value as

$$\epsilon_L(t) \approx \epsilon_L \quad (t \gg M_\Delta^{-1}). \quad (3.42)$$

This final lepton number asymmetry is calculated to be $\epsilon_L \sim 0.1$ for the generic choice of the model parameter values with $\lambda_{\cancel{L}}/\lambda_\Delta \sim 0.3 - 3$, as shown later in the numerical analysis. It should here be noted that once the AD-flatons are rotated rapidly with frequency $\sim M_\Delta$, the low-energy soft supersymmetry breaking terms have little effects on the leptogenesis for $M_\Delta \gg m_{3/2}$.

3.3.3 (iii) $t \gg M_\Delta^{-1}$

The coherent oscillation of the inflaton field dominates the energy density of the universe until the decay of the inflatons is completed at the time t_R ($\gg M_\Delta^{-1}$). Then, the universe is reheated to the temperature T_R . Until this time, the lepton number asymmetry is redshifted as matter, which is given for $H = H_R$ with Eqs. (3.38) and (3.42) as

$$n_L(t_R) = \epsilon_L(3/2)H_R^2(M/\lambda). \quad (3.43)$$

Then, the lepton-to-entropy ratio after the reheating is estimated with $s \sim 3H_R^2 M_P^2/T_R$ as

$$\begin{aligned} \frac{n_L}{s} &\sim \epsilon_L \frac{(M/\lambda)T_R}{2M_P^2} \\ &\sim 10^{-10} \left(\frac{\epsilon_L}{0.1} \right) \left(\frac{10^{-2}}{\lambda} \right) \left(\frac{M}{10^{18} \text{GeV}} \right) \left(\frac{T_R}{10^8 \text{GeV}} \right), \end{aligned} \quad (3.44)$$

where the reheating temperature is constrained as $T_R \lesssim 10^8 - 10^{10} \text{GeV}$ to avoid the overproduction of gravitinos [21, 22, 23]. This lepton number asymmetry is converted partially to the baryon number asymmetry through the electroweak anomalous effect. The chemical equilibrium between leptons and baryons leads the ratio $n_B \simeq -0.35n_L$ (without any preexisting baryon number asymmetry) [39]. Therefore, the sufficient baryon-to-entropy ratio is provided as required from the big-bang nucleosynthesis [11] and the cosmic microwave background [16],

$$\begin{aligned} \eta(\text{BBN}) &= (2.6 - 6.2) \times 10^{-10}, \\ \eta(\text{CMB}) &= (5.9 - 6.4) \times 10^{-10}, \end{aligned} \quad (3.45)$$

where $\eta \equiv n_B/n_\gamma \simeq 7n_B/s$. One may take seriously the non-thermal gravitino production. Then, the reheating temperature may be significantly lower than $10^8 - 10^{10} \text{GeV}$ [23]. Even in this case, if λ is small enough, the sufficient baryon number asymmetry can be generated.

3.3.4 Numerical analysis

We have made numerical calculations to confirm the generation of lepton number asymmetry in the present model with Higgs triplet. The values of the model parameters are

taken in some reasonable ranges as

$$\begin{aligned}
M &= 10^{18} \text{GeV}, \quad M_\Delta = m_{3/2} - 0.1 H_{\text{inf}}, \quad m_{3/2} = 10^3 \text{GeV}, \\
\lambda_{\cancel{L}}, \lambda_\Delta &= 0.3\lambda - 3\lambda, \quad \lambda = 10^{-2}, \\
c_a, C_a &= 0.5 - 2, \\
|a_{\cancel{L}}|, |a_\Delta|, |b_\Delta|, |A_{\cancel{L}}|, |A_\Delta|, |B_\Delta| &= 0.5 - 2,
\end{aligned} \tag{3.46}$$

and $[0, 2\pi]$ for the phases of coupling parameters. A typical example for the evolution of the AD-flatons is presented in the following by taking the parameter values rather arbitrarily in the above ranges as

$$\begin{aligned}
M_\Delta &= 10^{-4} H_{\text{inf}} = 10^9 \text{GeV} (H_{\text{inf}}/10^{13} \text{GeV}), \\
\lambda_{\cancel{L}} &= \lambda, \quad \lambda_\Delta = 2\lambda, \\
c_{\bar{\Delta}} &= 1, \quad c_\Delta = 0.5, \quad c_{\tilde{e}^c} = 1.5, \\
|a_{\cancel{L}}| &= 1, \quad |a_\Delta| = 0.5, \quad |b_\Delta| = 1, \\
\arg(a_{\cancel{L}}) &= -\pi/6, \quad \arg(a_\Delta) = -2\pi/3, \\
\arg(b_\Delta) &= 5\pi/6, \quad \delta = \pi/3.
\end{aligned} \tag{3.47}$$

(The effects of the low-energy soft supersymmetry breaking terms are in fact negligible for $M_\Delta \gg m_{3/2}$.) The initial values of the AD-flatons at $t = t_0$ ($H = H_{\text{inf}} \gg M_\Delta, m_{3/2}$) in Eq. (3.22) are determined with these parameter values as

$$\begin{aligned}
r_\Delta^{(0)} &= 0.752, & r_\Delta^{(0)} &= 0.144, & r_{\tilde{e}^c}^{(0)} &= 0.738, \\
\theta_\Delta^{(0)} &= 0, & \theta_\Delta^{(0)} &= -3.044, & \theta_{\tilde{e}^c}^{(0)} &= -1.327,
\end{aligned} \tag{3.48}$$

where $\theta_\Delta^{(0)} = 0$ is chosen by the $U(1)_{\text{em}}$ gauge transformation. Then, the asymptotic trajectory of the AD-flatons in the epoch $t_0 < t \ll M_\Delta^{-1} < m_{3/2}^{-1}$ is determined by the conditions $\partial U_1 / \partial \chi_a^* = 0$ as

$$\begin{aligned}
r_\Delta^{(1)} &= 0.812, & r_\Delta^{(1)} &= 0.209, & r_{\tilde{e}^c}^{(1)} &= 0.786, \\
\theta_\Delta^{(1)} &= 0.006, & \theta_\Delta^{(1)} &= -3.048, & \theta_{\tilde{e}^c}^{(1)} &= -1.348.
\end{aligned} \tag{3.49}$$

It is really observed that the asymptotic phases $\theta_a^{(1)}$ are in general slightly different from the initial phases $\theta_a^{(0)}$ in the multi-dimensional motion of the AD-flatons due to the apparent change of the mass terms in Eq. (3.31). (It is also checked that if the fine-tuning, $\arg(a_{\cancel{L}}) - \arg(a_\Delta) = \pi \bmod 2\pi$, is made, the alignment $\theta_a^{(1)} = \theta_a^{(0)}$ is realized, as expected.)

We have solved numerically the equations of motion (3.26) for the AD-flatons from $t = t_0$ ($H = H_{\text{inf}}$) to $t \sim 10^3 M_{\Delta}^{-1}$ with the initial conditions at $t = t_0$ in Eq. (3.25). (In practice, we have solved Eq. (3.28) for χ_a with Eq. (3.29) as functions of $z = \ln(t/t_0)$ since the time interval ranges over several orders. The D -flat condition (3.20) is checked to be hold.) The result is depicted in Fig. 3.1 in terms of the dimensionless fields χ_a for the case of Eq. (3.47) with $\lambda_{\cancel{\Delta}}/\lambda_{\Delta} = 0.5$ and $M_{\Delta} = 10^{-4} H_{\text{inf}}$ ($\gg m_{3/2}$). The dots represent the times of $t/t_0 = 1, 10, 10^2, 10^3, 10^4, 10^5$. The AD-flatons really exhibit the behavior as described in this section. Their phases θ_a and magnitudes $r_a = |\chi_a|$ normalized in Eq. (3.27) fluctuate gradually around the asymptotic values in Eq. (3.49) for $t_0 < t < 10^4 t_0$. Then, around $t \sim 10^4 t_0 \sim M_{\Delta}^{-1}$ they begin to rotate around the origin, which appears to be somewhat complicated in the multi-dimensional motion. This motion of the AD-flatons for $t \gtrsim M_{\Delta}^{-1}$ is driven mainly by the potential terms provided with the superpotential term $M_{\Delta} \bar{\Delta} \Delta$ of Higgs triplet mass.

The fraction of lepton number asymmetry $\epsilon_L(t)$ in Eq. (3.39) calculated from the time evolution of the AD-flatons is shown in Fig. 3.2, where the respective particle number asymmetries $\epsilon_a(t)$ in Eq. (3.40) are shown in Fig. 3.3. The fraction of Δ and $\bar{\Delta}$ are fluctuating even for $t \gtrsim 10^5 t_0$. However, since this fluctuation is due to the lepton number conserving B -term, the lepton number is fixed. (It is checked that the electric charge conservation is hold with $\epsilon_{\Delta}(t) - \epsilon_{\bar{\Delta}}(t) + \epsilon_{\bar{e}^c}(t) = 0$.) The lepton number asymmetry is really oscillating slowly in the time range $t_0 < t < 10^4 t_0$, which is due to the motion of the AD-flatons fluctuating around the asymptotic trajectory. Then, it changes to approach a nonzero value $\epsilon_L \sim 0.1$ for $t \gtrsim 10^4 t_0 \sim M_{\Delta}^{-1}$.

We have obtained similar numerical results in most cases by taking randomly about one hundred samples of the parameters in the ranges of Eq. (3.46). Then, we have confirmed that the minimum during the inflation for the initial values of the AD-flatons can really be formed on the flat manifold with

$$r_{\bar{\Delta}}^{(0)}, r_{\Delta}^{(0)}, r_{\bar{e}^c}^{(0)} \sim 0.1 - 1. \quad (3.50)$$

It is essential for admitting this sort of multi-dimensional motion of the AD-flatons that the relevant non-renormalizable superpotential terms are comparable, specifically in the present model

$$0.3 \lesssim \lambda_{\cancel{\Delta}}/\lambda_{\Delta} \lesssim 3 \quad (3.51)$$

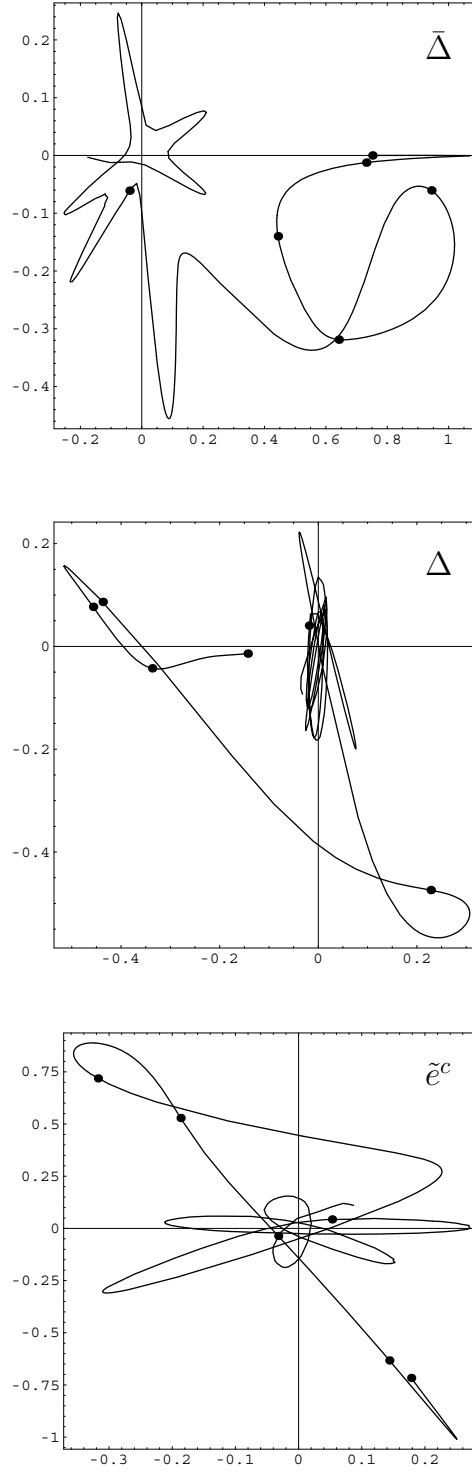


Figure 3.1: The motions of the AD-flatons, the real part (horizontal axis) and imaginary part (vertical axis), are depicted in terms of the dimensionless fields χ_a for the case with $\lambda_\psi/\lambda_\Delta = 0.5$ and $M_\Delta = 10^{-4}H_{\text{inf}} \gg m_{3/2}$. The dots represent the times of $t/t_0 = 1, 10, 10^2, 10^3, 10^4, 10^5$.

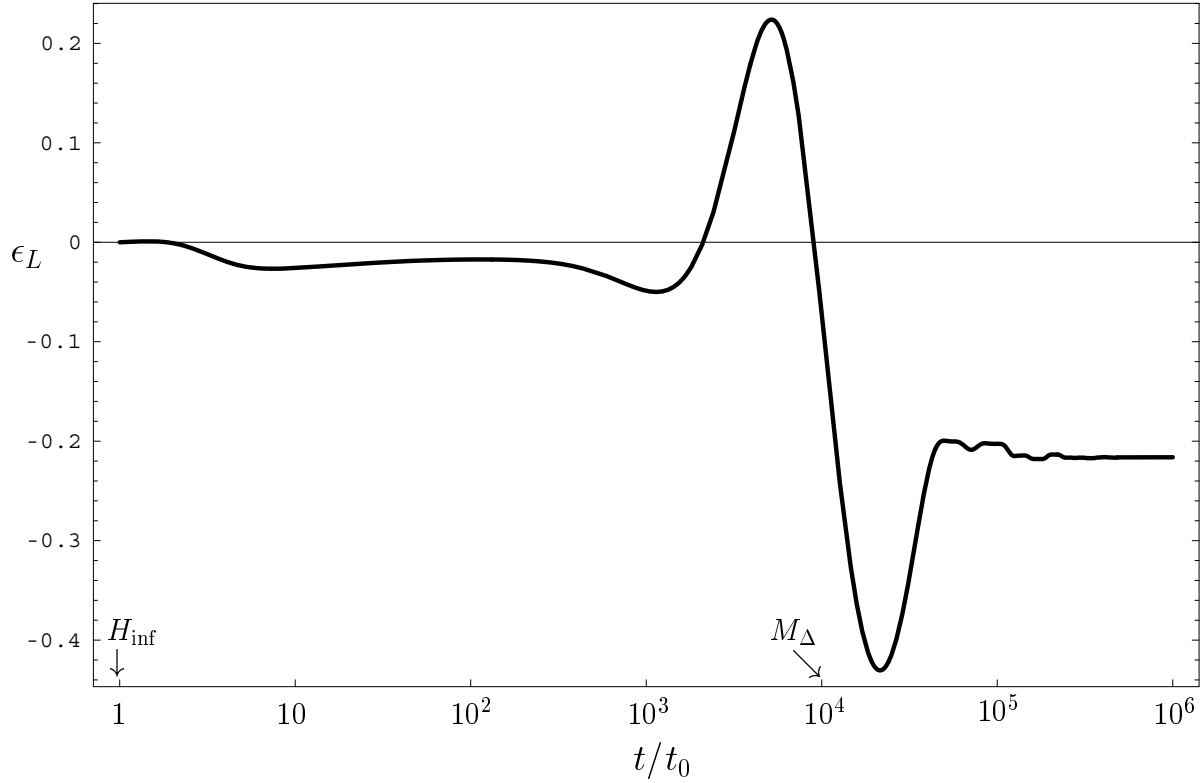


Figure 3.2: The fraction of lepton number asymmetry $\epsilon_L(t)$ is shown for the case with $\lambda_\psi/\lambda_\Delta = 0.5$ and $M_\Delta = 10^{-4}H_{\text{inf}} \gg m_{3/2}$.

with rather arbitrary values $0 < c_a \lesssim 1$ for the Hubble induced mass terms. This desired range of $\lambda_\psi/\lambda_\Delta$ has actually a reasonable size, in contrast to naive expectation, due to the effects of the phase dependent potential terms. If the difference between these couplings is larger than this range, we have found that the AD-flatons evolve along one of the flat directions as in the usual Affleck-Dine scenario.

As confirmed by these numerical calculations, it is quite an interesting feature of the present Affleck-Dine leptogenesis with Higgs triplet that the significant lepton number asymmetry is generated in the early epoch $t \sim M_\Delta^{-1}$ through the multi-dimensional motion of the AD-flatons. Then, for $M_\Delta \gg m_{3/2}$ the low-energy supersymmetry breaking terms with $m_{3/2}$ have little effect on the leptogenesis. This is because several scalar potential terms are provided for $H \sim M_\Delta$ with the superpotential mass term of Higgs triplet, which have different dependences on the phases of AD-flatons. The phase rotation of the AD-

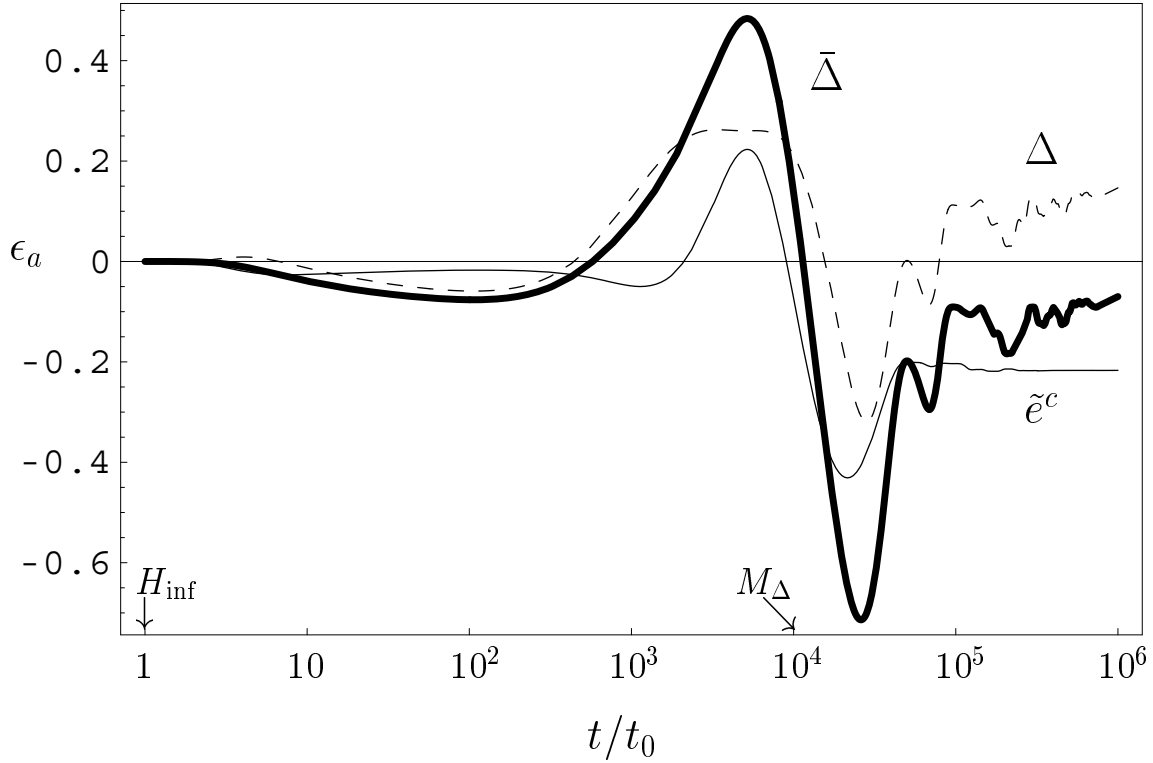


Figure 3.3: The fraction of particle number asymmetries $\epsilon_a(t)$ for the case with $\lambda_{\not{L}}/\lambda_{\Delta} = 0.5$ and $M_{\Delta} = 10^{-4}H_{\text{inf}} \gg m_{3/2}$.

flatons for $t \gtrsim M_{\Delta}^{-1}$ is indeed driven by such terms with M_{Δ} rather than the low-energy soft supersymmetry breaking terms with $m_{3/2}$.

3.4 Leptogenesis with Higgs triplets in TeV region

In this section, we examine the leptogenesis for the case of Higgs triplets with $M_{\Delta} \sim 1$ TeV in the light of experimental verification in TeV region [28]. In the case preceding section [27], the lepton number asymmetry is fixed readily in the early epoch by the very large Higgs triplet mass terms with $M_{\Delta} \gtrsim 10^9 \text{ GeV}$, which dominate over the thermal terms [46, 47]. On the other hand, the problem of asymmetry fixing becomes more important for $M_{\Delta} \sim 1 \text{ TeV}$ due to the thermal effects.

3.4.1 Thermal effects

We here consider the thermal terms for the scalar potential, which may provide significant effects on the scalar field evolution and hence the leptogenesis [44, 45, 46, 47].

The AD-flatons acquire the thermal mass term from the dilute thermal plasma as

$$m_{\text{th1}}|\phi|^2 = y^2 T_{\text{p}}^2 |\phi|^2, \quad (3.52)$$

where y represents the effective coupling of the relevant fields with the AD-flatons which is determined in terms of the f and h couplings and $|\phi_a|/|\phi|$. The temperature of this thermal plasma is given by

$$T_{\text{p}} \sim (T_R^2 H M_{\text{P}})^{1/4}. \quad (3.53)$$

This mass term appears under the condition $y|\phi| < T_{\text{p}}$. Then, the Hubble parameter H_{th} at the time when the thermal mass term begins to dominate over the Hubble induced mass terms are estimated as

$$H_{\text{th}} \sim \min \left[\frac{T_R^2 M_{\text{P}}}{y^4 (M/\lambda)^2}, (y^4 T_R^2 M_{\text{P}})^{1/3} \right]. \quad (3.54)$$

This estimate takes the maximal value as

$$H_{\text{th}}^{\text{max}} \sim 10^7 \text{GeV} \left(\frac{T_R}{10^8 \text{GeV}} \right) \left(\frac{M/\lambda}{10^{20} \text{GeV}} \right)^{-1/2} \quad (3.55)$$

with certain value of the relevant coupling

$$y \sim 10^{-4} \left(\frac{T_R}{10^8 \text{GeV}} \right)^{1/4} \left(\frac{M/\lambda}{10^{20} \text{GeV}} \right)^{-3/8}. \quad (3.56)$$

Hence, if the Higgs triplet is heavy enough as $M_{\Delta} > H_{\text{th}}^{\text{max}}$, the Higgs triplet mass terms dominate over the thermal mass terms.

The thermal-log term is more important for the asymmetry fixing with Higgs triplets in TeV region. The $\text{SU}(2)_W/\text{U}(1)_{I_3}$ gauge bosons acquire the very large masses through the gauge coupling to the Higgs triplet. Hence, the $\text{SU}(2)_W/\text{U}(1)_{I_3}$ gauge bosons decouples from the thermal plasma. Then, the *negative* thermal-log term appears through the modification of the gauge coupling of unbroken $\text{U}(1)_{I_3}$ due to this decoupling of gauge bosons:

$$V_{\text{th}} = -a\alpha_2^2 T_{\text{p}}^4 \ln \left[(|\Delta|^2 + |\bar{\Delta}|^2)/T_{\text{p}}^2 \right], \quad (3.57)$$

where $a \sim 6$ and $\alpha_2 = g_2^2/4\pi \sim 1/30$ with the $SU(2)_W$ gauge coupling g_2 .

If the Higgs triplet mass is rather small as $M_\Delta < a^{1/2}\alpha_2 H_{\text{th}}^{\text{max}} \sim 0.1 H_{\text{th}}^{\text{max}}$, the negative thermal-log term dominates over the Higgs triplet mass terms. Then, the situation of leptogenesis appears to be rather different. We examine the asymmetry fixing in the following for the case (i) with $M_\Delta > H_{\text{th}}$ and the case (ii) with $M_\Delta < H_{\text{th}}$ in order, by including the thermal terms in the scalar potential.

3.4.2 Case (i): asymmetry fixing with $M_\Delta > H_{\text{th}}$

The AD-flatons are scaled as $\bar{\phi} \propto H^{1/2}$ for some period after the inflation, as seen in Eq. (3.27). Then, the Higgs triplet mass terms and the thermal-log term, scaling as H , eventually become important for the dynamics of AD-flatons. The Higgs triplet mass terms $M_\Delta^2(|\Delta|^2 + |\bar{\Delta}|^2) \sim M_\Delta^2(M/\lambda)H$ may first dominate over the Hubble induced mass terms $\sim H^2|\phi_a|^2 \sim (M/\lambda)H^3$ at $H \sim M_\Delta$ under the condition

$$M_\Delta > H_{\text{th}2} = a^{1/2}\alpha_2 T_R \sqrt{M_{\text{P}}/(M/\lambda)}. \quad (3.58)$$

Here, the Hubble parameter H_{th} for $|V_{\text{th}}| \sim H^2|\phi_a|^2$ is estimated as

$$H_{\text{th}2} \sim 10\text{GeV} \left(\frac{T_R}{10^5\text{GeV}} \right) \left(\frac{M/\lambda}{10^{23}\text{GeV}} \right)^{-1/2}, \quad (3.59)$$

so that the condition (3.58) can be satisfied even with $M_\Delta \sim 1\text{TeV}$. In this case, the thermal-log term is still subdominant for $H \sim M_\Delta$, and the AD-flatons begin to rotate with frequency $\sim M_\Delta$ driven by the Higgs triplet mass terms [27].

Since $|\phi_a| \propto H$ for a while in this epoch, the thermal-log term $\propto H$ soon catches up the Higgs triplet mass terms $\propto H^2$. Then, two instantaneous minima $\phi_a(1)$ and $\phi_a(2)$ appear under the balance between the negative thermal-log term V_{th} of Eq. (3.57) and the potential terms in V of Eq. (3.21) as

$$\phi_a(1) : |\Delta(1)| \sim |\bar{\Delta}(1)| \sim |\tilde{e}^c(1)| \sim \frac{H_{\text{th}}}{M_\Delta} \bar{\phi}. \quad (3.60)$$

$$\phi_a(2) : |\Delta(2)| \simeq |\bar{\Delta}(2)| \sim \frac{H_{\text{th}}}{M_\Delta} \bar{\phi}, \quad |\tilde{e}^c(2)| = 0, \quad (3.61)$$

The main terms to determine these minima are given by

$$\begin{aligned} V_1 = & V_{\text{th}} + g_1^2(|\Delta|^2 - |\bar{\Delta}|^2 + |\tilde{e}^c|^2)^2 \\ & + (M_\Delta^2 + C_1 m_0^2)|\Delta|^2 + (M_\Delta^2 + C_2 m_0^2)|\bar{\Delta}|^2 \\ & + [B_\Delta m_0 M_\Delta \bar{\Delta} \Delta + \text{h.c.}] + C_3 m_0^2 |\tilde{e}^c|^2. \end{aligned} \quad (3.62)$$

The AD-flatons, however, have already sufficient angular momenta under the condition (3.58), so that they continue to rotate without trapped in these minima in the later epoch with $H < M_\Delta$. Specifically, \tilde{e}^c is rotating almost freely with the mass term $C_3 m_0^2 |\tilde{e}^c|^2$, separated from Δ and $\bar{\Delta}$. On the other hand, the rotation of Δ and $\bar{\Delta}$ is decelerated by the negative thermal-log term, but still driven by the phase dependent quartic terms in V . The evolution of AD-flatons is then described as

$$\begin{aligned} |\Delta| &\simeq |\bar{\Delta}| \sim (H_{\text{th}}/M_\Delta)\bar{\phi}, \\ \dot{\theta}_\Delta &\sim \dot{\theta}_{\bar{\Delta}} \sim (H_{\text{th}}/M_\Delta)\sqrt{M_\Delta H}, \end{aligned} \quad (3.63)$$

$$\begin{aligned} |\tilde{e}^c| &\sim \sqrt{(M/\lambda)/M_\Delta H}, \\ \dot{\theta}_{\tilde{e}^c} &\sim m_0, \end{aligned} \quad (3.64)$$

satisfying the D -flat condition.

The lepton number asymmetry is fixed by the rotation of AD-flatons [27] as

$$\epsilon_L(t) \approx \epsilon_L \sim 0.1(t \gg m_0^{-1}) \quad (3.65)$$

with

$$n_L(t) \equiv \epsilon_L(t)[H^2(M/\lambda)], \quad (3.66)$$

where $\epsilon_L(t)$ represents the fraction of lepton number asymmetry. This asymmetry fixing can also be seen in the rate equation,

$$\begin{aligned} \frac{d\epsilon_L}{dt} &= f_{\cancel{L}} = -\frac{2}{H^2(M/\lambda)} \sum_a Q_L(a) \text{Im} \left[\phi_a \frac{\partial(V + V_{\text{th}})}{\partial \phi_a} \right] \\ &\simeq -2 \frac{(\lambda_{\cancel{L}}/\lambda)}{H^2(M/\lambda)^2} \text{Im} [2M_\Delta \Delta^* \bar{\Delta} \tilde{e}^c \tilde{e}^c] - 2 \frac{(\lambda_{\cancel{L}}/\lambda)}{H^2(M/\lambda)^2} \text{Im} [A_{\cancel{L}} m_0 \bar{\Delta} \bar{\Delta} \tilde{e}^c \tilde{e}^c]. \end{aligned} \quad (3.67)$$

According to the evolution of AD-flatons in Eqs. (3.63) and (3.64), the lepton number violating source $f_{\cancel{L}}$ decreases as $H^3/H^2 \sim 1/t$, and oscillates around zero with frequency $\sim m_0$ due to the rapid rotation of \tilde{e}^c . Hence, the lepton number ceases to fluctuate for $t \gg m_0^{-1}$ upon integration of Eq. (3.67) in time.

The evolution of AD-flatons χ_a in the case (i) of $M_\Delta > H_{\text{th}}$ ($\sim 10\text{GeV}$) is shown in Fig. 3.4, which is determined by solving numerically the equations of motion with $M_\Delta = m_0 = 10^3\text{GeV}$, $T_R = 10^5\text{GeV}$, $M/\lambda = 10^{23}\text{GeV}$ and some arbitrary values of the other parameters in the reasonable range. It is clearly seen that the scale of Δ

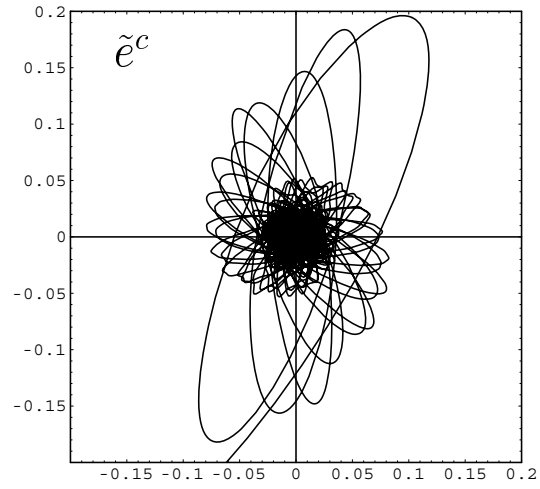
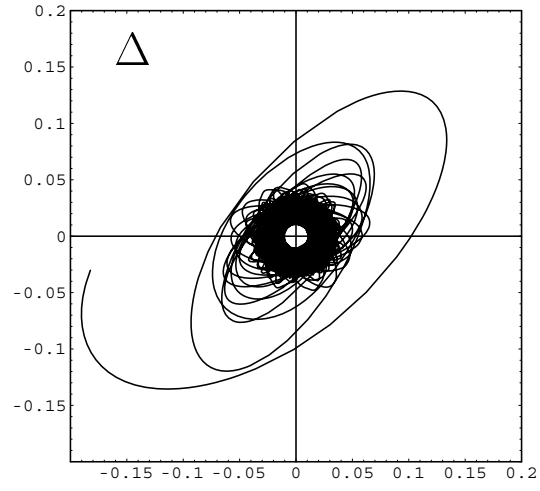
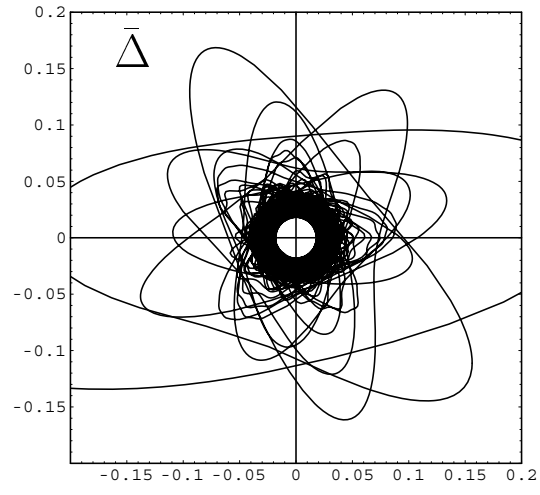


Figure 3.4: The evolution of AD-flatons χ_a in the case (i) of $M_\Delta > H_{\text{th}}$.

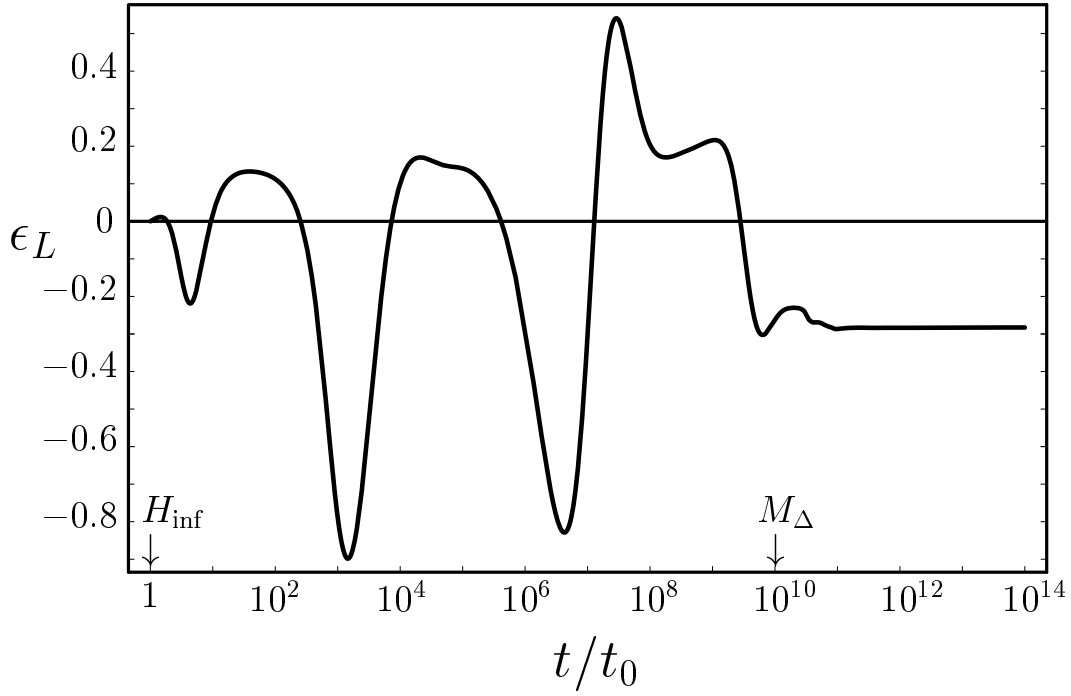


Figure 3.5: The time variation of the lepton number asymmetry in the case (i) of $M_\Delta > H_{\text{th}}$.

and $\bar{\Delta}$ trajectories is converging to $H_{\text{th}}/M_\Delta \sim 0.01$ in terms of $\chi \propto H^{1/2}$ (satisfying $|\Delta| \simeq |\bar{\Delta}|$ within errors of numerical calculation). The trajectory of \tilde{e}^c is, on the other hand, shrinking as $|\tilde{e}^c|/(HM/\lambda)^{1/2} \propto H^{1/2}$. This result confirms the expectation in Eqs. (3.63) and (3.64).

The time variation of the lepton number asymmetry is also shown in Fig. 3.5 corresponding to the evolution of AD-flatons in Fig. 3.4. This really confirms the asymmetry fixing by the redshift and rotation of AD-flatons.

In this way, the lepton-to-entropy ratio after the reheating is estimated from Eq. (3.65) as

$$\frac{n_L}{s} \sim 10^{-10} \left(\frac{\epsilon_L}{0.1} \right) \left(\frac{T_R}{10^5 \text{GeV}} \right) \left(\frac{M/\lambda}{10^{23} \text{GeV}} \right). \quad (3.68)$$

This lepton number asymmetry is converted to the baryon number asymmetry through the electroweak anomalous effect as $n_B = -(8/23)n_L$ [18, 39]. Therefore, the sufficient baryon number asymmetry can be provided for the nucleosynthesis with $\eta = (2.6 - 6.2) \times 10^{-10}$ [11] and for the cosmic microwave background $\eta = (5.9 - 6.4) \times 10^{-10}$ [16]. The condition (3.58) for the asymmetry fixing driven by the Higgs triplet mass terms can be satisfied

even for $M_\Delta \sim 1\text{TeV}$ by lowering H_{th} with larger M/λ and smaller T_R . The reheating temperature $T_R \sim 10^5\text{GeV}$ will be favorable for avoiding the gravitino problem [21, 22, 23]. The mass scale M/λ of the nonrenormalizable terms is, on the other hand, constrained as

$$M/\lambda \lesssim 10^{23}\text{GeV} \left(\frac{H_{\text{inf}}}{10^{13}\text{GeV}} \right)^{-1} \quad (3.69)$$

from the condition that the energy density of the AD-flatons does not exceed that of inflaton during the inflation as $H_{\text{inf}}^3(M/\lambda) \lesssim H_{\text{inf}}^2 M_{\text{P}}^2$.

3.4.3 Case (ii): asymmetry fixing with $M_\Delta < H_{\text{th}}$

The condition (3.58) for Higgs triplet mass driven rotation may not be satisfied with $M_\Delta \sim 1\text{TeV}$ for $T_R > 10^5\text{GeV}$ and/or $M/\lambda < 10^{23}\text{GeV}$. Then, with $H_{\text{th}} > M_\Delta$ the negative thermal-log term first dominates over the Hubble induced mass terms $H^2|\phi_a|^2$ at $H \sim H_{\text{th}}$, and after balancing with the ϕ_a^6 and ϕ_a^4 terms it soon competes with the ϕ_a^2 terms in V_1 of Eq. (3.62). The AD-flatons are already tracking the instantaneous minimum with fluctuating phases after the inflation [27]. Then, for $H \lesssim H_{\text{th}}$ this instantaneous minimum changes gradually to that of $\phi_a(1)$ in Eq. (3.60) due to the effect of thermal-log term. In this course, the phase of \tilde{e}^c is linked to those of Δ and $\bar{\Delta}$ by the quartic terms

$$\left\{ \frac{M_\Delta}{M/\lambda_{\bar{L}}} \Delta^* \bar{\Delta} + \frac{A_{\bar{L}}}{2} \frac{m_0}{M/\lambda_{\bar{L}}} \bar{\Delta} \bar{\Delta} \right\} \tilde{e}^c \tilde{e}^c. \quad (3.70)$$

For some while in this epoch $t \gtrsim H_{\text{th}}^{-1}$, these quartic terms are still larger than the mass term $\sim m_0^2 |\tilde{e}^c|^2$, and hence \tilde{e}^c together with Δ and $\bar{\Delta}$ move toward the minimum $\phi_a(1)$ with fluctuating phases:

$$|\phi_a| \sim \frac{H_{\text{th}}}{M_\Delta} \bar{\phi}, \quad \dot{\theta}_a \sim \frac{H_{\text{th}}}{M_\Delta} (M_\Delta H)^{1/2}. \quad (3.71)$$

This evolution of AD-flatons under the negative thermal-log term is characteristic in the case (ii) of $M_\Delta < H_{\text{th}}$ in contrast to the case (i) of $M_\Delta > H_{\text{th}}$.

If the Hubble parameter decreases further as

$$H < H_{\text{rot}} \sim M_\Delta \left(\frac{M_\Delta}{H_{\text{th}}} \right)^2, \quad (3.72)$$

the mass term $\sim m_0^2 |\tilde{e}^c|^2$ ($m_0 \sim M_\Delta \sim 10^3\text{GeV}$ henceforth) dominates over the quartic terms in Eq. (3.70). Then, \tilde{e}^c is liberated from Δ and $\bar{\Delta}$, and begins to rotate with

frequency $\sim m_0$. Since this rotation frequency is much larger than H in this epoch, the scaling of $|\tilde{e}^c|$ is no longer as $H^{1/2}$, but changes to H due to the friction force $3H(d\tilde{e}^c/dt)$. Accordingly, Δ and $\bar{\Delta}$ turn to move from the minimum $\phi_a(1)$ to the minimum $\phi_a(2)$.

The time variation of lepton number asymmetry is determined by this evolution of AD-flatons for $H \lesssim H_{\text{th}}$. In the transitional epoch with $H_{\text{rot}} \lesssim H \lesssim H_{\text{th}}$, according to Eq. (3.71) the lepton number asymmetry varies as

$$\epsilon_L(t) \sim \epsilon_L \left(\frac{H_{\text{th}}}{M_\Delta} \right)^2 \theta_L(t) \sin \theta_L(t) \quad (3.73)$$

with

$$\theta_L(t) \sim \theta_a(t) \sim \frac{H_{\text{th}}}{M_\Delta} \left(\frac{M_\Delta}{H} \right)^{1/2} \propto t^{1/2} \quad (3.74)$$

and $\epsilon_L \sim 0.01 - 0.1$ numerically. Hence, the lepton number asymmetry is amplified by the effect of negative thermal-log term from the preexisting asymmetry in the early epoch of $H_{\text{th}} < H < H_{\text{inf}}$.

For $H < H_{\text{rot}}$, the lepton number asymmetry is fixed by the rapid rotation of \tilde{e}^c with frequency $\sim m_0$, as in the case (i). The resultant asymmetry is given by considering the significant amplification in Eq. (3.73) as

$$\epsilon_L(t) \approx \left(\frac{H_{\text{th}}}{M_\Delta} \right)^4 \epsilon_L(t \gg H_{\text{rot}}^{-1}). \quad (3.75)$$

The evolution of AD-flatons χ_a in the case (ii) of $M_\Delta < H_{\text{th}}$ ($\sim 10^4 \text{GeV}$) is seen explicitly in Fig. 3.6, which is obtained with $M_\Delta = m_0 = 10^3 \text{GeV}$, $T_R = 10^6 \text{GeV}$, $M/\lambda = 10^{20} \text{GeV}$ and some arbitrary values of the other parameters in the reasonable. The Δ and $\bar{\Delta}$ fields first move to the minimum $\phi_a(1)$ for $H \lesssim H_{\text{th}}$, and then turn to approach the minimum $\phi_a(2)$ for $H \lesssim H_{\text{rot}}$. The \tilde{e}^c field first moves to the minimum $\phi_a(1)$ together with the Δ and $\bar{\Delta}$ fields, then it turns to decreases faster as $|\tilde{e}^c|/(MH/\lambda)^{1/2} \propto H^{1/2}$. (The trajectories end up just at the beginning of \tilde{e}^c rotation because of the limit of computer power.) This result confirms the characteristic evolution of AD-flatons in the case (ii) of $M_\Delta < H_{\text{th}}$.

The time variation of the lepton number asymmetry is also shown in Fig. 3.7 corresponding to the evolution of AD-flatons in Fig. 3.6. Here the absolute value of the asymmetry is depicted in log-scale. We really observe the amplification of asymmetry in the period of $H_{\text{rot}} \lesssim H \lesssim H_{\text{th}}$. For $H \lesssim 0.1 H_{\text{rot}}$, the asymmetry fixing is taking place

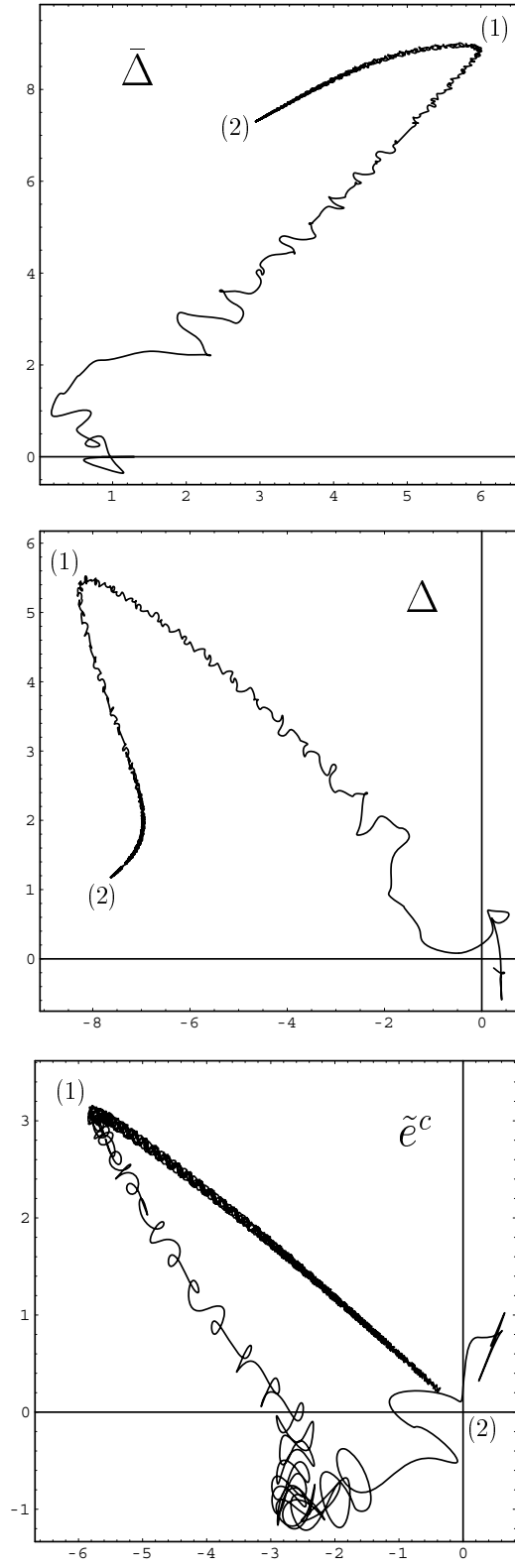


Figure 3.6: The evolution of AD-flatons χ_a in the case (ii) of $M_\Delta < H_{\text{th}}$. The minima $\phi_a(1)$ and $\phi_a(2)$ are indicated together.

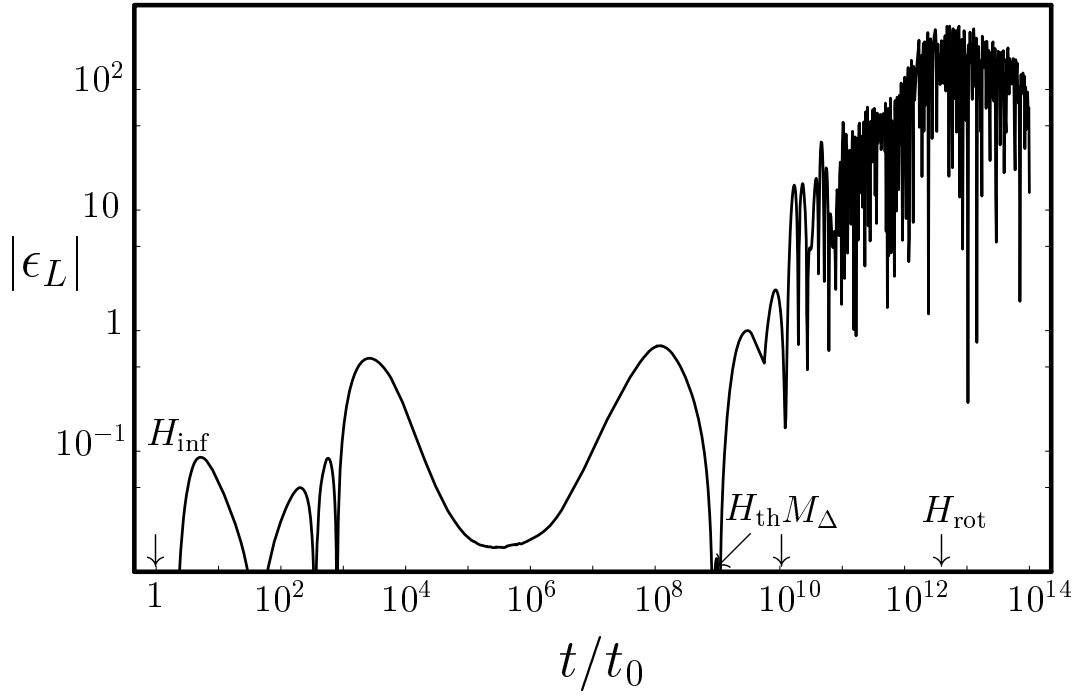


Figure 3.7: The time variation of the lepton number asymmetry in the case (ii) of $M_\Delta < H_{\text{th}}$. Here the absolute value of the asymmetry is depicted in log-scale.

by the rotation of \tilde{e}^c (though the time variation has not been traced further due to the computational limitation).

The resultant n_L/s is estimated from Eq. (3.75) as

$$\frac{n_L}{s} \sim 10^{-9} \left(\frac{\epsilon_L}{0.01} \right) \left(\frac{T_R}{10^6 \text{GeV}} \right) \left(\frac{M/\lambda}{10^{20} \text{GeV}} \right) \left(\frac{H_{\text{th}}/M_\Delta}{10} \right)^4, \quad (3.76)$$

where

$$H_{\text{th}} \sim 10^4 \text{GeV} \left(\frac{T_R}{10^6 \text{GeV}} \right) \left(\frac{M/\lambda}{10^{20} \text{GeV}} \right)^{-1/2}. \quad (3.77)$$

Therefore, even with $M_\Delta \sim 1 \text{TeV} < H_{\text{th}}$ the appropriate amount of n_L/s can be obtained for reasonable values of T_R and M/λ . Furthermore, if $H_{\text{th}} \gtrsim 10^2 M_\Delta$, much larger lepton number asymmetry will be obtained, e.g., $n_L/s \sim 10^{-5}$ with $T_R \sim 10^7 \text{GeV}$ and $M/\lambda \sim 10^{20} \text{GeV}$. Even if the asymmetry is overproduced, it may be diluted sufficiently by thermal inflation [49, 50].

3.5 Summary

We have examined the leptogenesis in the supersymmetric Higgs triplet model. The lepton number asymmetry is generated on the multi-dimensional flat manifold consisting of Δ , $\bar{\Delta}$, \tilde{e}^c . It is the essential point that several phase-dependent potential terms are provided with the superpotential terms $M_\Delta \bar{\Delta} \Delta$, $(\lambda_\ell/2M) \bar{\Delta} \bar{\Delta} e^c e^c$, $(\lambda_\Delta/2M) \bar{\Delta} \Delta \bar{\Delta} \Delta$ ($\lambda_\ell/\lambda_\Delta \sim 0.3 - 3$), which are significant for $H \sim H_{\text{inf}} - M_\Delta$. Then, soon after the inflation the lepton number asymmetry appears since the phases of AD-flatons fluctuate by the effects of such potential terms. It is slowly oscillating for a certain while, and then the leptogenesis is completed at the early time $\sim M_\Delta^{-1}$, when the AD-flatons begin to rotate around the origin due to the potential terms with Higgs triplet mass. The fraction of the resultant lepton number asymmetry amounts in general to $\epsilon_L \sim 0.1$ rather independently of M_Δ . Hence, in contrast to the usual Affleck-Dine scenario, the low-energy soft supersymmetry breaking terms have little effect on the leptogenesis. The role of the thermal effects is also different in the present scenario. The case of large Higgs triplet mass with $M_\Delta > H_{\text{th}}^{\text{max}}$ is primarily considered for the small neutrino masses. Then, the leptogenesis is completed at the early time $\sim M_\Delta^{-1}$ before the thermal effects become significant. Furthermore, even if M_Δ is rather small as in TeV region, the lepton number asymmetry really appears after the inflation via multiscalar coherent evolution of Δ , $\bar{\Delta}$ and \tilde{e}^c on the flat manifold. Then, if the Higgs triplet mass terms dominate over the negative thermal-log term for $H \sim M_\Delta$, the asymmetry is fixed readily to some significant value by the rotation of these AD-flatons with $M_\Delta \sim 1\text{TeV}$ for $T_R \sim 10^5\text{GeV}$ and $M/\lambda \sim 10^{23}\text{GeV}$. On the other hand, the negative thermal-log term may first become dominant with M_Δ as low as 1 TeV. Then, the lepton number asymmetry is amplified for some period, and fixed later by the rotation of \tilde{e}^c . Even with this amplification, the resultant lepton-to-entropy ratio can be appropriate for some reasonable values of T_R and M/λ .

Chapter 4

Right-handed neutrino model

A novel scenario of leptogenesis is investigated in the supersymmetric neutrino seesaw model. The right-handed sneutrino \tilde{N} and the ϕ field in the $\tilde{L}H_u$ direction of the slepton and Higgs doublets start together coherent evolution after the inflation with right-handed neutrino mass M_N smaller than the Hubble parameter of inflation. Then, after some period the motion of \tilde{N} and ϕ is drastically changed by the cross coupling $M_N h_\nu \tilde{N}^* \phi \phi$ from the $M_N NN$ and $h_\nu NLH_u$ terms, and the significant asymmetries of \tilde{N} and \tilde{L} are generated. The \tilde{L} asymmetry is fixed later by the thermal effects and/or the right-handed neutrino decay as the lepton number asymmetry for baryogenesis, while the \tilde{N} asymmetry disappears through the decays $\tilde{N} \rightarrow \bar{\tilde{L}}\tilde{H}_u, \tilde{L}H_u$ with almost the same rate but opposite final lepton numbers. This leptogenesis is distinctive at the point that the parameter set of h_ν and M_N can be taken as that of the mass explaining the solar and atmospheric neutrino oscillation.

4.1 Model

In the supersymmetric see-saw model, we investigate our leptogenesis scenario. The supersymmetric see-saw model motivated for the neutrino mass has a superpotential,

$$W = \frac{M_N}{2} NN + h_\nu NLH_u, \quad (4.1)$$

where N, L and H_u denote the right-handed neutrino (antineutrino strictly), the lepton doublet and the Higgs doublet superfields, respectively, and M_N is the mass matrix of the right-handed neutrino. The generation index is suppressed for simplicity. Through the

electroweak phase transition, the ordinary neutrino mass is given by

$$(m_\nu)_{ij} = \sum_k h_\nu^{ki}(M_W) h_\nu^{kj}(M_W) \frac{\langle H_u \rangle^2}{M_{N_k}}, \quad (4.2)$$

where $\langle H_u \rangle \simeq 174$ GeV. Hereafter, we take the basis that the right-handed neutrino mass is diagonal.

In the present scenario of leptogenesis, the mass of the right-handed neutrino relevant for leptogenesis must be smaller than the Hubble parameter $H_{\text{inf}} \sim 10^{13}$ GeV during the inflation. Then, the right-handed sneutrino can take very large value due to negative Hubble mass [26] or quantum fluctuation [42, 51]. On the other hand, the lightest right-handed neutrino mass M_{N_1} must be larger than the reheating temperature. Even if the lepton number asymmetry is generated in this scenario, the right-handed neutrino in thermal equilibrium washes out the lepton number asymmetry through the lepton number violating Majorana mass. Therefore, the condition $T_R < M_{N_1} < H_{\text{inf}}$ is required for the lightest right-handed neutrino mass. The lepton number asymmetry is generated via the coherent evolution of the right-handed sneutrino and the ϕ field in the $\tilde{L}H_u$, where the ϕ field is defined as D -flat configuration in $\tilde{L}H_u$,

$$\tilde{L} = \begin{pmatrix} \phi/\sqrt{2} \\ 0 \end{pmatrix}, H_u = \begin{pmatrix} 0 \\ \phi/\sqrt{2} \end{pmatrix}. \quad (4.3)$$

Hereafter, we consider one generation of \tilde{L} and \tilde{N} . In the basis that the M_N is diagonal, the largest element $h_{\nu LG}$ in the h_ν^{ij} , where the index j is taken for the right-handed sneutrino \tilde{N}_j satisfying $M_{N_j} < H_{\text{inf}}$, gives the largest potential for H_u field by $F_{H_u}^2 = |h_{\nu LG} \tilde{L} \tilde{N}|^2$ through the superpotential term $h_\nu N L H_u$. Since $\phi/\sqrt{2} = \tilde{L} = H_u$ by D flat condition, the generation of \tilde{L} with $h_{\nu LG}$ contributes ϕ field. Hence, the one generation of \tilde{L} and \tilde{N} with $h_{\nu LG}^j$ dominates the evolution of \tilde{L} 's and \tilde{N} 's even if other right-handed neutrino species satisfies $M_{N_k} < H_{\text{inf}}$. The lepton doublets are arranged with unitary transformation so that only one generation of \tilde{L}_i has the Yukawa coupling with a certain \tilde{N}_j . Hence, we choose the basis the $h_{\nu LG}$ is given by one generation of L and \tilde{N} . Since $\phi/\sqrt{2} = \tilde{L} = H_u$ by D flat condition, the generation of \tilde{L} with $h_{\nu LG}$ give almost all contribution to ϕ field. Hence, the one generation of \tilde{L} and \tilde{N} with $h_{\nu LG}$ dominates the evolution of \tilde{L} 's and \tilde{N} 's even if other right-handed neutrino species satisfies $M_{N_k} < H_{\text{inf}}$. Henceforth, we take the basis that $h_{\nu LG}$ is given by one generation of L and \tilde{N} and abbreviate $h_{\nu LG}$ as h_ν .

With very large value of right-handed sneutrino, some nonrenormalizable terms can be comparable to renormalizable terms. Hence, we include definitely the following non-renormalizable term,

$$W_{\text{non}} = \frac{e^{i\delta_N}}{4M} NNNN \quad (4.4)$$

where M represents very large mass scale such as Planck scale and the phase factor $e^{i\delta_N}$ is included with real M_N . The NNN term is discarded for simplicity by requiring the R parity. The $LH_u LH_u$ term is not considered either, since it does not provide a significant effect if the Yukawa coupling h_ν is not extremely small. If these terms are involved, our scenario of leptogenesis does not change substantially. As seen in later sections, we take $h_\nu = 2 \times 10^{-2}, 3 \times 10^{-3}$ for large and small h_ν value, respectively. Then, its value at the electroweak scale is evaluated as $h_\nu(M_W) \simeq 1.8 \times 10^{-2}, 2.8 \times 10^{-3}$ by considering the renormalization group effects given in Chap. 6. The ordinary neutrino masses with these $h_\nu(M_W)$ via seesaw mechanism are roughly estimated

$$m_\nu \sim \frac{h_\nu(M_W)^2 \langle H_u \rangle^2}{M_N} \quad (4.5)$$

$$\sim 10^{-1} \text{eV} \left(\frac{h_\nu(M_W)}{2 \times 10^{-2}} \right)^2 \left(\frac{10^{11} \text{GeV}}{M_N} \right) \quad (\text{large } h_\nu) \quad (4.6)$$

$$\sim 10^{-3} \text{eV} \left(\frac{h_\nu(M_W)}{3 \times 10^{-3}} \right)^2 \left(\frac{10^{11} \text{GeV}}{M_N} \right) \quad (\text{small } h_\nu) \quad (4.7)$$

depending on $h_\nu(M_W)$ and M_N . (The neutrino mixing is present in general with matrix form of h_ν .) Hence, the leptogenesis in the large h_ν case may be explained by the attractive mass scale of the atmospheric neutrino mass or solar one [2, 3, 4]. On the other hand, the neutrino mass relevant for the leptogenesis in the small h_ν case should be identified with the lightest one. It is interesting that the lightest neutrino mass is expected to be $m_\nu \sim 10^{-3}$ eV for the present leptogenesis, while $m_\nu \sim 10^{-9}$ eV is required for the conventional Affleck-Dine leptogenesis in the $\tilde{L}H_u$ flat direction.

4.2 multiscalar leptogenesis

The evolution of the scalar fields is governed by the equation of motion,

$$\ddot{\psi}_a + (3H + \Gamma_a)\dot{\psi}_a + \frac{\partial V}{\partial \psi_a^*} = 0 \quad (4.8)$$

where $\psi_a = \tilde{N}, \phi$. The decay rate Γ_a is included to consider effects of the right-handed sneutrino decay,

$$\begin{aligned}\Gamma_{\tilde{N}_i} &\simeq \frac{1}{4\pi} \sum_a (h_\nu^{ia})^2 M_{N_i}, \\ \Gamma_\phi &\ll H. \quad (H > m_{3/2})\end{aligned}\tag{4.9}$$

The decay of the ϕ field is negligible in the region that we consider. The Hubble parameter varies in time as $H = (2/3)t^{-1}$ in the matter-dominated universe, which the coherent oscillation of the inflaton dominates the energy density of the universe after the inflation. The scalar potential V is given by

$$\begin{aligned}V &= -c_N H^2 |\tilde{N}|^2 - c_\phi H^2 |\phi|^2 \\ &\quad + \left| M_N \tilde{N} + \frac{e^{i\delta_N}}{M} \tilde{N} \tilde{N} \tilde{N} + \frac{h_\nu}{2} \phi \phi \right|^2 + h_\nu^2 |\tilde{N}|^2 |\phi|^2 \\ &\quad + H \left(b_N \frac{M_N}{2} \tilde{N} \tilde{N} + a_N \frac{e^{i\delta_N}}{4M} \tilde{N} \tilde{N} \tilde{N} \tilde{N} + \text{h.c.} \right) \\ &\quad + H \left(a_h \frac{h_\nu}{2} \tilde{N} \phi \phi + \text{h.c.} \right) + V_{\text{th}}(\phi).\end{aligned}\tag{4.10}$$

The soft supersymmetry breaking terms with Hubble parameter H are induced by the nonzero energy density in the early universe. The thermal terms [46, 47] are also included in $V_{\text{th}}(\phi)$. The D^2 terms are vanishing for the ϕ field. The low-energy soft supersymmetry breaking terms with m_0 is irrelevant for the leptogenesis.

4.2.1 Large coupling : $h_\nu \gtrsim \sqrt{H_{\text{inf}}/M}$

First, we investigate the larger h_ν case. For this large h_ν , the evolution of the scalar fields starts as one dimensional motion of \tilde{N} since the ϕ field has large effective mass $h_\nu^2 |\tilde{N}|^2 |\phi|^2$. In large h_ν case, this coupling can be relevant to the operator responsible for the atmospheric or solar neutrino mass difference.

(i) Inflation epoch: $H = H_{\text{inf}}$

During the inflation, the Hubble parameter takes almost a constant value $H = H_{\text{inf}}$. (We henceforth take $H = 10^{13}$ GeV, typically.) Accordingly, the scalar fields settle into one of the minima of V with $H = H_{\text{inf}}$:

$$\phi(t_0) = 0,\tag{4.11}$$

$$\tilde{N}(t_0) = e^{i\theta_{\tilde{N}}} r_{\tilde{N}} \sqrt{H_{\text{inf}} M},\tag{4.12}$$

where $r_{\tilde{N}} \sim 0.1 - 1$ depending on c_N, a_N and δ_N . In large h_ν , the effective mass for ϕ through the quartic term $h_\nu^2 |\tilde{N}|^2 |\phi|^2$ dominates over the negative Hubble mass term $-c_\phi H^2 |\phi|^2$, then the minimum is $\phi = 0$. However, the nonzero quantum fluctuation of ϕ exists, which is given by

$$\langle \phi \rangle^2 \sim \frac{H_{\text{inf}}^4}{h_\nu^2 |\tilde{N}|^2}. \quad (4.13)$$

This nonzero value of ϕ by quantum fluctuation is necessary for ϕ to develop large value at later stage. The quantum fluctuation of \tilde{N} is much smaller than the value of (4.12).

(ii) Oscillation epoch: $H_{\text{inf}} > H > H_{\text{tr}}$

After the inflation, the Hubble parameter decrease as $H = (2/3)t^{-1}$ in the inflaton coherent oscillation dominated universe, that is, the matter-dominated universe. During this epoch the evolution of the scalar fields stays one dimensional. The right-handed sneutrino is scaled roughly as

$$\tilde{N} = e^{i\theta_{\tilde{N}}} r_{\tilde{N}}(t) \sqrt{H_{\text{inf}} M} \left(\frac{H}{H_{\text{inf}}} \right)^{1/2}. \quad (4.14)$$

The higher order potential terms suppressed by M are soon reduced by redshift, and the mass term of \tilde{N} dominates over the negative Hubble term at $H \sim M_N$. Then, driven by this mass terms the coherent oscillation (rotation strictly) of \tilde{N} starts. For $H \lesssim M_N$, the magnitude of the right-handed sneutrino oscillation is found to be scaled by redshift as

$$\tilde{N} = e^{i\theta_{\tilde{N}}(t)} r_{\tilde{N}}(t) \sqrt{M_N M} \left(\frac{H}{M_N} \right). \quad (4.15)$$

The phase of \tilde{N} does not stay constant any longer by phase dependent terms. The number asymmetry for scalar fields is defined as

$$n_{\psi_a} \equiv i(\psi_a^* \dot{\psi}_a - \dot{\psi}_a^* \psi_a) = \dot{\theta}_a |\psi_a|^2 \quad (4.16)$$

where dot represents a time derivative and θ_a is the phase of ϕ_a . Since nonzero time derivative of $\theta_{\tilde{N}}$ is derived through phase dependent terms i.e. $\dot{\theta}_{\tilde{N}} \neq 0$, the asymmetry of \tilde{N} appears. The B -term $b_N M_N H \tilde{N} \tilde{N}$ dominates phase dependent terms soon since the redshift of this term is the slowest in the phase dependent terms, which B -term $\propto H^3$ and other phase dependent terms $\propto H^4$. Hence, for this epoch the \tilde{N} oscillates slowly in $\ln t$ as investigated in the next subsection.

(iii) **Transition epoch:** $H_{\text{tr}} \gtrsim H > \Gamma_{\tilde{N}}$

Since the magnitude of \tilde{N} decreases with H as given in Eq. (4.15), the cross coupling $h_\nu M_N \tilde{N}^* \phi \phi$ from the $M_N N N$ and $h_\nu N L H_u$ become comparable to the quartic coupling $h_\nu^2 |\tilde{N}|^2 |\phi|^2$ with $|\tilde{N}| \sim M_N/h_\nu$ at $H = H_{\text{tr}}$. Here, H_{tr} is estimated as,

$$H_{\text{tr}} \simeq 10^8 \text{GeV} \left(\frac{M_N}{10^{11} \text{GeV}} \right)^{3/2} \left(\frac{10^{20} \text{GeV}}{M} \right)^{1/2} \left(\frac{2 \times 10^{-2}}{h_\nu} \right). \quad (4.17)$$

The minimum of potential become $\phi \neq 0$ if the phase dependent cross coupling dominates over thermal mass terms. Then, we study thermal mass terms at $H \sim H_{\text{tr}}$. The dominant part of thermal potential is given by

$$V_{\text{th1}} = (y T_p)^2 |\phi|^2 \quad (4.18)$$

where $y = h_t \sim 1$ is the top quark Yukawa coupling since the top quark is satisfied with the condition $y|\phi| < T_p$ with small $\phi \ll T_p$ [46]. The temperature T_p of the dilute plasma of inflaton decay products is given in terms of the reheating temperature T_R of the universe when the inflaton decay is completed:

$$T_p \sim (T_R^2 H M_P)^{1/4}, \quad (4.19)$$

where $M_P = 2.4 \times 10^{18} \text{GeV}$ is the reduced Planck mass. The condition that the cross coupling $M_N h_\nu \tilde{N}^* \phi \phi$ dominates over the thermal mass term $T_p^2 |\phi|^2$ at $H \sim H_{\text{tr}}$ is roughly given by

$$M_N > 3 \times 10^{10} \text{GeV} \left(\frac{T_R}{10^8 \text{GeV}} \right)^{4/5} \left(\frac{10^{20} \text{GeV}}{M} \right)^{1/5} \left(\frac{2 \times 10^{-2}}{h_\nu} \right)^{2/5}. \quad (4.20)$$

After the ϕ field develops large value, $|\phi| \sim M_N/h_\nu \gg T_p$, the masses of top quark and stop are much larger than T_p and decouple from thermal plasma. Then, thermal terms become negligibly small compared to the cross coupling term $M_N h_\nu \tilde{N}^* \phi \phi$ for $H_{\text{th}} < H < H_{\text{tr}}$.

Here, if accurately $\phi = 0$ for $H > H_{\text{tr}}$, the ϕ field stays the origin. However, quantum fluctuation exists, hence, ϕ has nonzero value for $H > H_{\text{tr}}$. As a result, ϕ has a new potential minimum,

$$\phi^2 \simeq \frac{-2M_N}{h_\nu} \tilde{N}, \quad (4.21)$$

which is provided by the phase dependent cross coupling term, $M_N h_\nu \tilde{N}^* \phi \phi$. For $H < H_{\text{tr}}$, \tilde{N} oscillates for the radial direction and rotates for the angular direction in the potential $V = M_N^2 |\tilde{N}|^2 + M_N h_\nu \tilde{N}^* \phi \phi + \text{H.c.}$. Then, the magnitude of the coherent oscillation of the radial direction decreases as $\tilde{N} \propto H$. Consequently, the magnitude of the scalar fields decrease as

$$|\tilde{N}(t)| = r_{\tilde{N}}(t) \frac{M_N}{h_\nu} \left(\frac{H}{H_{\text{tr}}} \right), \quad (4.22)$$

$$|\phi(t)| = r_\phi(t) \frac{M_N}{h_\nu} \left(\frac{H}{H_{\text{tr}}} \right)^{1/2}, \quad (4.23)$$

with $|F_N| \sim |F_\phi| \propto H^{3/2}$. Here, the cross coupling $M_N h_\nu \tilde{N}^* \phi \phi$ is dependent on the phases of \tilde{N} and ϕ and does not conserve the number of \tilde{N} and ϕ , either. Accordingly, through this drastic change in the multiscale coherent evolution, the significant asymmetries of \tilde{N} and \tilde{L} appear, which is really seen in the rate equations

$$\begin{aligned} \frac{d}{dt} \left(\frac{n_{\tilde{N}}}{H^2} \right) &\simeq -\frac{2}{H^2} \text{Im}[b_N M_N H \tilde{N} \tilde{N}] \\ &\quad -\frac{2}{H^2} \text{Im} \left[M_N \tilde{N} F_N^* + \frac{a_h h_\nu}{2} H \tilde{N} \phi \phi \right], \end{aligned} \quad (4.24)$$

$$\frac{d}{dt} \left(\frac{n_{\tilde{L}}}{H^2} \right) \simeq -\frac{2}{H^2} \text{Im} \left[\frac{h_\nu}{2} \phi \phi F_N^* + \frac{a_h h_\nu}{2} H \tilde{N} \phi \phi \right] \quad (4.25)$$

with $n_{\tilde{L}} = n_{H_u} = n_\phi/2$. The main lepton number generating sources are scaled as $\text{Im}[(h_\nu/2)\phi\phi F_N^*]/H^2 \simeq -\text{Im}[M_N \tilde{N} F_N^*]/H^2 \propto H^{5/2}/H^2$ with $|F_N| \propto H^{3/2}$, and hence the asymmetries $n_{\tilde{N}}$ and $n_{\tilde{L}}$ oscillate rapidly by the exchange $\tilde{N} \leftrightarrow \tilde{L}$. The sum $n_{\tilde{N}} + n_{\tilde{L}}$, however, varies rather moderately with the remaining sources $\propto H^3$, since the main sources are cancelled as $\text{Im}[F_N F_N^*] = 0$ with $F_N \simeq M_N \tilde{N} + (h_\nu/2)\phi\phi$.

(iv) Completion epoch: $\Gamma_{\tilde{N}} \gtrsim H \gg m_{3/2}$

For completion of the leptogenesis, we consider the decay effect of the right-handed sneutrino. The incoherent decay of \tilde{N} become significant with the dominant modes

$$\tilde{N} \rightarrow \bar{L} \tilde{H}_u [L = -1], \quad \tilde{L} H_u [L = +1], \quad (4.26)$$

where the decay products are ultra-relativistic with $h_\nu |\tilde{N}| \ll M_N/2$. The \tilde{N} decays at $H \sim \Gamma_{\tilde{N}}$, where $\Gamma_{\tilde{N}}$ is given by

$$\Gamma_{\tilde{N}} = \frac{h_\nu^2 M_N}{4\pi} \simeq 3 \times 10^6 \text{ GeV} \left(\frac{h_\nu}{2 \times 10^{-2}} \right)^2 \left(\frac{M_N}{10^{11} \text{ GeV}} \right). \quad (4.27)$$

The decay works as strong friction to the evolution of \tilde{N} as seen in Eq. (4.8). Hence, by this strong friction \tilde{N} is linked to ϕ , tracking the instantaneous minimum of V as $\tilde{N} = -(h_\nu/2M_N)\phi\phi$, then $|F_N| \sim 0 \ll |F_\phi| = h_\nu|\tilde{N}||\phi|$. Therefore, in the rate equations (4.41) and (4.42), the main lepton number generating source terms $M_N\tilde{N}F_N^*$ and $h_\nu\phi\phi F_N^*/2$ vanish.

The evolution of the phase is $d\theta_{\tilde{N}}/dt \simeq 2d\theta_\phi/dt \propto H$ since $n_\phi \simeq \dot{\theta}_\phi|\phi|^2$ is redshifted as $n_\phi \propto H^2$. Then, the \tilde{N} asymmetry remaining after the transition epoch diminishes rapidly through the decays as $n_{\tilde{N}} = 2(d\theta_{\tilde{N}}/dt)|\tilde{N}|^2 \propto H^3$. It is the essential point that the decay modes (4.26) have almost the same rate $\Gamma_{\tilde{N}}/2$ but the opposite final lepton numbers $L = \pm 1$. This means that the \tilde{N} asymmetry does not leave any significant lepton number asymmetry.

In this way, the \tilde{L} asymmetry is fixed to some significant value as the lepton number asymmetry for $t > \min[\Gamma_{\tilde{N}}^{-1}, H_{\text{th}}^{-1}]$,

$$n_{\tilde{L}} \simeq n_L \equiv \epsilon_L[(3/2)H^2M]. \quad (4.28)$$

This concludes that the thermal effect plays the positive role for the completion of leptogenesis, which is in salient contrast to the conventional Affleck-Dine mechanism where the thermal effect rather suppresses the asymmetry seriously.

The resultant lepton-to-entropy ratio after the reheating is completed is estimated with $s \simeq 3H_R^2 M_{\text{P}}^2/T_R$ as

$$\frac{n_L}{s} \sim 10^{-10} \left(\frac{\epsilon_L}{0.1} \right) \left(\frac{M}{10^{20} \text{GeV}} \right) \left(\frac{T_R}{10^8 \text{GeV}} \right). \quad (4.29)$$

Here the reheating temperature is restricted as $T_R \lesssim 10^8 - 10^{10} \text{GeV}$ to avoid the gravitino problem [21, 22]. The lepton number asymmetry is converted to the baryon number asymmetry through the electroweak anomalous effect as $n_B/s = -(8/23)n_L/s$ [39]. Hence, the sufficient baryon-to-entropy ratio can be provided for the nucleosynthesis and cosmic microwave background radiation with $\eta \simeq 6 \times 10^{-10}$ [11, 16].

4.2.2 Small coupling : $h_\nu \lesssim \sqrt{H_{\text{inf}}/M}$

Then, we discuss the smaller h_ν case, which is studied in our previous paper [29]. In this case, the \tilde{N} and ϕ fields together start coherent evolution with large initial field values after the inflation.

(i) Inflation epoch: $H = H_{\text{inf}}$

During the inflation, the scalar fields settle into one of the minima of V with almost constant Hubble parameter $H = H_{\text{inf}}$,

$$\phi(t_0) = e^{i\theta_\phi} r_\phi H_{\text{inf}}/h_\nu, \quad (4.30)$$

$$\tilde{N}(t_0) = e^{i\theta_{\tilde{N}}} r_{\tilde{N}} \sqrt{H_{\text{inf}} M}, \quad (4.31)$$

where $r_a \sim 0.1 - 1$ depending on c_a, a_N, δ_N and h_ν . This value of \tilde{N} is much larger than that of the quantum fluctuation (4.13). If $h_\nu < (H_{\text{inf}}/M)^{1/2}$, the initial values of $|\phi|$ and $|\tilde{N}|$ become much larger. However, these large values are due to an absence of a nonrenormalizable superpotential term $LLH_u H_u/M_\ell$, where M_ℓ is the Planck mass or a right-handed neutrino mass with $M_{N_i} > H_{\text{inf}}$. With an existence of this term, $\phi(t_0)$ can not develop far beyond $|\phi| \sim \sqrt{H_{\text{inf}} M_\ell}$. We take h_ν as typical value for definition,

$$h_\nu \sim 3 \times 10^{-3} \left(\frac{H_{\text{inf}}}{10^{13} \text{GeV}} \right)^{1/2} \left(\frac{M}{10^{18} \text{GeV}} \right)^{1/2}. \quad (4.32)$$

We will discuss the difference between this h_ν and smaller h_ν . When we use smaller h_ν , we will specifically point out below.

(ii) Oscillation epoch: $H_{\text{inf}} > H > H_{\text{tr}}$

After the inflation the Hubble parameter decreases as $H = (2/3)t^{-1}$ in the matter dominated universe, and the multiscalar coherent evolution of \tilde{N} and ϕ starts with the initial condition $(\tilde{N}, \phi) = (\tilde{N}_0, \phi_0)$ at $t = t_0 \sim H_{\text{inf}}^{-1}$, as given in Eqs. (4.30) and (4.31). The higher order potential terms suppressed by M are soon reduced by redshift, and the quartic couplings $h_\nu^2 |\phi|^4$ and $h_\nu^2 |\tilde{N}|^2 |\phi|^2$ dominate the scalar potential (4.10) in this epoch with h_ν as given in Eq. (4.32). Then, driven by these quartic couplings, the scalar fields oscillate in magnitude with scaling by redshift as

$$|\phi(t)| \sim |\tilde{N}(t)| \sim \sqrt{H_{\text{inf}} M} \left(\frac{H}{H_{\text{inf}}} \right)^{2/3}. \quad (4.33)$$

The field phases, however, remain almost constant except for the vicinities of $\tilde{N} = 0$ and $\phi = 0$, and the significant asymmetries of \tilde{N} and \tilde{L} do not appear in this epoch.

If smaller h_ν case $h_\nu < (H_{\text{inf}}/M)^{1/2}$, the scalar fields track the decreasing instantaneous minima,

$$\psi_a(t) = e^{i\theta_a} r_a \sqrt{HM}. \quad (4.34)$$

until $H = H_{\text{osc}} \equiv h_\nu^2 M$. The quartic terms dominate the scalar potential at $H \sim h_\nu^2 M$ and coherent oscillations start. After coherent oscillations start, the evolutions of the scalar fields are given by

$$|\phi(t)| \sim |\tilde{N}(t)| \sim \sqrt{H_{\text{osc}} M} \left(\frac{H}{H_{\text{osc}}} \right)^{2/3}. \quad (4.35)$$

(iii) Transition epoch: $H_{\text{tr}} \gtrsim H > H_{\text{th}}$

Since \tilde{N} and ϕ decrease with H as given in Eq. (4.33), the mass term $M_N^2 |\tilde{N}|^2$ and $M_N h_\nu \tilde{N}^* \phi \phi$ become comparable to the quartic couplings $h_\nu^2 |\phi|^4$ and $h_\nu^2 |\tilde{N}|^2 |\phi|^2$ with $|\tilde{N}| \sim |\phi| \sim M_N/h_\nu$ and the Hubble parameter

$$H_{\text{tr}} \sim 10^{10} \text{GeV} \left(\frac{h_\nu}{3 \times 10^{-3}} \right)^{-3/2} \left(\frac{10^{19} \text{GeV}}{M} \right)^{-3/4} \left(\frac{M_N}{10^{11} \text{GeV}} \right)^{3/2}. \quad (4.36)$$

where $h_\nu \sim (H_{\text{inf}}/M)^{1/2}$ with $H_{\text{inf}} = 10^{13} \text{GeV}$ is taken from Eq. (4.32). The thermal mass term should also be considered at $H \sim H_{\text{tr}}$, which is given by $(yT_p)^2 |\phi|^2$ with relevant coupling y under the condition $y|\phi| < T_p$ [?]. The temperature T_p of the dilute plasma of inflaton decay products is given in terms of the reheating temperature T_R of the universe after the inflaton decay is completed:

$$T_p \sim (T_R^2 H M_P)^{1/4}, \quad (4.37)$$

where $M_P = 2.4 \times 10^{18} \text{GeV}$ is the reduced Planck mass. The thermal mass is constrained at $H \sim H_{\text{tr}}$ as $yT_p < T_p^2/|\phi| \sim h_\nu T_p^2/M_N$ for $y|\phi| < T_p$ with $|\tilde{N}| \sim |\phi| \sim M_N/h_\nu$. Hence, the thermal mass term $(yT_p)^2 |\phi|^2$ is smaller than the $M_N^2 |\tilde{N}|^2$ and $M_N h_\nu \tilde{N}^* \phi \phi$ terms at $H \sim H_{\text{tr}}$ for the right-handed neutrino mass

$$M_N \gtrsim 10^9 \text{GeV} \left(\frac{h_\nu}{10^{-3}} \right)^{2/5} \left(\frac{10^{19} \text{GeV}}{M} \right)^{1/5} \left(\frac{T_R}{10^9 \text{GeV}} \right)^{4/5}. \quad (4.38)$$

In this situation, the $M_N^2 |\tilde{N}|^2$ and $M_N h_\nu \tilde{N}^* \phi \phi$ terms as well as the $h_\nu^2 |\phi|^4$ term dominate for $H \lesssim H_{\text{tr}}$, so that the motion of \tilde{N} and ϕ is changed drastically. Specifically, the

\tilde{N} field oscillates mainly driven by the mass term $M_N^2|\tilde{N}|^2$ with $|\tilde{N}| \propto H$. The motion of ϕ follows after \tilde{N} toward the new stable configuration with $(h_\nu/2)\phi\phi \simeq -M_N\tilde{N}$ so as to make $|F_N|^2 \sim |F_\phi|^2 \ll M_N^2|\tilde{N}|^2$ in V , where $F_N \simeq M_N\tilde{N} + (h_\nu/2)\phi\phi$ and $F_\phi = h_\nu\tilde{N}\phi$. Consequently, the scalar fields decrease roughly as

$$|\tilde{N}| \sim \frac{M_N}{h_\nu} \left(\frac{H}{H_{\text{tr}}} \right) \propto H, \quad (4.39)$$

$$|\phi| \sim \frac{M_N}{h_\nu} \left(\frac{H}{H_{\text{tr}}} \right)^{1/2} \propto H^{1/2}. \quad (4.40)$$

with $|F_N| \sim |F_\phi| \propto H^{3/2}$. Through this drastic change in the multiscalar coherent evolution, the significant asymmetries of \tilde{N} and \tilde{L} appear, which is really seen in the rate equations

$$\begin{aligned} \frac{d}{dt} \left(\frac{n_{\tilde{N}}}{H^2} \right) &\simeq -\frac{2}{H^2} \text{Im}[b_N M_N H \tilde{N} \tilde{N}] \\ &\quad -\frac{2}{H^2} \text{Im} \left[M_N \tilde{N} F_N^* + \frac{a_h h_\nu}{2} H \tilde{N} \phi \phi \right], \end{aligned} \quad (4.41)$$

$$\frac{d}{dt} \left(\frac{n_{\tilde{L}}}{H^2} \right) \simeq -\frac{2}{H^2} \text{Im} \left[\frac{h_\nu}{2} \phi \phi F_N^* + \frac{a_h h_\nu}{2} H \tilde{N} \phi \phi \right] \quad (4.42)$$

with $n_{\tilde{L}} = n_{H_u} = n_\phi/2$. As seen in large h_ν case, the main sources are scaled as $\text{Im}[(h_\nu/2)\phi\phi F_N^*]/H^2 \simeq -\text{Im}[M_N \tilde{N} F_N^*]/H^2 \propto H^{5/2}/H^2$ with $|F_N| \propto H^{3/2}$, and hence the asymmetries $n_{\tilde{N}}$ and $n_{\tilde{L}}$ oscillate rapidly by the exchange $\tilde{N} \leftrightarrow \tilde{L}$. The sum $n_{\tilde{N}} + n_{\tilde{L}}$, however, varies rather moderately with the remaining sources $\propto H^3$, since the main sources are cancelled as $\text{Im}[F_N F_N^*] = 0$ with $F_N \simeq M_N \tilde{N} + (h_\nu/2)\phi\phi$.

Here, the $M_N h_\nu \tilde{N}^* \phi \phi$ violates the lepton number. Accordingly, the lepton number asymmetry appear during this epoch. Through this drastic change in the multiscalar coherent evolution, the significant asymmetries of \tilde{N} and \tilde{L} appear, which is really seen in the rate equations. with $n_{\tilde{L}} = n_{H_u} = n_\phi/2$. The main sources are scaled as $\text{Im}[(h_\nu/2)\phi\phi F_N^*]/H^2 \simeq -\text{Im}[M_N \tilde{N} F_N^*]/H^2 \propto H^{5/2}/H^2$ with $|F_N| \propto H^{3/2}$, and hence the asymmetries $n_{\tilde{N}}$ and $n_{\tilde{L}}$ oscillate rapidly by the exchange $\tilde{N} \leftrightarrow \tilde{L}$. The sum $n_{\tilde{N}} + n_{\tilde{L}}$, however, varies rather moderately with the remaining sources $\propto H^3$, since the main sources are cancelled as $\text{Im}[F_N F_N^*] = 0$ with $F_N \simeq M_N \tilde{N} + (h_\nu/2)\phi\phi$.

(iv) Completion epoch: $H_{\text{th}} \gtrsim H \gg m_{3/2}$

After the transition epoch continues for some period, the thermal log term [47] may eventually dominates the evolution of ϕ before the right-handed sneutrino decay at $H =$

$\Gamma_{\tilde{N}}$. The thermal log term is mainly given by

$$V_{\text{th2}} = a_{\text{th}} \alpha_s^2 T_{\text{p}}^4 \ln(|\phi|^2/T_{\text{p}}^2) \quad (4.43)$$

($a_{\text{th}} = 9/8$) through the modification of $\text{SU}(3)_C$ coupling due to the decoupling of top quark from the plasma with large mass $h_t|\phi|/\sqrt{2} > T_{\text{p}}$. This thermal log term provides the effective mass term for the ϕ field giving $(a_{\text{th}} \alpha_s^2 T_{\text{p}}^4/|\phi|^2)\phi \propto H^{1/2}$ in $\partial V/\partial \phi^*$. This mass dominates over the term $F_N h_\nu \phi^* \propto H^2$ in $\partial V/\partial \phi^*$ ($|F_N| \sim |F_\phi| = h_\nu |\tilde{N}| |\phi|$) when the Hubble parameter is

$$H_{\text{th}} \sim 10^5 \text{GeV} \left(\frac{h_\nu}{2 \times 10^{-2}} \right)^{-1/3} \left(\frac{M_N}{10^{11} \text{GeV}} \right)^{-1/6} \left(\frac{T_{\text{R}}}{10^8 \text{GeV}} \right)^{4/3} \left(\frac{M}{10^{20} \text{GeV}} \right)^{-5/6}. \quad (4.44)$$

Then, the accelerating rotation of the ϕ field phase compensates the decreasing value of the field by this thermal log term as

$$|\phi| \propto H^{1/2} \rightarrow H^{3/2} \quad (4.45)$$

while keeping $|\tilde{N}| \propto H$. After a while the top quark enters the plasma at $H \sim 0.1 H_{\text{th}}$ with $|\phi| \sim T_{\text{p}}$ ($h_t \simeq 1$). Then, the thermal mass term $h_t^2 T_{\text{p}}^2 |\phi|^2$ dominates the scalar potential, and the ϕ field decreases as $|\phi| \propto H^{7/8}$. In the transition epoch, the significant exchange of asymmetries $n_{\tilde{N}} \leftrightarrow n_{\tilde{L}}$ has appeared through the \tilde{N} - ϕ couplings. This couplings is actually turned off in this epoch with the rapid decrease of $|\phi| \propto H^{3/2}$ and $H^{7/8}$ later due to the thermal terms, and the ϕ and \tilde{N} evolve almost independently. As a result, the \tilde{L} violating sources in Eq. (4.42) decreases fast enough as H^4/H^2 and $H^{11/4}/H^2$ later with rapidly varying phase of $\tilde{N}^* \phi \phi$.

In this way, the \tilde{L} asymmetry is fixed to some significant value as the lepton number asymmetry for $t > H_{\text{th}}^{-1}$,

$$n_{\tilde{L}} \simeq n_L \equiv \epsilon_L [(3/2) H^2 M], \quad (4.46)$$

since the \tilde{L} violating sources in Eq. (4.42) decreases fast enough as H^4/H^2 and $H^{11/4}/H^2$ later with rapidly varying phase of $\tilde{N}^* \phi \phi$. This concludes that the thermal effect plays the positive role for the completion of leptogenesis, which is in salient contrast to the conventional Affleck-Dine mechanism where the thermal effect rather suppresses the asymmetry seriously. The resultant lepton-to-entropy ratio after the reheating is estimated with $s \simeq 3 H_{\text{R}}^2 M_{\text{P}}^2 / T_{\text{R}}$ as

$$\frac{n_L}{s} \sim 10^{-10} \left(\frac{\epsilon_L}{1} \right) \left(\frac{M}{10^{18} \text{GeV}} \right) \left(\frac{T_{\text{R}}}{10^9 \text{GeV}} \right). \quad (4.47)$$

The lepton number asymmetry is converted to the baryon number asymmetry through the electroweak anomalous effect, then, the sufficient baryon-to-entropy ratio can be provided in small h_ν case.

The motion of \tilde{N} after the decoupling from ϕ for $H < H_{\text{th}} \ll M_N$ is determined by the $M_N^2 |\tilde{N}|^2$ and $b_N H M_N \tilde{N} \tilde{N}$ terms, and the analytic solution is obtained in a good approximation with $H \ll M_N$ for the two eigenmodes $\eta_R(t)$ and $\eta_I(t)$ in $\tilde{N}(t)$ as

$$\eta_{R,I}(t) \simeq \bar{\eta}_{R,I} \cos [M_N t + \sigma_{R,I}(|b_N|/3) \ln t + \delta_{R,I}] \quad (4.48)$$

with $\sigma_R = +1$, $\sigma_I = -1$, and

$$\tilde{N} \equiv H(M/M_N)^{1/2} (b_N/|b_N|)^{-1/2} (\eta_R + i\eta_I). \quad (4.49)$$

The parameters $\bar{\eta}_{R,I}$ and $\delta_{R,I}$ are determined as the result of \tilde{N} motion from $t = t_0 \sim H_{\text{inf}}^{-1}$ through $t > H_{\text{th}}^{-1} \gg M_N^{-1}$. The \tilde{N} asymmetry is evaluated with Eqs. (4.48) and (4.49) as

$$n_{\tilde{N}}(t) \simeq -2H^2 M \bar{\eta}_R \bar{\eta}_I \cos[(2|b_N|/3) \ln t + \delta_R - \delta_I], \quad (4.50)$$

where the rapid oscillations of η_R and η_I with $M_N t$ in Eq. (4.48) are cancelled.

This \tilde{N} asymmetry oscillates slowly in $\ln t$ for some while due to the b_N term, as seen in Eq. (4.50). Then, the incoherent decays of \tilde{N} become significant with the dominant modes where the decay products are ultra-relativistic with $h_\nu |\tilde{N}| \ll M_N/2$. The motion of \tilde{N} is significantly decelerated by these \tilde{N} decays at $H \sim \Gamma_{\tilde{N}} \simeq (h_\nu^2/4\pi) M_N$ ($\sim 10^5 \text{ GeV}$ numerically), so that it is linked again to ϕ , tracking the instantaneous minimum of V as $\tilde{N} \simeq -(h_\nu/2M_N)\phi\phi$ with $|\tilde{N}| \propto |\phi|^2 \propto H^{7/4}$ in magnitude and $d\theta_{\tilde{N}}/dt \simeq 2d\theta_\phi/dt \propto H^{1/4}$ in phase. Then, the \tilde{N} asymmetry remaining after the transition epoch diminishes rapidly through the decays as $n_{\tilde{N}} = 2(d\theta_{\tilde{N}}/dt)|\tilde{N}|^2 \propto H^{15/4}$. It is the essential point that the decay modes (4.26) have almost the same rate $\Gamma_{\tilde{N}}/2$ but the opposite final lepton numbers $L = \pm 1$. This means that the \tilde{N} asymmetry does not leave any significant lepton number asymmetry.

4.3 Numerical analysis

We here present the results of detailed numerical calculations for the leptogenesis in two parameter sets. Two parameter sets are listed in Table 5.1. The Case (1) and (2)

Table 4.1: Typical cases for the leptogenesis, where $H_{\text{inf}} = 10^{13}\text{GeV}$ is taken for definiteness. The Case (1) and (2) corresponds to the large h_ν and small h_ν , respectively.

	case (1)	case (2)
(h_ν, M_N, Γ_N)	$(2 \times 10^{-2}, 10^{11}\text{GeV}, 2 \times 10^6\text{GeV})$	$(3 \times 10^{-3}, 10^{11}\text{GeV}, 4 \times 10^4\text{GeV})$
(M, T_R)	$(10^{20}\text{GeV}, 10^8\text{GeV})$	$(5 \times 10^{18}\text{GeV}, 10^9\text{GeV})$
$(H_{\text{tr}}, H_{\text{th}})$	$(2 \times 10^8\text{GeV}, 5 \times 10^8\text{GeV})$	$(10^{10}\text{GeV}, 10^7\text{GeV})$
(a_N, δ_N)	$(1.3e^{i(2/3)\pi}, \pi/4)$	$(1.5e^{-i(5/4)\pi}, 3\pi/10)$
(b_N, a_h)	$(0.9e^{i(1/6)\pi}, 0.7e^{i(2/3)\pi})$	$(1.3e^{-i(2/3)\pi}, 0.8e^{i(1/4)\pi})$
(c_N, c_ϕ)	$(1.1, 0.9)$	$(1.2, 0.8)$
$\begin{pmatrix} r_N^{(0)} & r_\phi^{(0)} \\ \theta_N^{(0)} & \theta_\phi^{(0)} \end{pmatrix}$	$\begin{pmatrix} 0.869 & 5 \times 10^{-6} \\ 0.463 & -1.038 \end{pmatrix}$	$\begin{pmatrix} 1.282 & 1.148 \\ 1.138 & 0.608 \end{pmatrix}$
m_ν	$7.8 \times 10^{-2}\text{eV}$	$1.7 \times 10^{-3}\text{eV}$
$(\epsilon_L, n_L/s)$	$(-0.14, -1.2 \times 10^{-10})$	$(-1.1, -4.8 \times 10^{-10})$

corresponds to the large h_ν and small h_ν , respectively. Especially, the former case is in the parameter space where generates the lepton asymmetry through the operator relevant for the atmospheric neutrino.

The typical time variations of $n_{\tilde{N}}(t)$ and $n_{\tilde{L}}(t) \simeq n_L(t)$ are depicted in Fig. 4.1 in terms of the asymmetry fractions $\epsilon_a \equiv n_a/[(3/2)H^2M]$. The relevant scales, H_{inf} , M_N , H_{tr} , Γ_N and H_{th} , are marked together specifying the respective epochs.

We really observe the expected changes of the asymmetries through $H_{\text{inf}} \rightarrow H_{\text{tr}} \rightarrow \Gamma_N$ in Fig. 4.1 resulting in the desired lepton number asymmetry $\epsilon_L \sim 1$. In the large h_ν case, the phase dependent terms with M_N drives \tilde{N} to rotate at $t \sim M_N^{-1}$, the lepton number violating terms $h_\nu \tilde{N}^* \phi \phi$ forces ϕ to rotate together with the configuration $\phi \simeq (-2M_N \tilde{N}/h_\nu)^{1/2}$ at $t \sim H_{\text{tr}}^{-1}$, then, the \tilde{N} asymmetry diminishes rapidly by the friction term of the right-handed sneutrino decay at $t \sim \Gamma_N^{-1}$. On the other hand, in the small h_ν case, the effect of the phase dependent terms with M_N is small at $t \sim M_N^{-1}$, therefore, the angular momentum of scalar fields remain negligibly small and the significant asymmetries of \tilde{N} and \tilde{L} do not appear. The lepton number violating terms $h_\nu \tilde{N}^* \phi \phi$ generates dominant part of the \tilde{N} and ϕ asymmetry at $t \sim H_{\text{tr}}^{-1}$, then, $\epsilon_{\tilde{N}}$ are separated for $t > H_{\text{th}}^{-1}$; $\epsilon_{\tilde{L}}$ is fixed to $\epsilon \sim O(1)$ while $\epsilon_{\tilde{N}}$ oscillates slowly in $\ln t$ as given in Eq. (4.50).

It is also checked that the sum $n_{\tilde{N}} + n_{\tilde{L}}$ varies rather moderately in the transition

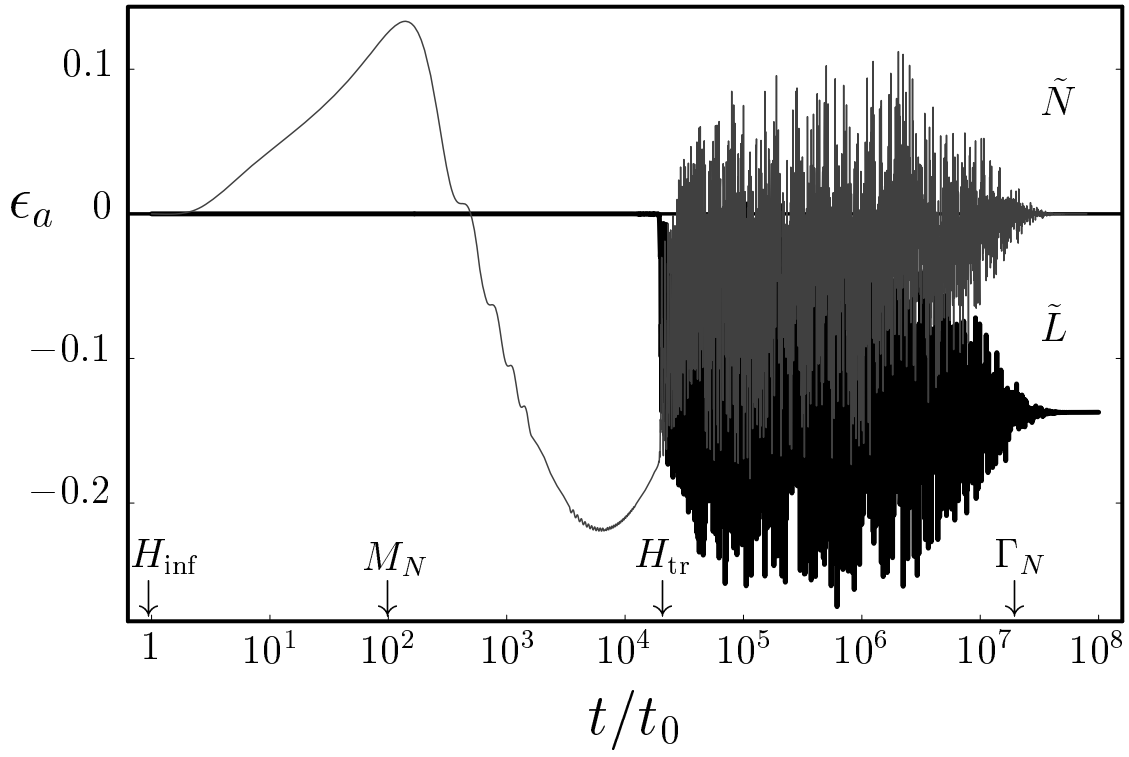


Figure 4.1: The time variation of particle number asymmetries is shown for the case (1) in Table 4.1.

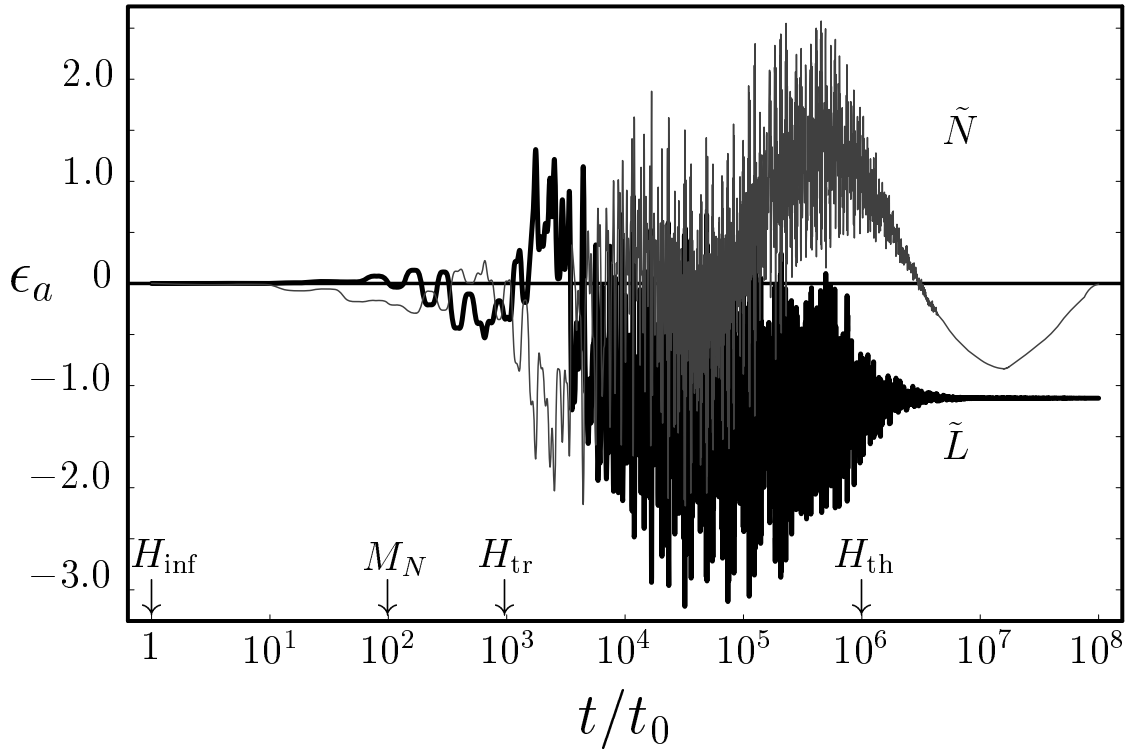


Figure 4.2: The time variation of particle number asymmetries is shown for the case (2) in Table 4.1.

epoch, while the respective asymmetries oscillate rapidly in both cases for $t > H_{\text{tr}}$.

4.4 Summary

In summary, we have investigated the leptogenesis via multiscalar coherent evolution in the supersymmetric seesaw model. The right-handed sneutrino \tilde{N} and the ϕ field in $\tilde{L}H_u$ of the slepton and Higgs doublets start together coherent evolution after the inflation with M_N smaller than H_{inf} . Then, after some period the motion of \tilde{N} and ϕ is drastically changed by the cross coupling $M_N h_\nu \tilde{N}^* \phi \phi$, and the significant asymmetries of \tilde{N} and \tilde{L} are generated. The \tilde{L} asymmetry is fixed later by the thermal effect as the lepton number asymmetry n_L . The \tilde{N} asymmetry, on the other hand, disappears through the incoherent decays $\tilde{N} \rightarrow \bar{\tilde{L}}\tilde{H}_u, \tilde{L}H_u$ with almost the same rate but opposite final lepton numbers. The sufficient amount of n_L for baryogenesis can be obtained with the lightest neutrino mass $m_\nu \lesssim 10^{-3}\text{eV}$ given by the seesaw mechanism with the right-handed neutrino mass $M_N \sim 10^{10} - 10^{13}\text{GeV} \lesssim H_{\text{inf}}$ for small h_ν case. On the other hand, for large h_ν case the light neutrino mass corresponding to leptogenesis operators can be the mass explaining the solar or atmospheric neutrino oscillation with the right-handed neutrino mass.

Chapter 5

Nonrenormalizable superpotential term

Flat manifold leptogenesis in the manner of Affleck and Dine is investigated with the slepton and Higgs fields, \tilde{L} , H_u , H_d , in the supersymmetric standard model. The multi-dimensional motion of these scalar fields is realized in the case that the $\tilde{L}H_u$ and H_uH_d directions are comparably flat with the relevant non-renormalizable superpotential terms. Soon after the inflation, the lepton number asymmetry appears to fluctuate due to this multi-dimensional motion involving certain CP violating phases. Then, it is fixed to some significant non-zero value for the successful baryogenesis when the scalar fields begin to oscillate with rotating phases driven by the quartic coupling from the superpotential term $\bar{h}_e L H_d e^c$ with $\bar{h}_e \sim 10^{-3}$. The Hubble parameter H_{osc} at this epoch for the completion of leptogenesis is much larger than the gravitino mass $m_{3/2} \sim 10^3 \text{GeV}$. The thermal terms may even play a cooperative role in this scenario of early leptogenesis. The lightest neutrino mass can be $m_{\nu_1} \sim 10^{-4} \text{eV}$, if the reheating temperature is allowed to be $T_R \sim 10^{10} \text{GeV}$.

5.1 Model

We investigate the supersymmetric standard model including the non-renormalizable superpotential terms,

$$W_{\text{non}} = \frac{\lambda_{\mathbb{L}_i}}{2M} (L_i H_u)(L_i H_u) + \frac{\lambda_H}{2M} (H_u H_d)(H_u H_d), \quad (5.1)$$

where M represents some very large mass scale such as the Planck scale, and the suitable basis is chosen for the relevant fields to give the positive and diagonal $\lambda_{\mathbb{L}_i}$ and positive λ_H .

The R -parity violating terms $(L_i H_u)(H_u H_d)$ are not included for simplicity. These terms do not alter the present leptogenesis scenario if they are not significantly large compared to W_{non} . We here assume the condition on the terms in W_{non} ,

$$\lambda_H \sim \lambda_{\psi_1} \ll \lambda_{\psi_2}, \lambda_{\psi_3}. \quad (5.2)$$

Then, the flat manifold for leptogenesis is formed with the \tilde{L}_1 , H_u and H_d fields. The lepton doublet L_1 includes the lightest neutrino ν_1 with mass

$$m_{\nu_1} = \lambda_{\psi_1} \frac{\langle H_u \rangle^2}{M} \sim 10^{-6} \text{eV} \left(\frac{10^{19} \text{GeV}}{M/\lambda_{\psi_1}} \right), \quad (5.3)$$

where $\sqrt{\langle H_u \rangle^2 + \langle H_d \rangle^2} = 174 \text{GeV}$ with $\langle H_u \rangle / \langle H_d \rangle \equiv \tan \beta$. The comparability of λ_{ψ_1} and λ_H would be understood by considering that these non-renormalizable terms stem from the physics at the Planck scale. On the other hand, as indicated from the solar and atmospheric neutrino puzzles, the other two neutrino masses are probably around 10^{-2}eV , apparently requiring $\lambda_{\psi_2}, \lambda_{\psi_3} \sim 10^4 (M/10^{19} \text{GeV})$. Such large couplings may be obtained effectively as $\lambda_{\psi_2}, \lambda_{\psi_3} \sim \lambda_{\psi_1} (M/M_{\nu^c})$ by the so-called seesaw mechanism with heavy right-handed neutrinos at an intermediate scale $M_{\nu^c} \ll M$ [7]. The see-saw contribution to λ_{ψ_1}/M should, however, be suppressed sufficiently for the successful leptogenesis.

The superpotential terms relevant for the flat manifold leptogenesis are given by

$$W = (h_e)_{ij} L_i H_d e_j^c + \mu H_u H_d + W_{\text{non}}. \quad (5.4)$$

The F terms except for the contributions of W_{non} are then calculated as

$$\begin{aligned} F_{L_i} &= (h_e)_{ij} H_d e_j^c, F_{e_j^c} = (h_e)_{ij} L_i H_d, \\ F_{H_u} &= \mu H_d, F_{H_d} = (h_e)_{ij} L_i e_j^c + \mu H_u. \end{aligned} \quad (5.5)$$

Among the slepton fields, only the sneutrino $\tilde{\nu}_1$ in \tilde{L}_1 associated with the lightest neutrino is considered to develop a very large coherent field value during the inflation, according to the condition (5.2). Then, it is usually supposed that the $\tilde{\nu}_1$ and H_d^0 are incompatible for the flat directions due to the F_{e^c} terms. However, this is not necessarily the case in the present scenario. In fact, the F_{e^c} terms provide the quartic term

$$\bar{h}_e^2 |\tilde{L}_1 H_d|^2 \quad (5.6)$$

with

$$\bar{h}_e^2 \equiv \sum_j |(h_e)_{1j}|^2. \quad (5.7)$$

The effective coupling is estimated as

$$\bar{h}_e \simeq \frac{m_e + \sin \theta_{12} m_\mu}{\langle H_d \rangle} \sim \begin{cases} 10^{-5} & (\theta_{12} \lesssim 10^{-2}) \\ 10^{-3} & (\theta_{12} \sim 1) \end{cases}, \quad (5.8)$$

where θ_{12} represents the ν_e - ν_μ mixing, and the effect of the ν_e - ν_τ mixing is assumed to be small enough. As explained in Sec. 5.2, while this quartic term is safely small during the inflation with $\bar{h}_e \sim 10^{-5} - 10^{-3}$, it in turn provides the driving force for the scalar fields to oscillate with rotating phases at some epoch after the inflation. This is one of the essential points in the present scenario for the flat manifold leptogenesis.

According to the above arguments, the flat manifold is specified by the D -flat condition for the $SU(2)_L \times U(1)_Y$ gauge interactions,

$$|\tilde{\nu}_1|^2 - |H_u^0|^2 + |H_d^0|^2 = 0, \quad (5.9)$$

and the other fields are vanishing. Henceforth, we adopt for simplicity the notation, $\tilde{L} \equiv \tilde{\nu}_1$, $H_u \equiv H_u^0$ and $H_d \equiv H_d^0$, suppressing the lepton generation indices. Including the contributions of W_{non} , this manifold is flat enough for both the $\tilde{L}H_u$ and H_uH_d directions in the case that $\lambda_{\tilde{L}}$ and λ_H are comparable,

$$0.3 \lesssim \lambda_{\tilde{L}}/\lambda_H \lesssim 3, \quad (5.10)$$

as observed in Ref. [27].

5.2 Flat Manifold Leptogenesis

We here describe the mechanism of leptogenesis on the flat manifold consisting of the scalar fields \tilde{L}, H_u, H_d , say *AD-flatons*. (The scalar fields associated with the flat potential are intrinsic in supersymmetric models, which are named flatons [49]. Here, we consider such fields as participants in leptogenesis/baryogenesis a la Affleck-Dine.) The scalar potential for the AD-flatons $\phi_a = \tilde{L}, H_u, H_d$ may be presented as

$$V = V_{\text{high}} + \bar{h}_e^2 |\tilde{L}H_d|^2 + V_{\text{low}}. \quad (5.11)$$

These three parts become dominant in the high, middle and low energy scales, respectively. The evolution of the AD-flaton fields is traced in the corresponding epochs starting with

the inflation. The high-energy part is provided from the superpotential W_{non} with the mass scale M and the corresponding soft supersymmetry breaking with the Hubble parameter H :

$$\begin{aligned}
V_{\text{high}} = & - \sum_a c_a H^2 |\phi_a|^2 \\
& + \left| \lambda_{\tilde{L}} \frac{\tilde{L}(\tilde{L}H_u)}{M} + \lambda_H \frac{H_d(H_uH_d)}{M} \right|^2 \\
& + \left| \lambda_H \frac{H_u(H_uH_d)}{M} \right|^2 + \left| \lambda_{\tilde{L}} \frac{H_u(\tilde{L}H_u)}{M} \right|^2 \\
& + \left[\frac{\lambda_{\tilde{L}}}{2M} a_{\tilde{L}} H(\tilde{L}H_u)(\tilde{L}H_u) + \text{h.c.} \right] \\
& + \left[\frac{\lambda_H}{2M} a_H H(H_uH_d)(H_uH_d) + \text{h.c.} \right] \\
& + (g^2 + g'^2)(|\tilde{L}|^2 - |H_u|^2 + |H_d|^2)^2.
\end{aligned} \tag{5.12}$$

The last term with the gauge couplings g and g' of the $\text{SU}(2)_L$ and $\text{U}(1)_Y$, respectively, is also included here to realize the D -flat condition (5.9) for the very large $|\tilde{L}|$, $|H_u|$ and $|H_d|$. The low-energy part V_{low} includes the remaining terms, which are related to the parameters $m_{3/2}, |\mu| \sim 10^3 \text{GeV}$. It will be clarified in the following that the quartic term $\bar{h}_e^2 |\tilde{L}H_d|^2$ plays a crucial role to complete the flat manifold leptogenesis. On the other hand, the low-energy part V_{low} is actually irrelevant for the leptogenesis. This is in salient contrast to the conventional flat direction Affleck-Dine mechanism. In this section, we do not either consider explicitly the thermal terms [46, 47, 44, 45]. It will be seen in Secs. 5.3 and 5.4 that the thermal terms do not alter essentially the present scenario of flat manifold leptogenesis. They may even play a cooperative role for leptogenesis.

5.2.1 $H = H_{\text{inf}}$

During the inflation the Hubble parameter takes almost a constant value H_{inf} , which is typically 10^{14}GeV or so. In this epoch, the AD-flaton fields quickly settle into one of the minima of the scalar potential (5.11) with $H = H_{\text{inf}}$. The potential minima is almost determined by the high-energy part V_{high} as

$$\phi_a^{(0)} = e^{i\theta_a^{(0)}} r_a^{(0)} \sqrt{H_{\text{inf}}(M/\lambda)}, \tag{5.13}$$

with λ representing the mean value of $\lambda_{\not{L}}$ and λ_H . The generation of these non-trivial minima (5.13) with $r_a^{(0)} \sim 0.1 - 1$ far apart from the origin on the multi-dimensional flat manifold depends rather complicatedly on the parameters, c_a , $\lambda_{\not{L}}$, λ_H , $a_{\not{L}}$ and a_H [27]. As usually considered, at least one of c_a 's should be positive so that the origin stays unstable in the inflation epoch. It is also essential for the flat manifold formation that $\lambda_{\not{L}}$ and λ_H are comparable, as given in Eq. (5.10). Otherwise, the potential minima would be developed along either the $\tilde{L}H_u$ direction or the H_uH_d direction.

By comparing $V_{\text{high}} \sim H_{\text{inf}}^3(M/\lambda)$ and $\bar{h}_e^2|\tilde{L}H_d|^2 \sim \bar{h}_e^2H_{\text{inf}}^2(M/\lambda)^2$, the following condition is expected to be satisfied for the flatness of the \tilde{L} - H_u - H_d manifold during the inflation:

$$H_{\text{inf}} > H_{\text{osc}} \equiv \bar{h}_e^2(M/\lambda). \quad (5.14)$$

The critical value H_{osc} of the Hubble parameter for which the \bar{h}_e quartic term becomes comparable to V_{high} may be estimated in terms of m_{ν_1} with Eqs. (5.3) and (5.8):

$$H_{\text{osc}} \sim 10^9 \text{GeV} \left(\frac{\bar{h}_e}{10^{-5}} \right)^2 \left(\frac{10^{-6} \text{eV}}{m_{\nu_1}} \right). \quad (5.15)$$

Hence, the condition (5.14) can be satisfied readily since H_{inf} is typically 10^{14}GeV or so. Here, it may be noticed that if $\bar{h}_e \sim 10^{-3}$ with large ν_e - ν_μ mixing, H_{osc} could be comparable to H_{inf} . Remarkably, even in such an extreme case with $H_{\text{osc}} \sim H_{\text{inf}}$ the successful leptogenesis can be realized, as confirmed by the numerical calculations in Sec. 5.4.

5.2.2 $H_{\text{osc}} < H < H_{\text{inf}}$

After the inflation the inflaton oscillates coherently, and it dominates the energy density of the universe. In this epoch with $H > H_{\text{osc}}$, the high-energy part V_{high} is still dominant, and the evolution of the AD-flaton fields is essentially the same as in the case of the model with triplet Higgs [27]. We recapitulate the main results with suitable changes of notation, showing especially the fluctuating behavior of the lepton number asymmetry after the inflation.

The AD-flaton fields are moving toward the origin with the initial conditions at $t = t_0 \sim H_{\text{inf}}^{-1}$ after the inflation,

$$\phi_a(t_0) = \phi_a^{(0)}, \quad \dot{\phi}_a(t_0) = 0. \quad (5.16)$$

The evolution of the AD-flaton fields is governed by the equations of motion,

$$\ddot{\phi}_a + 3H\dot{\phi}_a + \frac{\partial V}{\partial \phi_a^*} = 0. \quad (5.17)$$

The Hubble parameter varies in time as $H = (2/3)t^{-1}$ in the matter-dominated universe. The AD-flaton fields may be represented suitably in terms of the dimensionless fields χ_a [26] as

$$\phi_a = \chi_a \sqrt{H(M/\lambda)} \equiv e^{i\theta_a} r_a \sqrt{H(M/\lambda)}. \quad (5.18)$$

Then, the equations of motion (5.17) are rewritten with $z = \ln(t/t_0)$ as

$$\frac{d^2 \chi_a}{dz^2} + \frac{\partial U}{\partial \chi_a^*} = 0, \quad (5.19)$$

and the initial conditions from Eq. (5.16) are given as

$$\chi_a(0) = e^{i\theta_a^{(0)}} r_a^{(0)}, \quad \frac{d\chi_a}{dz}(0) = \frac{1}{2}\chi_a(0). \quad (5.20)$$

It should be noticed in Eq. (5.19) that the first-order z -derivative is absent due to the parametrization of ϕ_a in Eq. (5.18). The dimensionless effective potential is given dominantly by

$$\begin{aligned} U(\chi_a) &\simeq \frac{4}{9H^3(M/\lambda)} V_{\text{high}} - \frac{1}{4} |\chi_a|^2 \\ &+ \frac{4}{9} (H_{\text{osc}}/H) |\chi_{\tilde{L}} \chi_{H_d}|^2. \end{aligned} \quad (5.21)$$

The second term is due to the time variation of the factor $\sqrt{H(M/\lambda)}$ in Eq. (5.18), which apparently provides the change of the mass terms in $U(\chi_a)$,

$$c_a \rightarrow c_a + \frac{9}{16}. \quad (5.22)$$

The third contribution from the \bar{h}_e quartic term is small enough in this epoch with $H > H_{\text{osc}}$, while it will in turn play a crucial role in the next epoch. The low-energy part V_{low} is clearly negligible for $H_{\text{osc}} \gg m_{3/2}, |\mu|$.

The behavior of the AD-flaton phases θ_a is described in this epoch as follows. The initial conditions at $t = t_0$ ($z = 0$) are given from Eq. (5.20) as

$$\theta_a(0) = \theta_a^{(0)}, \quad \frac{d\theta_a}{dz}(0) = 0. \quad (5.23)$$

On the other hand, the asymptotic trajectory of the AD-flaton fields is found by the conditions $\partial U/\partial \chi_a^* = 0$ in this epoch with the small enough \bar{h}_e quartic term as

$$\theta_a = \theta_a^{(1)}. \quad (5.24)$$

It is remarkable in the multi-dimensional motion of the AD-flaton fields with $\lambda_{\not{L}} \sim \lambda_H$ that the direction of this trajectory is somewhat different from the initial direction, i.e.,

$$\theta_a^{(1)} \neq \theta_a^{(0)}. \quad (5.25)$$

This is because the apparent change of the mass terms in Eq. (5.22) due to the redshift induces the new balance among the $\lambda_{\not{L}}\text{-}\lambda_H$ cross term, $a_{\not{L}}$ term and a_H term in $U(\chi_a)$, which have different dependences on θ_a . (If the fine-tuning is made as $\arg(a_{\not{L}}) - \arg(a_H) = \pi \bmod 2\pi$, the initial balance is maintained independently of $|\chi_a|$ so as to realize $\theta_a^{(0)} = \theta_a^{(1)}$.) Without the $d\chi_a/dz$ (friction) term in Eq. (5.19), the AD-flaton phases θ_a slowly fluctuate around $\theta_a^{(1)}$ starting from $\theta_a^{(0)}$ as a function of $z = \ln(t/t_0)$ in the epoch $H_{\text{inf}}^{-1} \sim t_0 \leq t < H_{\text{osc}}^{-1}$. That is, in the motion on the multi-dimensional flat manifold

the AD-flaton fields no longer track exactly behind the decreasing instantaneous minimum of the scalar potential. This is in salient contrast to the conventional Affleck-Dine mechanism on the one-dimensional flat direction, where the AD-flaton phase is fixed for a long time until the low-energy supersymmetry breaking terms become important.

In this way, through this fluctuating motion of the (almost) homogeneous coherent AD-flaton fields $\phi_a(t)$, the particle number asymmetries are generated soon after the inflation as

$$\Delta n_a \equiv n_a - \bar{n}_a = i(\phi_a^* \dot{\phi}_a - \dot{\phi}_a^* \phi_a). \quad (5.26)$$

The fractions of the respective asymmetries are also calculated by considering the redshift in the matter-dominated universe as

$$\epsilon_a(t) \equiv \Delta n_a / [(3/2)H^2(M/\lambda)] = -2r_a^2 \frac{d\theta_a}{dz}. \quad (5.27)$$

The lepton number asymmetry is particularly given as the \tilde{L} asymmetry,

$$\epsilon_L(t) = \epsilon_{\tilde{L}}(t). \quad (5.28)$$

Since the AD-flaton phases are fluctuating in this early epoch, as mentioned so far, the lepton number asymmetry is oscillating in time as $|\epsilon_L(t)| \sim |d\theta_a/dz| \lesssim |\theta_a^{(0)} - \theta_a^{(1)}| \sim 0.01 - 0.1$ ($r_a \sim 0.1 - 1$) numerically for the reasonable parameter values.

5.2.3 $m_{3/2} \ll H \lesssim H_{\text{osc}}$

The high-energy potential terms and the \bar{h}_e quartic term are redshifted for $H \gtrsim H_{\text{osc}}$ after the inflation as

$$V_{\text{high}} \sim H^3(M/\lambda), \quad (5.29)$$

$$\bar{h}_e^2 |\tilde{L} H_d|^2 \sim \bar{h}_e^2 H^2 (M/\lambda)^2 \quad (5.30)$$

with $|\phi_a| \sim \sqrt{H(M/\lambda)}$ in Eq. (5.18). Then, the \bar{h}_e quartic term eventually dominates in the present epoch with $H \lesssim H_{\text{osc}}$, playing the crucial role for the flat manifold leptogenesis. Specifically, this quartic term acts in some sense as positive mass-squared terms for the \tilde{L} and H_d fields, driving the AD-flaton fields to oscillate. Once the oscillation begins, the lepton number asymmetry is fixed to some non-zero value as

$$\epsilon_L(t) = \epsilon_L \quad (t \gg H_{\text{osc}}^{-1}). \quad (5.31)$$

This asymptotic behavior of $\epsilon_L(t)$ in the later time is in accordance with the fact that the lepton number violating terms in V_{high} are redshifted rapidly to be much smaller than the lepton number conserving terms including the \bar{h}_e quartic term. (See Sec. 5.4 for the numerical results.) It is also obvious that for $H \gg m_{3/2}, |\mu|$ the low-energy part V_{low} still provides negligible effects in this epoch of leptogenesis.

The coherent oscillation of the inflaton field dominates the energy density of the universe until the decay of inflatons is completed at the time $t_R (\gg H_{\text{osc}}^{-1})$. Then, the universe is reheated to the temperature T_R . Until this time the lepton number asymmetry is redshifted as matter, which is given at $t = t_R$ ($H = H_R$) with Eqs. (5.27), (5.28) and (5.31) as

$$n_L(t_R) = \epsilon_L (3/2) H_R^2 (M/\lambda). \quad (5.32)$$

Then, the lepton-to-entropy ratio after the reheating is determined with $s \simeq 3H_R^2 M_{\text{P}}^2 / T_R$ as

$$\begin{aligned} \frac{n_L}{s} &\simeq \epsilon_L \frac{(M/\lambda) T_R}{2M_{\text{P}}^2} \\ &\sim 10^{-10} \left(\frac{\epsilon_L}{0.1} \right) \left(\frac{10^{-6} \text{eV}}{m_{\nu_1}} \right) \left(\frac{T_R}{10^9 \text{GeV}} \right), \end{aligned} \quad (5.33)$$

where $M_{\text{P}} = m_{\text{P}} / \sqrt{8\pi} = 2.4 \times 10^{18} \text{GeV}$ is the reduced Planck mass, and the relation (5.3) between M/λ and m_{ν_1} is considered. This lepton number asymmetry is converted partially

to the baryon number asymmetry through the electroweak anomalous effect. The chemical equilibrium between leptons and baryons leads the ratio $n_B = -(8/23)n_L$ (without any preexisting baryon number asymmetry) [39]. Therefore, the sufficient baryon-to-entropy ratio can be provided as required from the nucleosynthesis with $\eta = (2.6 - 6.2) \times 10^{-10}$ [11].

It should here be noted that the reheating temperature may be constrained as $T_R \lesssim 10^8 - 10^{10} \text{ GeV}$, or even more severely, for $m_{3/2} \sim 1 \text{ TeV}$ to avoid the gravitino problem [21, 22, 23]. Hence, the desired mass of the lightest neutrino is very small generally as $m_{\nu_1} \lesssim 10^{-6} \text{ eV}$. It will, however, be found in Sec. 5.4 that there is some range of the model parameters for the successful leptogenesis with relatively large $m_{\nu_1} \sim 10^{-4} \text{ eV}$, if the reheating temperature is allowed to be $T_R \sim 10^{10} \text{ GeV}$ for $m_{3/2} \sim \text{several TeV}$ with small hadronic branching ratio of gravitino decay $B_h \sim 0.01$ [22]. Then, the prediction for the neutrinoless double beta decay with very small m_{ν_1} [45] could be evaded in the case of \tilde{L} - H_u - H_d flat manifold leptogenesis.

5.3 Thermal Effects

We now discuss that the thermal terms for the scalar potential [44, 45, 46, 47] do not alter essentially the present scenario of flat manifold leptogenesis. Before the reheating after inflation is completed, there is already a dilute plasma of the inflaton decay products with temperature

$$T_p \sim (T_R^2 H M_P)^{1/4}. \quad (5.34)$$

Then, the AD-flatons acquire the thermal mass terms in this plasma,

$$V_{\text{th1}} = c_{\text{th}} y^2 T_p^2 |\phi_a|^2 \quad (y|\phi_a| < T_p), \quad (5.35)$$

where y is the relevant coupling constant, and c_{th} is the positive constant, e.g., $c_{\text{th}} = 3/4$ for a quark superfield. One can readily estimate the Hubble parameter H_{th1} when the thermal mass terms begin to dominate over the Hubble induced mass terms:

$$H_{\text{th1}} \sim \min \left[\frac{T_R^2 M_P}{y^4 (M/\lambda)^2}, (y^4 T_R^2 M_P)^{1/3} \right]. \quad (5.36)$$

The thermal log terms are also given mainly through the modification of the $\text{SU}(3)_C$ gauge coupling as

$$V_{\text{th2}} = a_{\text{th}} \alpha_s^2(T) T_p^4 \ln(|\phi_a|^2/T_p^2) \quad (5.37)$$

with $a_{\text{th}} \sim 1$ depending on the particle contents. The Hubble parameter H_{th2} for the thermal log terms to be comparable to the Hubble induced mass terms is also estimated with $|\phi_a| \sim \sqrt{H(M/\lambda)}$ as

$$H_{\text{th2}} \sim \alpha_s [T_R^2 M_P / (M/\lambda)]^{1/2}. \quad (5.38)$$

Then, the thermal effects become important for the Hubble parameter

$$H_{\text{th}} \sim \max[H_{\text{th1}}, H_{\text{th2}}]. \quad (5.39)$$

It really takes the maximal value as

$$\begin{aligned} H_{\text{th}}^{\text{max}} &\sim H_{\text{th2}}/\alpha_s \\ &\sim 5 \times 10^8 \text{GeV} \left(\frac{T_R}{10^9 \text{GeV}} \right) \left(\frac{m_{\nu_1}}{10^{-6} \text{eV}} \right)^{1/2} \end{aligned} \quad (5.40)$$

with certain value of the relevant coupling,

$$y \sim 3 \times 10^{-3} \left(\frac{T_R}{10^9 \text{GeV}} \right)^{1/4} \left(\frac{m_{\nu_1}}{10^{-6} \text{eV}} \right)^{3/8}, \quad (5.41)$$

where Eq. (5.3) is considered for m_{ν_1} and M/λ . It is readily seen that $H_{\text{osc}} > H_{\text{th}}$ for a wide range of the model parameters. Then, the leptogenesis is completed dominantly by the \bar{h}_e quartic term. On the other hand, one may obtain $H_{\text{th}} \gtrsim H_{\text{osc}}$ for certain model parameter range with $\bar{h}_e \sim 10^{-5}$, $(M/\lambda) \lesssim 10^{18} \text{GeV}$ and $T_R \gtrsim 10^9 \text{GeV}$. Then, the oscillation of AD flaton fields is driven by the thermal terms rather than the \bar{h}_e quartic term. In any case, the lepton number asymmetry fluctuating after the inflation is fixed to some significant non-zero value in the early epoch with $H \gg m_{3/2}$. The thermal terms do not severely suppress the lepton number generation, but even play a cooperative role in the flat manifold leptogenesis.

5.4 Numerical Analysis

We here present the results of detailed numerical calculations for the flat manifold leptogenesis. The characteristic features in the multi-dimensional motion of the AD-flaton fields are confirmed, and the reasonable range of the model parameters is identified for the sufficient leptogenesis.

The values of the various model parameters are taken in the following range:

$$\begin{aligned}
M &= 10^{17} \text{GeV}, \quad H_{\text{inf}} = 10^{14} \text{GeV}, \quad t_0 = (2/3)H_{\text{inf}}^{-1}, \\
\bar{h}_e &= 10^{-5} - 10^{-3}, \quad T_R = 10^5 \text{GeV} - 10^{10} \text{GeV}, \\
\lambda_{\not{L}}, \lambda_H &= 0.1\lambda - 10\lambda, \quad \lambda = 10^{-3} - 1, \\
|a_{\not{L}}|, |a_H|, c_a &= 0 - 2,
\end{aligned}$$

and $[0, 2\pi]$ for the phases of coupling parameters. Here, the parameters relevant to the low-energy part V_{low} are not presented explicitly. It has been checked numerically that the effects of V_{low} is negligible in the present scenario of flat manifold leptogenesis. While the fixed value of the mass scale M in W_{non} is presented for definiteness, the results are really obtained as a function of M/λ . The value of $\tan\beta$ is determined in Eq. (5.8) for given \bar{h}_e with $\theta_{12} \simeq 0$ (small ν_e - ν_μ mixing) or $\theta_{12} \simeq \pi/4$ (large ν_e - ν_μ mixing).

By choosing randomly the model parameter values, we have first determined the initial values of the AD-flaton fields in Eq. (5.16) just after the inflation. (The initial phase of H_u is chosen as $\theta_{H_u}^{(0)} = 0$ without loss of generality by making a $U(1)_Y$ transformation.) Then, we have solved the equations of motion (5.17) for a sufficiently long time interval from $t = t_0$ ($H = H_{\text{inf}}$) to $t \sim 10^8 t_0$, evaluating the particle number asymmetries $\epsilon_a(t)$ as functions of time. (In practice, we have solved Eq. (5.19) for χ_a with Eq. (5.20) as functions of $z = \ln(t/t_0)$, since the time interval ranges over many orders. The D -flat condition (5.9) is checked to be hold within numerical errors.) The dominant contributions to the thermal terms $V_{\text{th1}} + V_{\text{th2}}$ are also taken into account for the evolution of the AD-flaton fields. The relevant parameters are taken for the thermal mass terms as $y = m_q/\langle H_d \rangle$ and $c_{\text{th}} = 3/4$ with the $q = d, s$ quarks, $y = m_c/\langle H_u \rangle$ and $c_{\text{th}} = 3/4$ with the c quark, and $y = m_\mu/\langle H_d \rangle$ and $c_{\text{th}} = 1/4$ with the muon. These Yukawa couplings may be close to the optimal value as given in Eq. (5.41), depending on $\tan\beta$. As for the thermal log term, $a_{\text{th}} = 9/8$ is taken due to the decoupling of the top quark from the thermal plasma.

We have actually made calculations by taking hundreds of the parameter sets. Some typical cases are listed in Table 5.1, where the sufficient lepton number asymmetry is obtained. The cases (1) and (2) correspond to the small \bar{h}_e (small ν_e - ν_μ mixing) and the large \bar{h}_e (large ν_e - ν_μ mixing), respectively. Although different values are taken for M/λ and T_R in the cases (1) and (2), the resultant ϵ_L has only moderate dependence on these parameters. It should here be noticed that $H_{\text{osc}} \sim H_{\text{inf}}$ in the case (2). Then, the \bar{h}_e

Table 5.1: Typical cases for the flat manifold leptogenesis, where $M = 10^{17}\text{GeV}$ and $H_{\text{inf}} = 10^{14}\text{GeV}$ are taken for definiteness. The index a denotes the AD-flatons as $\phi_a = \tilde{L}, H_u, H_d$ in order.

	case (1)	case (2)	case (3)
h_e	3×10^{-5}	10^{-3}	10^{-3}
$(\tan \beta, \theta_{12})$	$(10.2, 0)$	$(2.1, \pi/4)$	$(2.1, \pi/4)$
$(M/\lambda, T_R)$	$(10^{19}\text{GeV}, 10^9\text{GeV})$	$(10^{20}\text{GeV}, 10^8\text{GeV})$	$(10^{18}\text{GeV}, 10^{10}\text{GeV})$
$(H_{\text{osc}}, H_{\text{th}}^{\text{max}})$	$(9 \times 10^9\text{GeV}, 5 \times 10^8\text{GeV})$	$(10^{14}\text{GeV}, 10^7\text{GeV})$	$(10^{12}\text{GeV}, 10^{10}\text{GeV})$
$(\lambda_{\tilde{L}}, \lambda_H)$	$(1.0 \times 10^{-2}, 1.5 \times 10^{-2})$	$(1.5 \times 10^{-3}, 0.5 \times 10^{-3})$	$(4.0 \times 10^{-1}, 1.0 \times 10^{-1})$
$(a_{\tilde{L}}, a_H)$	$(1.0e^{i(1/4)\pi}, 1.0e^{i(1/2)\pi})$	$(1.5e^{-i(1/3)\pi}, 0.5e^{-i\pi})$	$(2.0e^{i(1/3)\pi}, 0.4e^{i\pi})$
c_a	$(1.5, 1.0, 0.5)$	$(1.0, 1.0, 1.0)$	$(2.0, 2.0, 0.5)$
$\begin{pmatrix} r_a^{(0)} \\ \theta_a^{(0)} \end{pmatrix}$	$\begin{pmatrix} 0.738 & 0.753 & 0.148 \\ 1.208 & 0 & 3.108 \end{pmatrix}$	$\begin{pmatrix} 0.397 & 0.954 & 0.868 \\ -1.170 & 0 & 0.237 \end{pmatrix}$	$\begin{pmatrix} 0.313 & 0.640 & 0.558 \\ -2.040 & 0 & 2.783 \end{pmatrix}$
$\begin{pmatrix} r_a^{(1)} \\ \theta_a^{(1)} \end{pmatrix}$	$\begin{pmatrix} 0.775 & 0.823 & 0.277 \\ 1.236 & 0.039 & 3.101 \end{pmatrix}$	$\begin{pmatrix} 0.392 & 1.047 & 0.971 \\ -1.188 & -0.007 & 0.226 \end{pmatrix}$	$\begin{pmatrix} 0.282 & 0.711 & 0.654 \\ -2.019 & 0.005 & 2.819 \end{pmatrix}$
m_{ν_1}	$3.0 \times 10^{-6}\text{eV}$	$3.7 \times 10^{-7}\text{eV}$	$1.0 \times 10^{-4}\text{eV}$
$(\epsilon_L, n_L/s)$	$(-0.24, -2.1 \times 10^{-10})$	$(-0.17, -1.5 \times 10^{-10})$	$(-0.11, -1.0 \times 10^{-10})$

quartic term as well as the high-energy part V_{high} may be important to determine the potential minimum in the inflation epoch. We have really confirmed that even in such an extreme case the multi-dimensional motion of the AD-fields can be realized producing the significant lepton number asymmetry.

We have also searched the specific parameter range allowing for somewhat high $T_R \sim 10^{10}\text{GeV}$, where the sufficient lepton number asymmetry is obtained with relatively large $m_{\nu_1} \sim 10^{-4}\text{eV}$ for the lightest neutrino. A typical example is presented as the case (3) in Table 5.1.

The time evolution of the AD-flaton fields has been determined precisely by these numerical calculations. In Fig. 5.1, the multi-dimensional motion of the AD-flaton fields is typically depicted in terms of the dimensionless fields χ_a for the case (1) in Table 5.1. In Fig. 3.66, is also shown the time variation of the particle number asymmetries, or the contributions to the hypercharge asymmetry, $\epsilon_{\tilde{L}}$ (bold line), $-\epsilon_{H_u}$ (slim line) and ϵ_{H_d} (dashed line), which are evaluated with the solutions of χ_a . Here, we can check the hypercharge conservation (within the numerical errors), $\epsilon_{\tilde{L}} - \epsilon_{H_u} + \epsilon_{H_d} = 0$. The lepton number asymmetry is given just by $\epsilon_L = \epsilon_{\tilde{L}}$. These asymmetries are really fluctuating after the inflation, and then fixed to certain values for $t \gg H_{\text{osc}}^{-1}$.

As for the thermal effects, we have observed that they do not alter essentially the

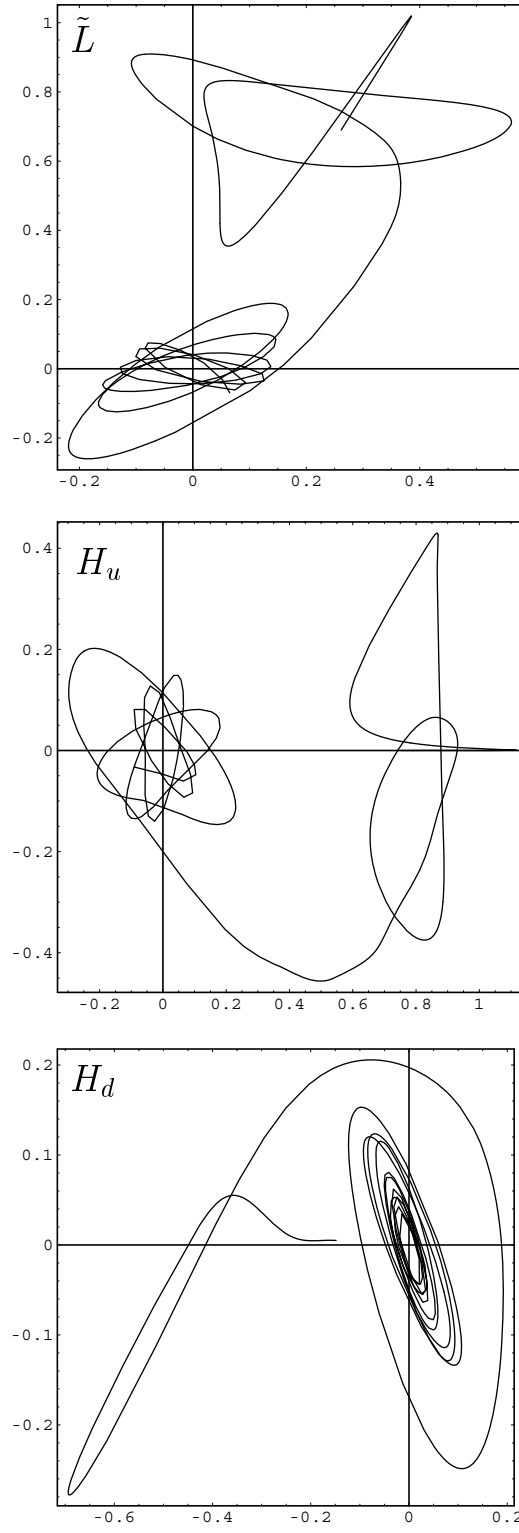


Figure 5.1: The motions of the AD-flaton fields, the real part (horizontal axis) and imaginary part (vertical axis), are depicted in terms of the dimensionless fields χ_a for the case (1) in Table 5.1.

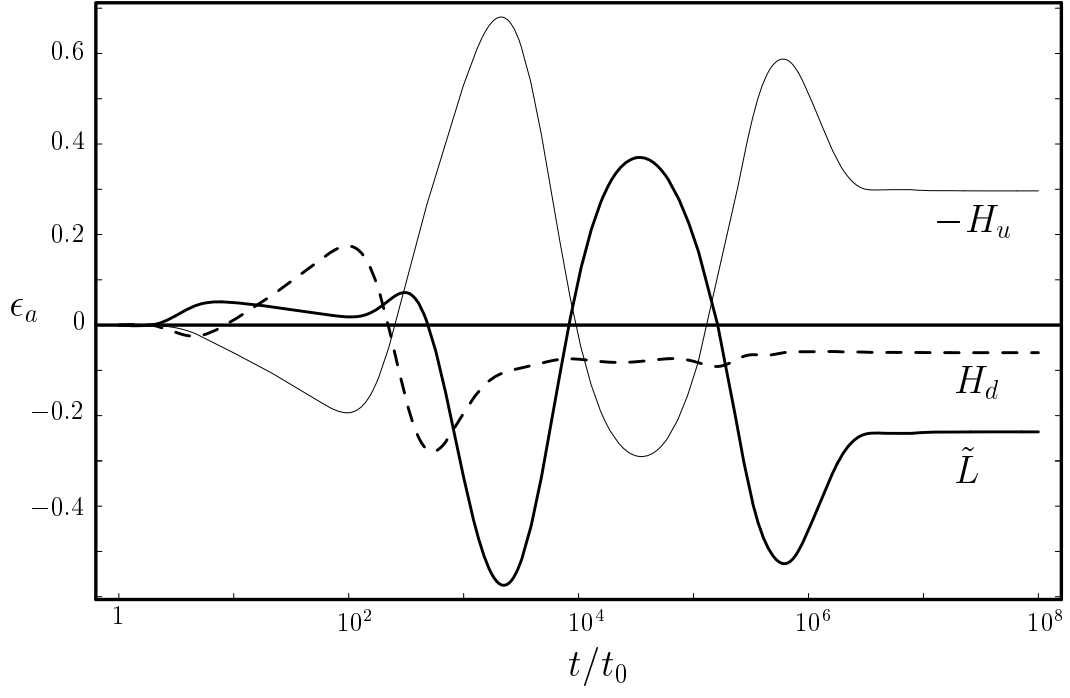


Figure 5.2: The time variation of particle number asymmetries is shown for the case (1) in Table 5.1.

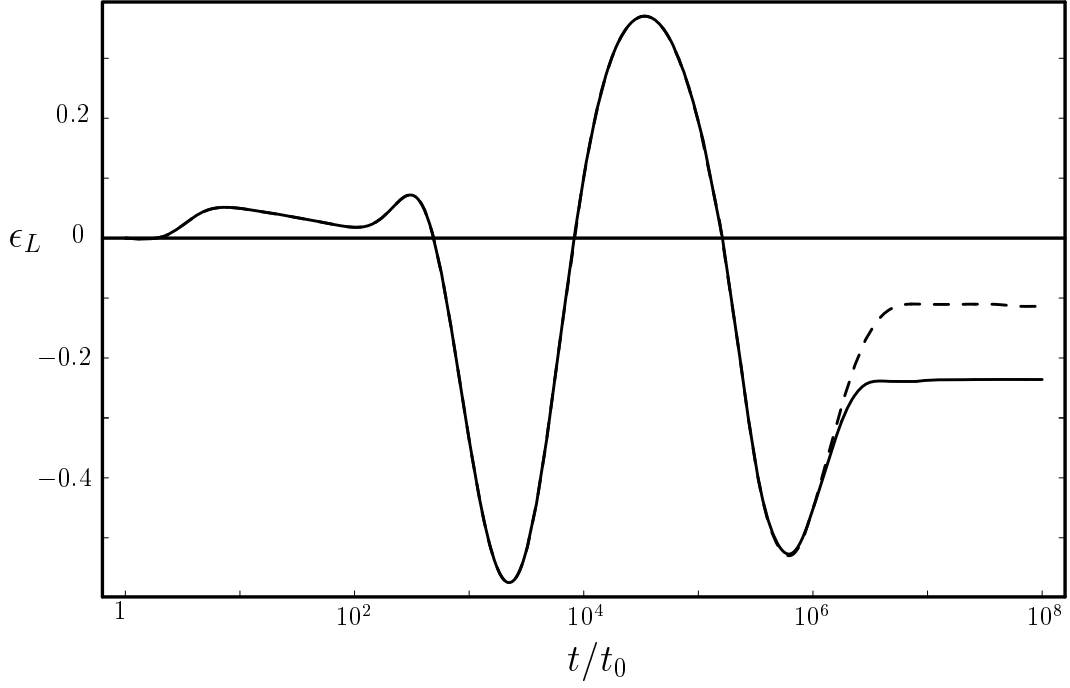


Figure 5.3: The time variation of the lepton number asymmetry is shown for the case (1) in Table 5.1, where the solid and dashed lines represent the results with and without the thermal terms, respectively.

present scenario of flat manifold leptogenesis. In a wide range of the model parameter space, the thermal effects on the final lepton number asymmetry ϵ_L are found to be small for $H_{\text{osc}} \gg H_{\text{th}}$, particularly with lower reheating temperature $T_R \lesssim 10^8 \text{GeV}$. It should, however, be noted that the lepton number asymmetry varies slowly with $z = \ln(t/t_0)$, as seen in Fig. 3.66. Then, it actually takes a rather long term ranging over some orders around $t \sim H_{\text{osc}}^{-1}$ to fix completely the lepton number asymmetry by driving the AD-flaton oscillation. In such a situation, when $H_{\text{th}}^{\text{max}}$ is smaller only by a few orders than H_{osc} , as seen for the case (1) of Table 5.1, the thermal terms become dominant at the late stage of leptogenesis for driving the AD-flaton oscillation. In Fig. 5.3, the time variation of the lepton number asymmetry $\epsilon_L(t)$ is shown for the case (1) in Table 5.1, where the solid and dashed lines represent the results with and without the thermal terms, respectively. In this case, the thermal log term is considered to provide the dominant effect. We really observe here that the lepton number asymmetry is finally fixed by the thermal terms, though the \bar{h}_e quartic term first triggers the AD-flaton oscillation. The resultant ϵ_L is changed by some factor ~ 1 due to the thermal effects. We may even have $H_{\text{osc}} \lesssim H_{\text{th}}^{\text{max}}$ for some cases with smaller $\bar{h}_e \sim 10^{-5}$, $M/\lambda \lesssim 10^{18} \text{GeV}$ and higher $T_R \gtrsim 10^9 \text{GeV}$. Then, the AD-flaton oscillation to complete the leptogenesis is driven mainly by the thermal terms rather than the \bar{h}_e quartic term. In any case, the thermal terms do not provide severe suppression, but may even play a cooperative role for the flat manifold leptogenesis.

The magnitudes of AD-flaton fields are found to be scaled roughly as

$$|\phi_a| \propto H^{\alpha(t)}. \quad (5.42)$$

In Fig. 5.4, this redshift is shown typically for the case (1) of Table 5.1 in terms of the dimensionless variables $r_a(t) \propto H^{\alpha(t)-1/2}$. It is observed up to some fluctuating behavior that the power of redshift $\alpha(t)$ eventually changes as

$$\alpha(t) \approx \begin{cases} 1/2 & (t < H_{\text{osc}}^{-1}) \\ 2/3 & (H_{\text{osc}}^{-1} \lesssim t < H_{\text{th}}^{-1}) \\ 7/8 & (H_{\text{th}}^{-1} \lesssim t < m_{3/2}^{-1}) \\ 1 & (t \gtrsim m_{3/2}^{-1}) \end{cases}. \quad (5.43)$$

We here find especially that in the late epoch $H_{\text{th}}^{-1} \lesssim t < m_{3/2}^{-1}$ the evolution of the AD-flatons is determined dominantly by the thermal terms, while the leptogenesis is already completed during the epoch $H_{\text{osc}}^{-1} \lesssim t \lesssim H_{\text{th}}^{-1}$. The redshift of the AD-flaton fields changes

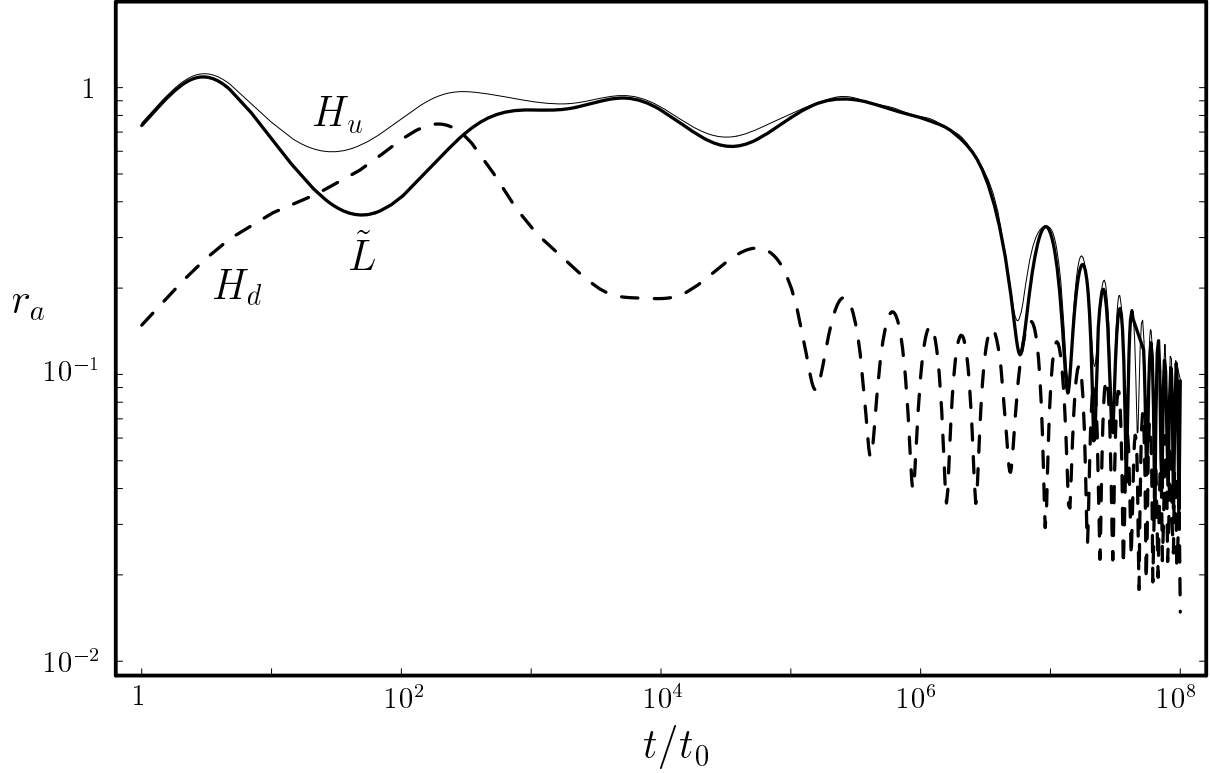


Figure 5.4: The time variation of the AD-flaton field magnitudes is shown in terms of r_a for the case (1) in Table 5.1.

finally to $|\phi_a| \propto H$, when the low-energy soft supersymmetry breaking mass terms become dominating.

In Fig. 5.5, the time variation of the scalar potential terms is also shown in terms of the dimensionless effective potential $U(\chi_a)$ in Eq.(5.21), where the symbols indicate the respective terms as $[c]$: Hubble induced negative mass-squared terms, $[a]$: Hubble induced A terms, $[F]$: $|F|^2$ terms from W_{non} , $[\bar{h}_e]$: $|\tilde{L}H_d|^2$ term, $[\text{th}]$: thermal terms. It is observed that in the epoch with $H > H_{\text{osc}}$ the $[c]$, $[a]$ and $[F]$ terms in V_{high} really dominate being scaled as H^0 in terms of the $U(\chi_a)$. Then, the $[\bar{h}_e]$ and even $[\text{th}]$ terms catches up them around $H \sim H_{\text{osc}}$. Soon after that, the $[\text{th}]$ term dominates over the $[\bar{h}_e]$ and $[c]$ terms, and the $[a]$ and $[F]$ terms including the lepton number violation decrease rapidly, so that the lepton number asymmetry is fixed to some non-zero value. The D^2 term is not shown here for simplicity. Since $D = (g^2 + g'^2)^{1/2}(|\tilde{L}|^2 - |H_u|^2 + |H_d|^2)$ is calculated by using the

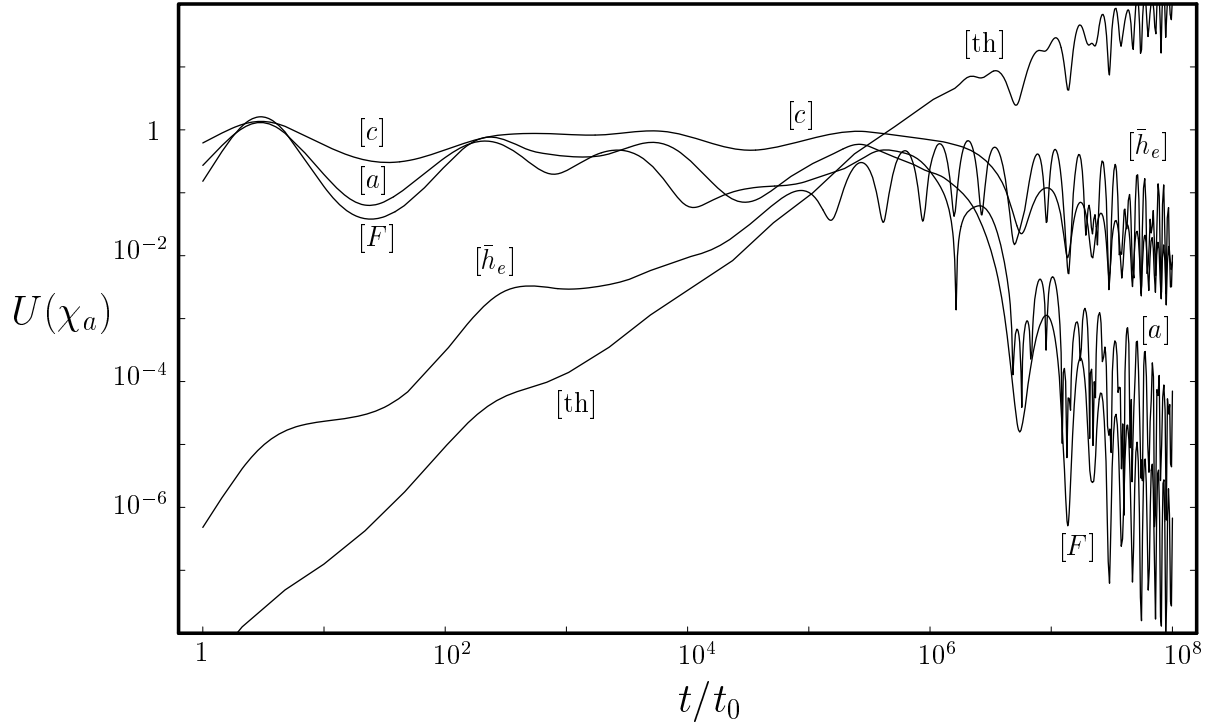


Figure 5.5: The time variation of the scalar potential terms is shown in terms of $U(\chi)$ for the case (1) in Table 5.1. The respective terms are indicated as [c]: Hubble induced negative mass-squared terms, [a]: Hubble induced A terms, [F]: $|F|^2$ terms from W_{non} , $[\bar{h}_e]$: $|\tilde{L}H_d|^2$ term, [th]: thermal terms.

solutions of $\phi_a(t)$, it is very sensitive to the numerical errors for the cancellation among $|\phi_a|^2$ terms by several orders. We have really checked that the D^2 contribution is smaller than 10^{-3} in the unit of $U(\chi_a)$, though it apparently exhibits a violent oscillation within this small range. This oscillating behavior is regarded to be an artifact within the intrinsic numerical errors due to the fine cancellation among the large $|\phi_a|^2$ terms in calculating the D term. The D^2 term is anyway small enough compared to the leading terms in the $U(\chi_a)$, and the D -flat condition (5.9) is maintained quite well through the evolution of the AD-flaton fields.

It has been argued that the comparability of $\lambda_{\tilde{L}}$ and λ_H is essential for the flat manifold leptogenesis. In Fig. 5.6, the resultant lepton number asymmetries are plotted depending on the ratio $\lambda_{\tilde{L}}/\lambda_H$, where the relevant parameter values are taken randomly. It is clearly seen that the flat manifold leptogenesis can be realized naturally under the

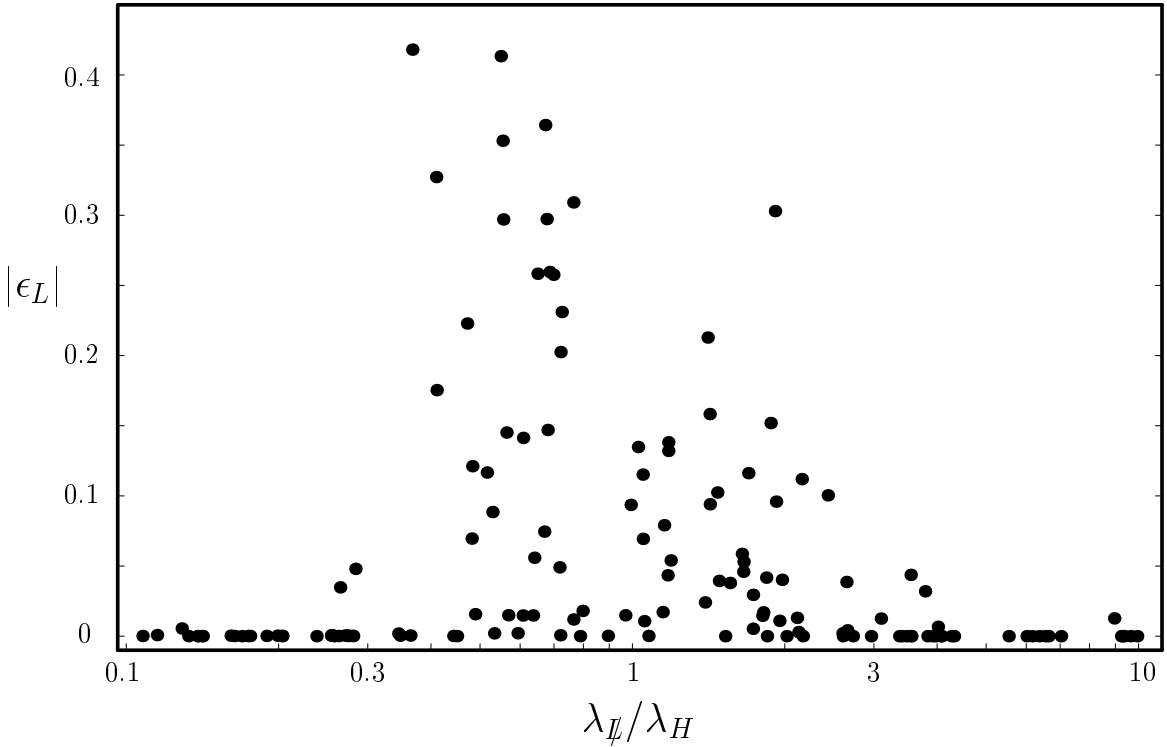


Figure 5.6: A scatter plot is presented for the resultant lepton number asymmetries depending on the ratio λ_{ψ}/λ_H , where the relevant parameter values are taken randomly.

flatness condition (5.10).

5.5 Summary

We have investigated the flat manifold leptogenesis a la Affleck-Dine with the slepton and Higgs fields, \tilde{L} , H_u , H_d , in the supersymmetric standard model. The multi-dimensional motion of these AD-flaton fields is indeed realized in the case that the $\tilde{L}H_u$ and H_uH_d directions are comparably flat with the relevant non-renormalizable superpotential terms. Soon after the inflation, the lepton number asymmetry appears to fluctuate due to this multi-dimensional motion involving certain CP violating phases. Then, the lepton number asymmetry is fixed to some significant non-zero value for the successful baryogenesis when the scalar fields begin to oscillate with rotating phases driven by the quartic coupling from the superpotential term $\bar{h}_e L H_d e^c$ with $\bar{h}_e \sim 10^{-5} - 10^{-3}$. The Hubble parameter H_{osc} at this epoch for the completion of leptogenesis is much larger than the gravitino

mass $m_{3/2} \sim 10^3 \text{GeV}$. The thermal terms do not alter this scenario of flat manifold leptogenesis in the early epoch. They may even play a cooperative role for leptogenesis. The lightest neutrino mass can be $m_{\nu_1} \sim 10^{-4} \text{eV}$, if the reheating temperature is allowed to be $T_R \sim 10^{10} \text{GeV}$. Clearly, this flat manifold leptogenesis is not restricted by the physics at the electroweak scale such as the low-energy supersymmetry breaking terms.

Chapter 6

Phenomenological signature

In this chapter, we examine phenomenological signatures in the leptogenesis models. The neutrino mass is considered to be one of them, as discussed above. We consider the lepton flavor violating processes such as $\mu \rightarrow 3e$ and $\mu \rightarrow e\gamma$ and the muon anomalous magnetic moment in this chapter. The additional coupling of the Higgs triplet with lepton and that of the right-handed neutrino with lepton introduce the lepton flavor violation. We study the phenomenological effects of the couplings.

6.1 Higgs Triplet model

In this section, we discuss the Higgs triplet model introduced in Chapter. 3. Lepton flavor violating processes are investigated in the light of neutrino masses and experimentally verifiable leptogenesis. Then, the Higgs triplet mass M_Δ is expected to be in the range of $1 - 100\text{TeV}$. The branching ratios of these charged lepton decays are evaluated in terms of M_Δ and the coupling $fL\Delta L$ of Higgs triplet Δ with lepton doublet pairs LL , which is proportional to the neutrino mass matrix. They may be reached in the future collider experiments. In particular, the $\mu \rightarrow 3e$ decay would be observed indicating the existence of Higgs triplets with $M_\Delta \sim 1 - 100\text{TeV}$ for $|f| \sim 0.1 - 1$, while the $\mu \rightarrow e\gamma$ decay can be significant irrespective of M_Δ in the supersymmetric model due to the flavor violation in the slepton mass matrices induced by the renormalization effects.

6.1.1 Lepton flavor violation

In this section, we examine the lepton flavor violating couplings provided with Higgs triplets, including the renormalization group effects.

The lepton basis is taken with the diagonal Yukawa coupling h at M_W in Eqs. (3.2) and (3.8):

$$h_{ij} = h_i \delta_{ij}. \quad (6.1)$$

(Henceforth M_W is omitted for the quantities at the electroweak scale.) Then, the lepton flavor violation, which is provided by the f coupling at M_W , is linked directly to the neutrino mass matrix, as seen in Eq. (3.6) [52, 53, 54]. This is a very interesting feature of Higgs triplet model. Specifically, the f coupling is given in terms of the neutrino masses (m_i), mixing angles (θ_{ij}) and CP violating phases ($\delta, \alpha_1, \alpha_2$) as

$$f_{ij} = |f| \sum_k U_{ik}^* U_{jk} \frac{m_k}{m_{\text{atm}}}, \quad (6.2)$$

where $m_{\text{atm}} \equiv \sqrt{\Delta m_{\text{atm}}^2}$ with $\Delta m_{\text{atm}}^2 \sim 3 \times 10^{-3} \text{eV}^2$. The explicit form of the Maki-Nakagawa-Sakata (MNS) matrix U (lepton mixing matrix) [55] is given in a review of the Particle Data [11]. The mean magnitude of the f coupling is given suitably by

$$|f| \equiv \frac{m_{\text{atm}}}{\sqrt{2} \langle \Delta^0 \rangle}, \quad (6.3)$$

which is constrained, as in Eq. (3.9), with $\langle \Delta^0 \rangle$ in terms of ξ and M_Δ .

The flavor violation appears in the h coupling at certain unification scale M_G such as the grand unification or gravitational scale through the renormalization effects. The renormalization group equations for the gauge couplings and gaugino masses are given by

$$16\pi^2 \frac{dg_1}{dt} = \left(\frac{33}{5} + \frac{9}{5} n_\Delta \right) g_1^3, \quad 16\pi^2 \frac{dM_1}{dt} = 2 \left(\frac{33}{5} + \frac{9}{5} n_\Delta \right) g_1^2 M_1, \quad (6.4)$$

$$16\pi^2 \frac{dg_2}{dt} = (1 + 2n_\Delta) g_2^3, \quad 16\pi^2 \frac{dM_2}{dt} = 2(1 + 2n_\Delta) g_2^2 M_2, \quad (6.5)$$

$$16\pi^2 \frac{dg_3}{dt} = -3g_3^3, \quad 16\pi^2 \frac{dM_3}{dt} = -6g_3^2 M_3, \quad (6.6)$$

where g_a and M_a are the gauge couplings and gaugino masses of $U(1)_Y, SU(2)_L$ and $SU(3)_C$ gauge group, respectively, $n_\Delta = 2$ is the contribution of the additional Higgs triplets, and t is the scaling parameter, which is related to the renormalization scale μ , $t = \ln \mu$. Here, we used the GUT convention for the normalization of the $U(1)_Y$ gauge coupling $g_Y^2 = (3/5)g_1^2$. Hence, the Higgs triplet would spoil the gauge coupling unification. However, if we introduce more multiplet to complete a certain representation of GUT, the gauge coupling unification is saved. For example, the introduction of extra

multiplets $(6, 1, -2/3)$ and $(3, 2, 1/6)$ saves the gauge coupling unification in the framework of the SU(5) GUT [52]. The renormalization group equations for the Yukawa couplings are given by

$$16\pi^2 \frac{df}{dt} = f \left(-\frac{9}{5}g_1^2 - 7g_2^2 + h^\dagger h + 6f^\dagger f + \text{Tr} f^\dagger f \right) + h^T h^* f, \quad (6.7)$$

$$16\pi^2 \frac{dh}{dt} = h \left[-\frac{9}{5}g_1^2 - 3g_2^2 + 3h^\dagger h + 3f^\dagger f + \text{Tr} \left(h^\dagger h + 3y_d^\dagger y_d \right) \right], \quad (6.8)$$

$$16\pi^2 \frac{dy_d}{dt} = y_d \left[-\frac{7}{15}g_1^2 - 3g_2^2 - \frac{16}{3}g_3^2 + y_d^\dagger y_d + y_u^\dagger y_u + \text{Tr} \left(y_e^\dagger y_e + 3y_d^\dagger y_d \right) \right], \quad (6.9)$$

$$16\pi^2 \frac{dy_u}{dt} = y_u \left(-\frac{13}{15}g_1^2 - 3g_2^2 - \frac{16}{3}g_3^2 + 3y_u^\dagger y_u + 3y_d^\dagger y_d + \text{Tr} y_u^\dagger y_u \right), \quad (6.10)$$

where y_d and y_u are the Yukawa couplings of the down and up quarks. The renormalization group equations for the masses of the sleptons and squarks are given by

$$\begin{aligned} 16\pi^2 \frac{dM_L^2}{dt} = & -\frac{6}{5}M_1^2 g_1^2 - 6M_2^2 g_2^2 + M_L^2 (h^\dagger h + 3f^\dagger f) + (h^\dagger h + 3f^\dagger f) M_L^2 \\ & + 2(h^\dagger M_{H_d}^2 h + h^\dagger M_{\tilde{e}^c} h + 3f^\dagger M_{\tilde{L}}^{2T} f + 3f^\dagger M_{\tilde{\delta}}^2 f) \\ & + 2(A_h^\dagger A_h + 3A_f^\dagger A_f), \end{aligned} \quad (6.11)$$

$$\begin{aligned} 16\pi^2 \frac{dM_{\tilde{e}^c}^2}{dt} = & -\frac{24}{5}M_1^2 g_1^2 + (2M_{\tilde{e}^c}^2 + 4M_{H_d}^2) h h^\dagger \\ & + 2h h^\dagger M_{\tilde{e}^c} + 4h^\dagger M_{\tilde{e}^c} h + 4A_h A_h^\dagger, \end{aligned} \quad (6.12)$$

$$\begin{aligned} 16\pi^2 \frac{dM_{\tilde{d}^c}^2}{dt} = & -\frac{8}{15}M_1^2 g_1^2 - \frac{32}{3}M_3^2 g_3^2 + 2M_{\tilde{d}^c}^2 y_d y_d^\dagger + 2y_d y_d^\dagger M_{\tilde{d}^c}^2 \\ & + 4(y_d M_{H_d}^2 y_d^\dagger + y_d M_{\tilde{q}} y_d^\dagger) + 4A_d A_d^\dagger, \end{aligned} \quad (6.13)$$

$$\begin{aligned} 16\pi^2 \frac{dM_{\tilde{u}^c}^2}{dt} = & -\frac{32}{5}M_1^2 g_1^2 - \frac{32}{3}M_3^2 g_3^2 + (2M_{\tilde{u}^c}^2 + 4M_{H_u}^2) y_u y_u^\dagger \\ & + 2y_u y_u^\dagger M_{\tilde{u}^c} + 4y_u M_{\tilde{q}} y_u^\dagger + 4A_u A_u^\dagger, \end{aligned} \quad (6.14)$$

$$\begin{aligned} 16\pi^2 \frac{dM_{\tilde{q}}^2}{dt} = & -\frac{2}{15}M_1^2 g_1^2 - 6M_2^2 g_2^2 - \frac{32}{3}M_3^2 g_3^2 \\ & + (M_{\tilde{q}}^2 + 2M_{H_u}^2) y_u^\dagger y_u + (M_{\tilde{q}}^2 + 2M_{H_d}^2) y_d^\dagger y_d + (y_u^\dagger y_u + y_d^\dagger y_d) M_{\tilde{q}}^2 \\ & + 2y_u^\dagger M_{\tilde{u}^c} y_u + 2y_d^\dagger M_{\tilde{d}^c} y_d + 2A_u A_u^\dagger + 2A_d A_d^\dagger, \end{aligned} \quad (6.15)$$

where $M_{\tilde{\delta}}$ is the soft mass for the Higgs triplet Δ and A_x is the soft-breaking trilinear

coupling of x term. The renormalization group equations for the soft masses are given by

$$16\pi^2 \frac{dM_\delta^2}{dt} = -\frac{24}{15}M_1^2 g_1^2 - 16M_2^2 g_2^2 + 2 \left(M_\delta^2 \text{Tr} f^\dagger f + 2\text{Tr} f^\dagger M_L^2 f + \text{Tr} A_f^\dagger A_f \right), \quad (6.16)$$

$$16\pi^2 \frac{dM_\delta^2}{dt} = -\frac{24}{15}M_1^2 g_1^2 - 16M_2^2 g_2^2, \quad (6.17)$$

$$16\pi^2 \frac{dM_{H_d}^2}{dt} = -\frac{6}{5}M_1^2 g_1^2 - 6M_2^2 g_2^2 + 2M_{H_d}^2 \left(\text{Tr} h h^\dagger + 3\text{Tr} y_d y_d^\dagger \right) + 2 \left[3\text{Tr} \left(y_d^\dagger M_{\tilde{d}^c}^2 y_d + h^\dagger M_L^2 h \right) \right] + 2 \left(\text{Tr} A_d A_d^\dagger + \text{Tr} A_h A_h^\dagger \right), \quad (6.18)$$

$$16\pi^2 \frac{dM_{H_u}^2}{dt} = -\frac{6}{5}M_1^2 g_1^2 - 6M_2^2 g_2^2 + 6M_{H_u}^2 \text{Tr} y_u y_u^\dagger + 6\text{Tr} \left(y_u^\dagger M_{\tilde{u}^c}^2 y_u + y_u M_{\tilde{q}}^2 y_u^\dagger \right) + 6\text{Tr} A_u A_u^\dagger, \quad (6.19)$$

where M_δ is the soft mass for the Higgs triplet $\bar{\Delta}$. The renormalization group equation for the soft-breaking trilinear coupling are given by,

$$16\pi^2 \frac{dA_f}{dt} = 2f \left(\frac{9}{5}M_1 g_1^2 + 7M_2 g_2^2 + 3\text{Tr} f^\dagger A_f \right) + (h^T h^* + 9f f^\dagger) A_f + A_f \left(-\frac{9}{5}g_1^2 - 7g_2^2 + h^\dagger h + 9f^\dagger f + \text{Tr} f^\dagger f \right), \quad (6.20)$$

$$16\pi^2 \frac{dA_h}{dt} = 2h \left[\frac{9}{5}M_1 g_1^2 + 3M_2 g_2^2 + 2h^\dagger A_h + 3f^\dagger A_f + \text{Tr} \left(A_h h^\dagger + 3A_d Y_d^\dagger \right) \right] + A_h \left[-\frac{9}{5}g_1^2 - 3g_2^2 + 5h^\dagger h + 3f^\dagger f + \text{Tr} \left(h h^\dagger + 3y_d y_d^\dagger \right) \right], \quad (6.21)$$

$$16\pi^2 \frac{dA_d}{dt} = 2y_d \left[\frac{7}{15}M_1 g_1^2 + 3M_2 g_2^2 + \frac{16}{3}M_3 g_3^2 + 2y_d^\dagger A_d + y_u^\dagger A_u + \text{Tr} \left(A_h h^\dagger + 3A_d y_d^\dagger \right) \right] + A_d \left[-\frac{7}{15}g_1^2 - 3g_2^2 - \frac{16}{3}g_3^2 + 5y_d^\dagger y_d + y_u^\dagger y_u + \text{Tr} \left(h h^\dagger + 3y_d y_d^\dagger \right) \right], \quad (6.22)$$

$$16\pi^2 \frac{dA_u}{dt} = 2y_u \left[\frac{13}{15}M_1 g_1^2 + 3M_2 g_2^2 + \frac{16}{3}M_3 g_3^2 + 2y_u^\dagger A_u + y_d^\dagger A_d + 3\text{Tr} A_u y_u^\dagger \right] + A_u \left(-\frac{13}{15}g_1^2 - 3g_2^2 - \frac{16}{3}g_3^2 + 5y_u^\dagger y_u + y_d^\dagger y_d + 3\text{Tr} y_u y_u^\dagger \right), \quad (6.23)$$

In the bottom-up view point $M_W \rightarrow M_G$, the relevant couplings at M_G are evaluated with those at M_W as

$$h_{ij}(M_G) = c_{hi} h_i \delta_{ij} + (\Delta_f h)_{ij}, \quad (6.24)$$

$$f_{ij}(M_G) = c_{fij} f_{ij} + (\Delta_f f)_{ij}, \quad (6.25)$$

where the sum is not taken over i, j . The factors $c_{hi}, c_{fij} \sim 1$ are provided by the gauge and h couplings. The remaining terms provided by the f coupling are calculated in the leading-log approximation as

$$(\Delta_f h)_{ij} \simeq (3/2)h_i (f^\dagger f)_{ij} t_G, \quad (6.26)$$

$$(\Delta_f f)_{ij} \simeq 3 (f f^\dagger f)_{ij} t_G, \quad (6.27)$$

where

$$t_G \equiv \frac{1}{8\pi^2} \ln(M_G/M_W) \sim 0.4. \quad (6.28)$$

The flavor violation also appears in the soft supersymmetry breaking terms. We may assume the universality of the soft supersymmetry breaking terms at the unification scale M_G , i.e., the soft masses of scalar fields are given by the common mass m_0 , and the A -terms are given by $a_0 m_0$ with $a_0 \sim 1$. Then, in the top-down view point $M_G \rightarrow M_W$ the soft mass terms at M_W are calculated particularly for the left-handed slepton doublets \tilde{L} and the right-handed charged slepton singlets \tilde{l}^c [52] as

$$(M_{\tilde{L}}^2)_{ij} = c_{\tilde{L}} m_0^2 \delta_{ij} + (\Delta_{h+f} M_{\tilde{L}}^2)_{ij}, \quad (6.29)$$

$$(M_{\tilde{l}^c}^2)_{ij} = c_{\tilde{l}^c} m_0^2 \delta_{ij} + (\Delta_h M_{\tilde{l}^c}^2)_{ij}. \quad (6.30)$$

Here, the contributions of the gauge couplings are included in the factors $c_{\tilde{L}}, c_{\tilde{l}^c} \sim 1$, and those of the h and f couplings are given by

$$\Delta_{h+f} M_{\tilde{L}}^2 \simeq -m_0^2 [(3 + a_0^2)h^\dagger(M_G)h(M_G) + (9 + 3a_0^2)f^\dagger(M_G)f(M_G)] t_G, \quad (6.31)$$

$$\Delta_h M_{\tilde{l}^c}^2 \simeq -m_0^2 (6 + 2a_0^2)h^\dagger(M_G)h(M_G) t_G. \quad (6.32)$$

The A_h term of the h coupling is also given at M_W by

$$(A_h)_{ij} = a_h m_0 h_{ij}(M_G) + (\Delta A_h)_{ij} \quad (6.33)$$

with $a_h \sim a_0$ including the effects of gauge couplings and

$$\Delta A_h \simeq -(9/2)a_0 m_0 h(M_G) [h^\dagger(M_G)h(M_G) + f^\dagger(M_G)f(M_G)] t_G. \quad (6.34)$$

The charged slepton mass matrix is given in the basis of $(\tilde{l}, \tilde{l}^{c*})$ by

$$\mathcal{M}_{\tilde{l}}^2 = \begin{pmatrix} M_{\tilde{l}LL}^2 & M_{\tilde{l}LR}^2 \\ M_{\tilde{l}RL}^2 & M_{\tilde{l}RR}^2 \end{pmatrix}, \quad (6.35)$$

where the submatrices are given by

$$M_{iLL}^2 = M_L^2 + M_l^2, \quad (6.36)$$

$$M_{iRR}^2 = M_{lc}^2 + M_l^2, \quad (6.37)$$

$$M_{iLR}^2 = M_{iRL}^{2\dagger} = \langle H_d \rangle A_h + \tan \beta \mu M_l, \quad (6.38)$$

with $\tan \beta \equiv \langle H_u \rangle / \langle H_d \rangle$. The sneutrino mass matrix is also given by

$$M_{\tilde{\nu}}^2 = M_L^2, \quad (6.39)$$

where the tiny lepton number violating term related to the Majorana neutrino mass matrix is neglected in a good approximation. The flavor changing components are particularly calculated in the leading order of $|f|^2$ as

$$\frac{(M_{iLL}^2)_{ij}|_{i \neq j}}{m_0^2} \simeq -3(3 + a_0^2)(1 + c_{hi}h_i^2 t_G) t_G (f^\dagger f)_{ij}, \quad (6.40)$$

$$\frac{(M_{iRR}^2)_{ij}|_{i \neq j}}{m_0^2} \simeq -6(3 + a_0^2) c_{hi} h_i^2 t_G^2 (f^\dagger f)_{ij}, \quad (6.41)$$

$$\frac{(M_{iLR}^2)_{ij}|_{i \neq j}}{m_0^2} \simeq -(9/2) a_0 c_{hi} \frac{m_{l_i}}{m_0} (1 + 3h_i^2 t_G) t_G (f^\dagger f)_{ij}, \quad (6.42)$$

$$\frac{M_{\tilde{\nu}}^2|_{i \neq j}}{m_0^2} \simeq -3(3 + a_0^2)(1 + c_{hi}h_i^2 t_G) t_G (f^\dagger f)_{ij}, \quad (6.43)$$

where the values of f and h couplings are taken at M_W . It is noticed that these leading contributions of flavor violation are determined essentially by $t_G(f^\dagger f)_{ij}$ ($i \neq j$) [52] with the significant log factor $t_G \sim 0.4$ in the present scheme of $M_\Delta \sim 10^3 \text{ GeV}$.

6.1.2 Lepton flavor violating processes

We investigate the charged lepton processes in order, to which the supersymmetric Higgs triplets in TeV region may provide significant contributions. Such effects are expected to show the evidence of Higgs triplets particularly related to the neutrino masses and mixings.

The leading contribution to the $\mu \rightarrow 3e$ decay is provided at the tree level mediated by the Higgs triplet as shown in Fig. 6.1. The supersymmetric contributions, on the other hand, appear at the one-loop level through the flavor violation in the slepton sectors [56]. They are, however, negligible compared to the tree-level contribution for $M_\Delta \sim 10^3 \text{ GeV}$.

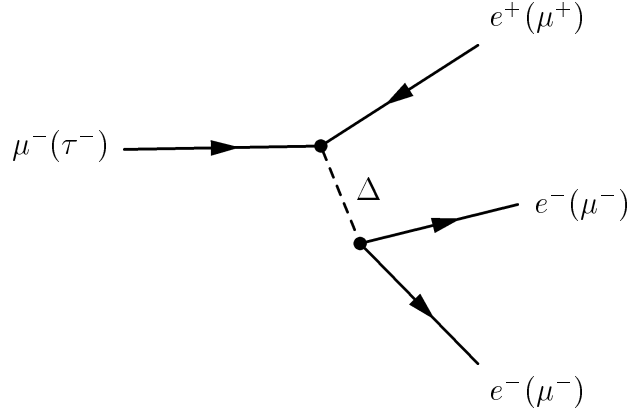


Figure 6.1: The tree diagram mediated by the Higgs triplet is shown.

The branching ratio is calculated [57] as

$$\begin{aligned}
 \text{Br}(\mu \rightarrow 3e) &= \frac{|f_{ee}^* f_{\mu e}|^2}{8g^4} \left(\frac{M_W}{m_\Delta} \right)^4 \\
 &= 3 \times 10^{-13} \left(\frac{1\text{TeV}}{m_\Delta} \right)^4 \left(\frac{|I_{\mu \rightarrow 3e}|}{0.01} \right)^2 \left(\frac{|f|}{0.1} \right)^4,
 \end{aligned} \tag{6.44}$$

where

$$f_{ee}^* f_{\mu e} \equiv I_{\mu \rightarrow 3e} |f|^2, \tag{6.45}$$

and the mass of scalar Higgs triplet is given including the contribution of soft supersymmetry breaking ($c_\Delta \sim 1$) by

$$m_\Delta = \sqrt{M_\Delta^2 + c_\Delta m_0^2}. \tag{6.46}$$

The experimental bound is, on the other hand, placed as $\text{Br}(\mu \rightarrow 3e) < 1.0 \times 10^{-12}$ [58]. The flavor changing factor $|I_{\mu \rightarrow 3e}| = 0.01$ is taken in Eq. (6.44) as a reference value. Its value is evaluated precisely from Eq. (6.3) with the neutrino masses and MNS matrix U , which are inferred from the data of neutrino experiments [2, 3, 4, 48]. Numerically, we have $|I_{\mu \rightarrow 3e}| \lesssim 0.03$ (HI), $\lesssim 0.06$ (DG), and $\lesssim 0.2$ (IH), respectively, for the hierarchical (HI) case $m_1 \ll m_2 \ll m_3$, the degenerate (DG) case $m_1 \sim m_2 \sim m_3$, and the inverted-hierarchical (IH) case $m_1 \sim m_2 \gg m_3$.

A detailed estimate of $\text{Br}(\mu \rightarrow 3e)$ is presented in Fig. 6.2 depending on the Higgs triplet mass m_Δ . Typical values of the neutrino masses and mixings are taken in the HI

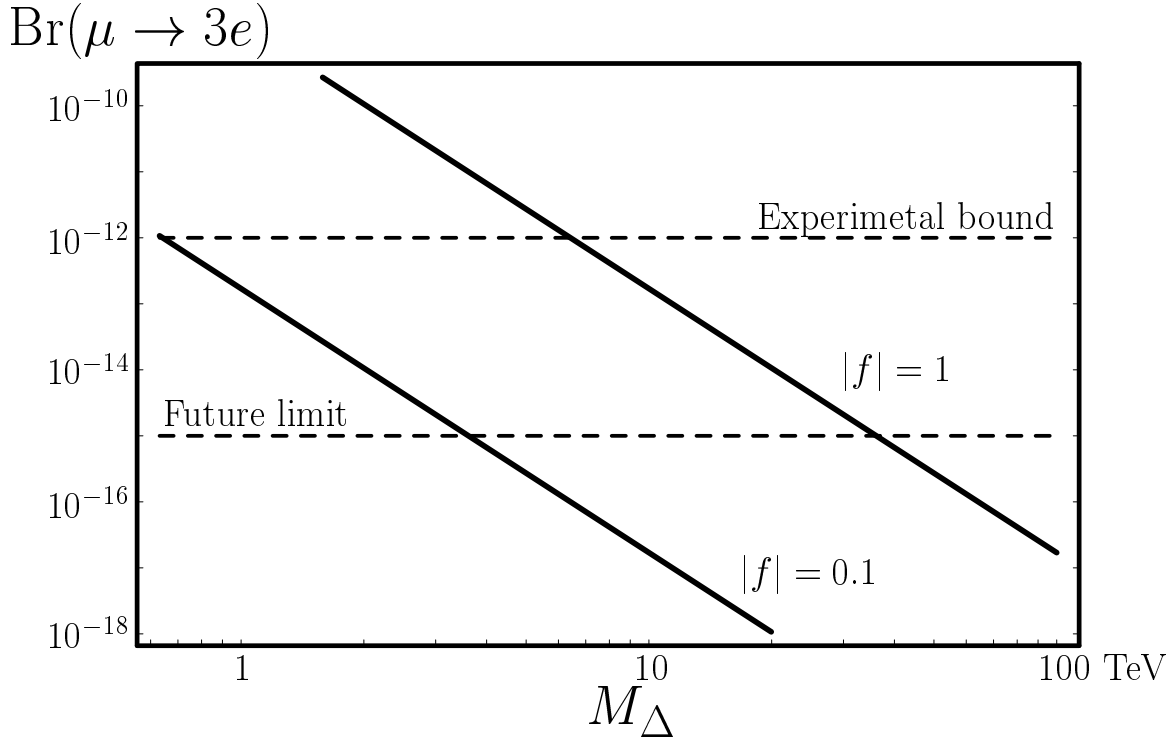


Figure 6.2: A typical estimate of the branching ratio of $\mu \rightarrow 3e$ is shown depending on the Higgs triplet mass m_Δ for $|f| = 1$ and $|f| = 0.1$.

case as

$$(m_1, m_2, m_3) = (10^{-3}\text{eV}, 8 \times 10^{-3}\text{eV}, 5 \times 10^{-2}\text{eV}),$$

$$(\sin \theta_{12}, \sin \theta_{23}, \sin \theta_{13}) = (1/2, 1/\sqrt{2}, 0.1),$$

and the zero CP violating phases, which provides

$$I_{\mu \rightarrow 3e} = 0.7 \times 10^{-2}.$$

The upper and lower solid lines represent the results for $|f| = 1$ and $|f| = 0.1$, respectively. The present experimental bound 1.0×10^{-12} and a future sensitivity $\sim 10^{-15}$ achieved by proposed experiments [59] are also shown with the upper and lower dashed lines, respectively. It is interesting here that through the $\mu \rightarrow 3e$ decay the evidence of Higgs triplets may be seen up to the mass $M_\Delta \simeq m_\Delta = 100\text{TeV}$ for $|f| \sim 1$. This will be promising especially for obtaining the experimental evidence of leptogenesis in TeV region with the supersymmetric Higgs triplets. On the other hand, as discussed later, the Higgs

triplet contributions to the $\mu \rightarrow e\gamma$ decay are significant even for $M_\Delta \gg 100\text{TeV}$ through renormalization effects.

The branching ratio of $\tau \rightarrow 3\mu$ is also estimated as

$$\text{Br}(\tau \rightarrow 3\mu) = 2 \times 10^{-11} \left(\frac{1\text{TeV}}{m_\Delta} \right)^4 \left(\frac{|I_{\tau \rightarrow 3\mu}|}{0.2} \right)^2 \left(\frac{|f|}{0.1} \right)^4, \quad (6.47)$$

where

$$f_{\mu\mu}^* f_{\tau\mu} \equiv I_{\tau \rightarrow 3\mu} |f|^2. \quad (6.48)$$

We have numerically $|I_{\tau \rightarrow 3\mu}| \simeq 0.1 - 0.3$ (HI), $\simeq 0.1 - 0.2$ (DG), and $\simeq 0.1 - 0.3$ (IH), respectively. This Higgs triplet contribution to the $\tau \rightarrow 3\mu$ decay is far below the experimental bound $\text{Br}(\tau \rightarrow 3\mu) < 3.8 \times 10^{-7}$ [60] for $m_\Delta \sim 1\text{TeV}$ and $|f| \lesssim 0.1$. Similar estimates are made for the leptonic three-body decays, $\tau \rightarrow \bar{e}\mu\mu$, and so on [54].

The flavor changing radiative decays such as $\mu \rightarrow e\gamma$ and $\tau \rightarrow \mu\gamma$ are induced by the one-loop diagrams as shown in Fig. 6.3. In the Higgs triplet model, the non-supersymmetric contribution is given by the L - Δ loop, which is almost independent of the mass of the internal lepton for $m_l \ll m_\Delta$ [53, 54]. The supersymmetric partner of this contribution is given by the \tilde{L} - $\tilde{\Delta}$ loop. The flavor violation appears even in the internal slepton line through the renormalization effects, though its contribution is sufficiently small for $|f| \lesssim 10^{-1}$. The flavor violation in the slepton mass matrices also provides the supersymmetric contributions of the \tilde{l} - $\tilde{\chi}^0$ (neutralino) loop and the $\tilde{\nu}$ - $\tilde{\chi}^-$ (chargino) loop, as in the minimal supersymmetric standard model [56]. For the case of very large Higgs triplet mass such as $M_\Delta \sim 10^{11} - 10^{14}\text{GeV}$, the \tilde{l} - $\tilde{\chi}^0$ and $\tilde{\nu}$ - $\tilde{\chi}^-$ contributions are dominant [52], while the L - Δ and \tilde{L} - $\tilde{\Delta}$ contributions are negligible due to the suppression factor $(m_0/M_\Delta)^2$. On the other hand, for the case of $M_\Delta \sim m_0 \sim 1\text{TeV}$, as motivated for the direct detection of Higgs triplet, these contributions may be comparable.

In this interesting case of $M_\Delta \sim m_0 \sim 1\text{TeV}$, we investigate the charged lepton radiative decays and their intimate relation to the leptonic three-body decays of charged leptons through the neutrino mass matrix proportional to the f coupling. In particular, the supersymmetric contributions of the \tilde{l} - $\tilde{\chi}^0$ and $\tilde{\nu}$ - $\tilde{\chi}^-$ loops may become most significant for certain range of the model parameters, while those of the \tilde{L} - $\tilde{\Delta}$ loop are comparable to or even larger than their non-supersymmetric partners of the L - Δ loop for $M_{\tilde{\Delta}} = M_\Delta < m_\Delta$. Then, the relations between the decays $\mu \rightarrow 3e$, etc. and the decays $\mu \rightarrow e\gamma$, etc., as found in the non-supersymmetric case [53, 54], may be modified to some extent, since

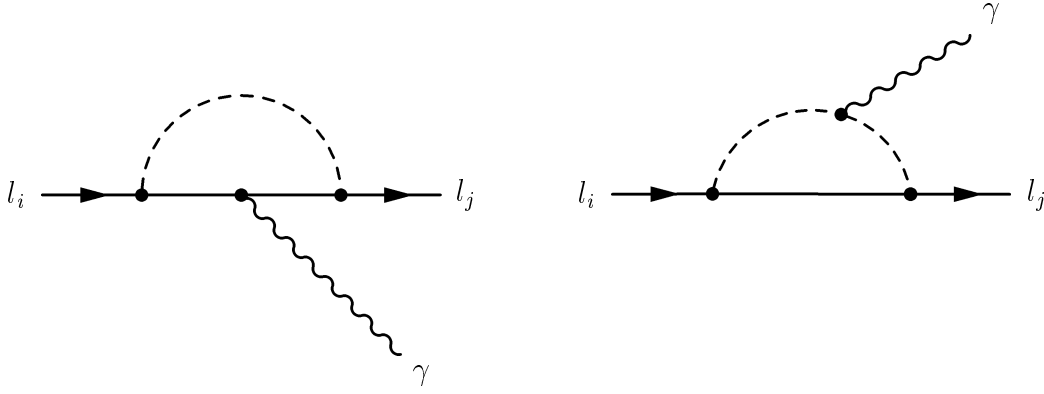


Figure 6.3: The loop diagrams contributing $l_i \rightarrow l_j \gamma$ process is shown.

the radiative decays are enhanced due to the supersymmetric contributions [52] with the log-factor $t_G \sim 0.4$.

We now estimate the branching ratio of $\mu \rightarrow e \gamma$ decay. The decay amplitude is generally given by

$$T(\mu \rightarrow e \gamma) = e \epsilon^{\alpha*} \bar{u}_e [i \sigma_{\alpha\beta} q^\beta (A_L P_L + A_R P_R)] u_\mu. \quad (6.49)$$

Then, the decay rate is given by

$$\Gamma(\mu \rightarrow e \gamma) = \frac{e^2}{16\pi} m_\mu^3 (|A_L|^2 + |A_R|^2), \quad (6.50)$$

and the branching ratio is calculated by

$$\text{Br}(\mu \rightarrow e \gamma) = \frac{\Gamma(\mu \rightarrow e \gamma)}{G_F^2 m_\mu^5 / 192 \pi^3}. \quad (6.51)$$

The left-handed and right-handed decay amplitudes are calculated in the leading order by combining the one-loop contributions:

$$A_{L,R} = A_{L,R}^{\tilde{\chi}^0} + A_{L,R}^{\tilde{\chi}^-} + A_{L,R}^\Delta + A_{L,R}^{\tilde{\Delta}}. \quad (6.52)$$

The formulas for calculating the contributions $A_{L,R}^{\tilde{\chi}^0}$ and $A_{L,R}^{\tilde{\chi}^-}$ of the neutralinos and charginos are presented in the literature [56]. The contributions $A_{L,R}^\Delta$ and $A_{L,R}^{\tilde{\Delta}}$ of the supersymmetric Higgs triplets are calculated as later. Then, the decay amplitudes are given specifically as

$$A_L = \frac{m_\mu}{32\pi^2} I_{\mu \rightarrow e \gamma} |f|^2 \left[\frac{G_L^{\tilde{\chi}}}{m_0^2} + \frac{G_L^\Delta}{m_\Delta^2} + \frac{G_L^{\tilde{\Delta}}}{M_\Delta^2} \right], \quad (6.53)$$

$$A_R = \frac{m_\mu}{32\pi^2} I_{\mu \rightarrow e \gamma} |f|^2 \left[\frac{G_R^{\tilde{\chi}}}{m_0^2} + \frac{G_R^\Delta}{m_\Delta^2} + \frac{G_R^{\tilde{\Delta}}}{M_\Delta^2} \right], \quad (6.54)$$

where

$$\sum_k f_{ek}^* f_{\mu k} \equiv I_{\mu \rightarrow e\gamma} |f|^2. \quad (6.55)$$

These leading contributions to the decay amplitudes are proportional to the flavor changing factor $(f^\dagger f)_{e\mu} = \sum_k f_{ek}^* f_{\mu k}$ ($f = f^\Gamma$), as seen in Eq. (6.55). This is realized for the $\tilde{l}-\tilde{\chi}^0$ and $\tilde{\nu}-\tilde{\chi}^-$ loops by using the mass-insertion method with the flavor changing elements of slepton mass matrices in Eqs. (6.40) – (6.43). As for the L - Δ and \tilde{L} - $\tilde{\Delta}$ loops, the flavor-dependence of the masses of intermediate states can be neglected in a good approximation. Then, the factor $(f^\dagger f)_{e\mu}$ is extracted from the two vertices in the loop diagram. It should, however, be remarked that the contribution of $k = \tau$ in Eq. (6.55) may be modified to some extent for $\tan \beta \gtrsim 30$. This is because the renormalization effects on the $\tilde{\tau}$ and $\tilde{\nu}_\tau$ masses by the Yukawa coupling h_τ becomes significant especially for the $\tilde{\tau}$ - $\tilde{\Delta}^{++}$ and $\tilde{\nu}_\tau$ - $\tilde{\Delta}^+$ loops. Furthermore, the renormalization effects may modify significantly the flavor structure of these amplitudes for the large f coupling as $|f| \sim 0.5 - 1$. At present, there is no strong motivation to pursue such special cases.

As a typical example, the factors $G_{L,R}^{\tilde{\chi}}$, $G_{L,R}^\Delta$ and $G_{L,R}^{\tilde{\Delta}}$ are evaluated numerically as

$$\begin{aligned} G_L^{\tilde{\chi}} &= 0.20, \quad G_L^\Delta = 0.8 \times 10^{-3}, \quad G_L^{\tilde{\Delta}} = 1.0 \times 10^{-3}, \\ G_R^{\tilde{\chi}} &= 1.35, \quad G_R^\Delta = 0.17, \quad G_R^{\tilde{\Delta}} = 0.21, \end{aligned} \quad (6.56)$$

by taking the parameters as $M_{\tilde{\Delta}} = M_\Delta = 700\text{GeV}$, $m_\Delta = 1000\text{GeV}$, $m_0 = 700\text{GeV}$, $a_0 = 1$, $\tan \beta = 3$, $\mu = 1000\text{GeV}$, $M_1 = 300\text{GeV}$ and $M_2 = 600\text{GeV}$ (M_1 and M_2 are the gaugino masses of $U(1)_Y$ and $SU(2)_L$, respectively). Here, $G_R^{\tilde{\chi}}$ is somewhat enhanced by $\tan \beta$ coming from the $\tilde{\mu}_L$ - $\tilde{\mu}_R$ flip with $(M_{\tilde{L}LR}^2)_{\mu\mu}$ and the μ_R - $\tilde{\mu}_L$ - \tilde{H}_d^0 vertex [52, 56]. The small ratio $G_L^\Delta/G_R^\Delta = G_L^{\tilde{\Delta}}/G_R^{\tilde{\Delta}} = m_e/m_\mu$ is attributed to the chirality flip of the external charged leptons. Then, the branching ratio is estimated as

$$\text{Br}(\mu \rightarrow e\gamma) = 7 \times 10^{-12} \left(\frac{G}{3}\right)^2 \left(\frac{1\text{TeV}}{m_\Delta}\right)^4 \left(\frac{|I_{\mu \rightarrow e\gamma}|}{0.1}\right)^2 \left(\frac{|f|}{0.1}\right)^4, \quad (6.57)$$

which should be compared to the experimental bound $\text{Br}(\mu \rightarrow e\gamma) < 1.2 \times 10^{-11}$ [11]. Here, we take $G = 3$ as a reference value for

$$G \equiv \left(\sum_{K=L,R} \left| r_{\tilde{\chi}} G_K^{\tilde{\chi}} + G_K^\Delta + r_{\tilde{\Delta}} G_K^{\tilde{\Delta}} \right|^2 \right)^{1/2} \quad (6.58)$$

with $r_{\tilde{\chi}} \equiv (m_{\Delta}/m_0)^2$ and $r_{\tilde{\Delta}} \equiv (m_{\Delta}/M_{\Delta})^2$. This net G factor is actually calculated depending on the various parameters, as seen from Eq. (6.56). It is usually of $O(1)$ for the reasonable parameter range. The weights of supersymmetric contributions are relatively enhanced in G due to $r_{\tilde{\chi}}, r_{\tilde{\Delta}} > 1$ for $m_{\Delta} > m_0, M_{\Delta}$ from Eq. (6.46), compared to the non-supersymmetric ones. We have also numerically $|I_{\mu \rightarrow e\gamma}| \lesssim 0.2$ (HI), $\lesssim 0.1$ (DG), and $\lesssim 0.2$ (IH), respectively. This expected branching ratio $\text{Br}(\mu \rightarrow e\gamma)$ really becomes larger by one order or so due to the supersymmetric contributions than that of the non-supersymmetric case [53, 54]. It should also be remarked that the $\mu \rightarrow e\gamma$ decay can be a good test to distinguish the supersymmetric Higgs triplets from the non-supersymmetric ones. This is because in the non-supersymmetric model the left-handed decay amplitude $A_L = A_L^{\Delta}$ is much smaller than the right-handed one $A_R = A_R^{\Delta}$ due to the suppression with m_e/m_{μ} .

We here present the formulas for calculating the one-loop contributions of supersymmetric Higgs triplets to the decay amplitudes of $l_j \rightarrow l_i + \gamma$. The charged slepton mass eigenstates are determined by diagonalizing the mass matrix $\mathcal{M}_{\tilde{l}}^2$ in Eq. (6.35) with a unitary matrix $U^{\tilde{l}}$:

$$\tilde{l}_a = U_{ai}^{\tilde{l}} \tilde{l}_{Li} + U_{ai+3}^{\tilde{l}} \tilde{l}_{Ri} \quad (a = 1 - 6), \quad (6.59)$$

where $\tilde{l}_L \equiv \tilde{l}$ and $\tilde{l}_R \equiv \tilde{l}^{c*}$. The sneutrino mass eigenstates are determined by diagonalizing the mass matrix $\mathcal{M}_{\tilde{\nu}}^2$ in Eq. (6.39) with a unitary matrix $U^{\tilde{\nu}}$:

$$\tilde{\nu}_b = U_{bi}^{\tilde{\nu}} \tilde{\nu}_{Li} \quad (b = 1 - 3), \quad (6.60)$$

where $\tilde{\nu}_{Li} \equiv \tilde{\nu}_i$. The interactions of bileptons with scalar Higgs triplet are given from Eq. (3.2) by

$$\begin{aligned} \mathcal{L}_{\Delta} = & -\frac{1}{\sqrt{2}} f_{ij} \bar{l}_i^c P_L l_j \Delta^{++} - \frac{1}{2} f_{ij} \bar{l}_i^c P_L \nu_j \Delta^+ \\ & -\frac{1}{2} f_{ij} \bar{\nu}_i^c P_L l_j \Delta^+ + \frac{1}{\sqrt{2}} f_{ij} \bar{\nu}_i^c P_L \nu_j \Delta^0 + \text{H.c.} \end{aligned} \quad (6.61)$$

The interactions of bisleptons with Higgsino triplet are given in terms of the mass eigenstates in Eqs. (6.59) and (6.60) by

$$\begin{aligned} \mathcal{L}_{\tilde{\Delta}} = & -\sqrt{2} \mathcal{F}_{ia}^{\tilde{l}} \bar{l}_i^c P_L \tilde{\Delta}^{++} \tilde{l}_a - \mathcal{F}_{ib}^{\tilde{l}} \bar{l}_i^c P_L \tilde{\Delta}^+ \tilde{\nu}_b \\ & -\mathcal{F}_{ia}^{\tilde{l}} \bar{\nu}_i^c P_L \tilde{\Delta}^+ \tilde{l}_a + \sqrt{2} \mathcal{F}_{ib}^{\tilde{\nu}} \bar{\nu}_i^c P_L \tilde{\Delta}^0 \tilde{\nu}_b + \text{H.c.}, \end{aligned} \quad (6.62)$$

where

$$\mathcal{F}_{ia}^{\tilde{l}} = (fU^{\tilde{l}\dagger})_{ia}, \quad \mathcal{F}_{ib}^{\tilde{\nu}} = (fU^{\tilde{\nu}\dagger})_{ib}. \quad (6.63)$$

The contributions of L - Δ loops are calculated by using the interactions in Eq. (6.61) as

$$A_R^\Delta = \frac{1}{32\pi^2} \frac{m_{l_j}}{m_\Delta^2} \sum_k f_{ik}^* f_{jk} [F_1(0) + 4F_1(x_k) - 2F_2(x_k)], \quad (6.64)$$

$$A_L^\Delta = (m_{l_i}/m_{l_j}) A_R^\Delta, \quad (6.65)$$

where $x_k \equiv (m_{l_k}/m_\Delta)^2$ with the scalar Higgs triplet mass m_Δ in Eq. (6.46). The functions F_1 and F_2 are given by

$$F_1(x) = \frac{1 - 6x + 3x^2 + 2x^3 - 6x^2 \ln x}{6(1-x)^4}, \quad (6.66)$$

$$F_2(x) = \frac{2 + 3x - 6x^2 + x^3 + 6x \ln x}{6(1-x)^4}. \quad (6.67)$$

The contributions of \tilde{L} - $\tilde{\Delta}$ loops are also calculated by using the interactions in Eq. (6.62) as

$$A_R^{\tilde{\Delta}} = \frac{1}{32\pi^2} \frac{m_{l_j}}{M_{\tilde{\Delta}}^2} \left\{ \sum_a \mathcal{F}_{ia}^{\tilde{l}*} \mathcal{F}_{ja}^{\tilde{l}} [-2F_1(x_a) + 4F_2(x_a)] + \sum_b \mathcal{F}_{ib}^{\tilde{\nu}*} \mathcal{F}_{jb}^{\tilde{\nu}} F_2(x_b) \right\}, \quad (6.68)$$

$$A_L^{\tilde{\Delta}} = (m_{l_i}/m_{l_j}) A_R^{\tilde{\Delta}}, \quad (6.69)$$

where $x_a \equiv (M_{\tilde{l}_a}/M_{\tilde{\Delta}})^2$ and $x_b \equiv (M_{\tilde{\nu}_b}/M_{\tilde{\Delta}})^2$, and the Higgsino triplet mass is given by $M_{\tilde{\Delta}} = M_\Delta$.

Here, two remarks should be made. (i) The suppression factor $m_{l_i}/m_{l_j} \ll 1$ appears in the left-handed contributions where the chirality is flipped in the final state l_i . This is due to the fact that only the left-handed lepton doublets participate in the f coupling of bileptons and Higgs triplet. (ii) These amplitudes are approximately proportional to $(f^\dagger f)_{ij}$. In the amplitudes $A_{L,R}^\Delta$ we have $F_{1,2}(x_k) \simeq F_{1,2}(0)$ for $x_k \ll 1$, so that the factor $(f^\dagger f)_{ij} = \sum_k f_{ik}^* f_{jk}$ ($f = f^T$) is extracted. Similarly, in the amplitudes $A_{L,R}^{\tilde{\Delta}}$ we may neglect the mass differences among the sleptons for small enough $|f| \lesssim 0.1$, so that the factor $(f^\dagger f)_{ij} = \sum_a \mathcal{F}_{ia}^{\tilde{l}*} \mathcal{F}_{ja}^{\tilde{l}} = \sum_b \mathcal{F}_{ib}^{\tilde{\nu}*} \mathcal{F}_{jb}^{\tilde{\nu}}$ is extracted again with unitarity of $U^{\tilde{l}}$ and $U^{\tilde{\nu}}$. In other words, the flavor mixing of the intermediate sleptons is actually ineffective for $A_{L,R}^{\tilde{\Delta}}$ in the leading order of $|f|^2$.

By these formulas, we can make a similar estimate on the branching ratio of $\tau \rightarrow \mu\gamma$ as

$$\text{Br}(\tau \rightarrow \mu\gamma) = 3 \times 10^{-11} \left(\frac{G}{3}\right)^2 \left(\frac{1\text{TeV}}{m_\Delta}\right)^4 \left(\frac{|I_{\tau \rightarrow \mu\gamma}|}{0.5}\right)^2 \left(\frac{|f|}{0.1}\right)^4, \quad (6.70)$$

where

$$\sum_k f_{\mu k}^* f_{\tau k} \equiv I_{\tau \rightarrow \mu\gamma} |f|^2. \quad (6.71)$$

We have numerically $|I_{\tau \rightarrow \mu\gamma}| \simeq 0.4 - 0.5$ (HI), $\simeq 0.1 - 0.4$ (DG), and $\simeq 0.4 - 0.5$ (IH), respectively. This Higgs triplet contribution to the $\tau \rightarrow \mu\gamma$ decay is much smaller than the experimental bound $\text{Br}(\tau \rightarrow \mu\gamma) < 3.1 \times 10^{-7}$ [61] for $m_\Delta \sim 1\text{TeV}$ and $|f| \lesssim 0.1$.

6.1.3 Muon anomalous magnetic moment

The contributions of the f coupling to the muon anomalous magnetic moment mainly appear through the Δ - L and $\tilde{\Delta}$ - \tilde{L} loops. The magnitude of these contributions are estimated roughly for $M_\Delta \sim m_0$ as

$$\begin{aligned} |\Delta_f a_\mu| &\sim \frac{1}{8\pi^2} \left(\frac{m_\mu}{m_\Delta}\right)^2 \sum_k |f_{\mu k}|^2 \\ &\sim 10^{-12} \left(\frac{1\text{TeV}}{m_\Delta}\right)^2 \left(\frac{|f|}{0.1}\right)^2. \end{aligned} \quad (6.72)$$

Hence, the contributions of the f coupling to the muon anomalous magnetic moment are found to be harmlessly small.

6.1.4 Muonium to antimuonium conversion

The muonium atom consists of one anti-muon and one electrons, namely, $(\mu^+ e^-)$. A conversion of muonium into antimuonium conserves lepton number and violates the lepton family number by two units. The doubly charged boson in the Higgs triplet contributes this conversion process as shown in Fig. 6.4.

To discuss the muonium-antimuonium conversion, we take the effective four fermion interaction of the (V-A) type, which is given by

$$\mathcal{H}_{M\bar{M}} = \left(\frac{G_{M\bar{M}}}{2}\right) \bar{\mu} \gamma_\sigma (1 - \gamma_5) e \bar{\mu} \gamma^\sigma (1 - \gamma_5) e + \text{H.c.}, \quad (6.73)$$

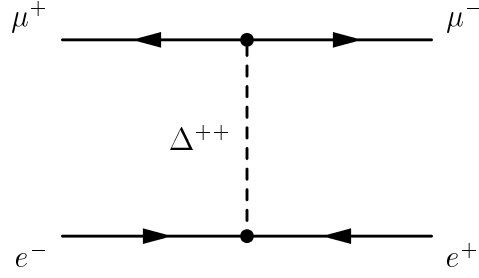


Figure 6.4: A muonium to anitmuonium conversion process with an intermediate Higgs triplet is shown.

where $G_{M\bar{M}}$ is coupling constant characterizing the strength of the muonium to antimuonium conversion. The $G_{M\bar{M}}$ are estimated in Higgs triplet model as

$$G_{M\bar{M}} = \frac{f_{ee}f_{\mu\mu}}{8\sqrt{2}m_{\Delta}^2} = \frac{f_{ee}f_{\mu\mu}}{2g^2} \left(\frac{M_W}{m_{\Delta}} \right)^2 G_F, \quad (6.74)$$

where G_F is the Fermi coupling constant. In the absence of an external magnetic field, this effective four fermion interaction cause a small mass splitting as

$$\delta \equiv 2\langle \bar{M} | \mathcal{H}_{M\bar{M}} | M \rangle = \frac{8G_{M\bar{M}}}{\sqrt{2}n^2\pi a^3}, \quad (6.75)$$

where n is the principal quantum number of the muonium atom and a is a Bohr radius of the muonium atom. The conversion probability in a zero magnetic field is given by

$$P_{M\bar{M}} \simeq \frac{\delta^2}{2\Gamma_{\mu}^2} \simeq 2.6 \times 10^{-5} \left(\frac{G_{M\bar{M}}}{G_F} \right)^2, \quad (6.76)$$

where Γ_{μ} is the muon decay rate.

The experimental upper bound for a conversion of muonium into antimuonium at PSI is given by [62]

$$G_{M\bar{M}} \lesssim 3.0 \times 10^{-3} G_F. \quad (6.77)$$

By using (6.74), this bound is reduced to the constraint for the Higgs triplet mass and couplings,

$$f_{ee}f_{\mu\mu} \left(\frac{10^3 \text{GeV}}{m_{\Delta}} \right)^2 \lesssim 4.0 \times 10^{-1}. \quad (6.78)$$

Hence,

$$|f| \lesssim 2.0 \left(\frac{0.1}{|I_{M \rightarrow \bar{M}}|} \right)^{-1/2} \left(\frac{10^3 \text{GeV}}{m_\Delta} \right)^{-1}, \quad (6.79)$$

where

$$f_{ee} f_{\mu\mu} = I_{M \rightarrow \bar{M}} |f|^2. \quad (6.80)$$

Numerically, we have $|I_{\mu \rightarrow 3e}| \lesssim 0.1$ (HI), $\sim 0.3 - 0.7$ (DG), and $\sim 0.2 - 0.7$ (IH), respectively, for the hierarchical (HI) case $m_1 \ll m_2 \ll m_3$, the degenerate (DG) case $m_1 \sim m_2 \sim m_3$, and the inverted-hierarchical (IH) case $m_1 \sim m_2 \gg m_3$.

Also, the future bound using high-quality muon beam produced at PRISM facility is proposed as [63]

$$G_{M\bar{M}} \lesssim 10^{-4} G_F. \quad (6.81)$$

This bound is reduced to

$$|f| \lesssim 0.4 \left(\frac{0.1}{|I_{M \rightarrow \bar{M}}|} \right)^{-1/2} \left(\frac{10^3 \text{GeV}}{m_\Delta} \right)^{-1}, \quad (6.82)$$

This bound for $|f|$ seems to be loose in the hierarchy case compared with the processes, $\mu \rightarrow 3e$ and $\mu \rightarrow e\gamma$. However, if a signature of $\mu \rightarrow 3e$ or $\mu \rightarrow e\gamma$ is found, future muonium-antimuonium conversion could confirm the Higgs triplet model. On the other hand, in the inverted hierarchy and degenerate cases, future muonium-antimuonium conversion may judge the region $|f| \gtrsim 0.1$, hence, muonium-antimuonium conversion is also available to examine Higgs triplet models.

6.2 Right-handed neutrino model

In this section, we consider the phenomenology of the supersymmetric seesaw model discussed in Chap. 4. The right-handed neutrino is considered to be very heavy compared to the electroweak scale. Hence, the amplitudes of the lepton flavor violation through loop diagrams mediated right-handed neutrino are negligibly small because the amplitudes are proportional to inverse powers of the right-handed neutrino mass. However, in supersymmetric models, the lepton flavor violating right-handed neutrino Yukawa coupling leads to lepton flavor violation in the slepton masses through the renormalization group effects.

We will discuss the lepton flavor violating processes, $\mu \rightarrow e\gamma$ and $\tau \rightarrow \mu\gamma$. Also, under some assumption about the right-handed neutrino mass and coupling, we will judge our leptogenesis by these lepton flavor violating processes.

6.2.1 Lepton flavor violation

We here discuss the lepton flavor violating couplings provided with the right-handed neutrino, including the renormalization group effects. The superpotential relevant for lepton flavor violation is given by

$$W = h_\nu LH_u N + h_l LH_d e^c + \frac{M_N}{2} NN. \quad (6.83)$$

We work in the left-handed lepton and right-handed neutrino diagonal basis where the charged lepton mass matrix and the right-handed neutrino mass matrix M_N are diagonal. Then, the neutrino Yukawa coupling h_ν is not generally diagonal in this basis and leads the lepton flavor violation. By the seesaw mechanism, the neutrino mass matrix is given by

$$m_{\nu ij} = \sum_k h_{\nu ik} h_{\nu kj} \frac{\langle H_u \rangle^2}{M_{Nk}}. \quad (6.84)$$

We assume that M_{Nij} is proportional to the unit matrix below for simplicity. Then, the neutrino mass (6.84) is reduced to

$$m_{\nu ij} = (h_\nu^T h_\nu)_{ij} \frac{\langle H_u \rangle^2}{M_N}. \quad (6.85)$$

For the smallness of the neutrino mass, the right-handed neutrino mass is supposed to be very heavy, $M_N \sim 10^8 - 10^{13}$ GeV.

The flavor violation appears through the renormalization effects. The renormalization group equations for the gauge couplings and gaugino masses are given by

$$16\pi^2 \frac{dg_1}{dt} = \frac{33}{5} g_1^3, \quad 16\pi^2 \frac{dM_1}{dt} = \frac{66}{5} g_1^2 M_1, \quad (6.86)$$

$$16\pi^2 \frac{dg_2}{dt} = g_2^3, \quad 16\pi^2 \frac{dM_2}{dt} = 2g_2^2 M_2, \quad (6.87)$$

$$16\pi^2 \frac{dg_3}{dt} = -3g_3^3, \quad 16\pi^2 \frac{dM_3}{dt} = -6g_3^2 M_3. \quad (6.88)$$

The renormalization group equations for the Yukawa couplings are given by

$$16\pi^2 \frac{dh_l}{dt} = h_l \left[-\frac{9}{5}g_1^2 - 3g_2^2 + 3h_l^\dagger h_l + h_\nu^\dagger h_\nu + \text{Tr} \left(h_l^\dagger h_l + 3y_d^\dagger y_d \right) \right], \quad (6.89)$$

$$16\pi^2 \frac{dh_\nu}{dt} = h_\nu \left[-\frac{3}{5}g_1^2 - 3g_2^2 + 3h_\nu^\dagger h_\nu + h_l^\dagger h_l + \text{Tr} \left(h_\nu^\dagger h_\nu + 3y_u^\dagger y_u \right) \right], \quad (6.90)$$

$$16\pi^2 \frac{dy_d}{dt} = y_d \left[-\frac{7}{15}g_1^2 - 3g_2^2 - \frac{16}{3}g_3^2 + y_d^\dagger y_d + y_u^\dagger y_u + \text{Tr} \left(h_l^\dagger h_l + 3y_d^\dagger y_d \right) \right], \quad (6.91)$$

$$16\pi^2 \frac{dy_u}{dt} = y_u \left[-\frac{13}{15}g_1^2 - 3g_2^2 - \frac{16}{3}g_3^2 + 3y_u^\dagger y_u + 3y_d^\dagger y_d + \text{Tr} \left(h_\nu^\dagger h_\nu + 3y_u^\dagger y_u \right) \right] \quad (6.92)$$

The renormalization group equations for the masses of the sleptons and squarks are given by

$$\begin{aligned} 16\pi^2 \frac{dM_L^2}{dt} = & -\frac{6}{5}M_1^2 g_1^2 - 6M_2^2 g_2^2 + M_L^2 \left(h_l^\dagger h_l + h_\nu^\dagger h_\nu \right) + \left(h_l^\dagger h_l + h_\nu^\dagger h_\nu \right) M_L^2 \\ & + 2 \left(h_l^\dagger M_{H_d}^2 h_l + h_l^\dagger M_{\tilde{e}^c} h_l + h_\nu^\dagger M_{H_u}^2 h_\nu + h_\nu^\dagger M_{\tilde{\nu}}^2 h_\nu \right) \\ & + 2 \left(A_l^\dagger A_l + A_\nu^\dagger A_\nu \right), \end{aligned} \quad (6.93)$$

$$\begin{aligned} 16\pi^2 \frac{dM_{\tilde{e}^c}^2}{dt} = & -\frac{24}{5}M_1^2 g_1^2 + 2M_{\tilde{e}^c}^2 h_l^\dagger h_l + 2h_l^\dagger h_l M_{\tilde{e}^c}^2 \\ & + 4 \left(h_l^\dagger M_{\tilde{e}^c} h_l + h_l M_{H_d}^2 h_l^\dagger \right) + 4A_l A_l^\dagger, \end{aligned} \quad (6.94)$$

$$16\pi^2 \frac{dM_{\tilde{\nu}}^2}{dt} = 2M_{\tilde{\nu}}^2 h_\nu^\dagger h_\nu + 2h_\nu^\dagger h_\nu M_{\tilde{\nu}}^2 + 4 \left(h_\nu^\dagger M_{H_u}^2 h_\nu + h_\nu^\dagger M_{\tilde{\nu}} h_\nu + A_\nu^\dagger A_\nu \right), \quad (6.95)$$

$$\begin{aligned} 16\pi^2 \frac{dM_{\tilde{d}^c}^2}{dt} = & -\frac{8}{15}M_1^2 g_1^2 - \frac{32}{3}M_3^2 g_3^2 + 2M_{\tilde{d}^c}^2 y_d^\dagger y_d + 2y_d^\dagger y_d M_{\tilde{d}^c}^2 \\ & + 4 \left(y_d M_{H_d}^2 y_d^\dagger + y_d M_{\tilde{q}} y_d^\dagger \right) + 4A_d A_d^\dagger, \end{aligned} \quad (6.96)$$

$$\begin{aligned} 16\pi^2 \frac{dM_{\tilde{u}^c}^2}{dt} = & -\frac{32}{15}M_1^2 g_1^2 - \frac{32}{3}M_3^2 g_3^2 + (2M_{\tilde{u}^c}^2 + 4M_{H_u}^2) y_u^\dagger y_u \\ & + 4y_u M_{\tilde{q}^c} y_u^\dagger + 2y_u y_u^\dagger M_{\tilde{u}^c} + 4A_u A_u^\dagger, \end{aligned} \quad (6.97)$$

$$\begin{aligned} 16\pi^2 \frac{dM_{\tilde{q}}^2}{dt} = & -\frac{2}{15}M_1^2 g_1^2 - 6M_2^2 g_2^2 - \frac{32}{3}M_3^2 g_3^2 \\ & + (M_{\tilde{q}}^2 + 2M_{H_u}^2) y_u^\dagger y_u + (M_{\tilde{q}}^2 + 2M_{H_d}^2) y_d^\dagger y_d + \left(y_u^\dagger y_u + y_d^\dagger y_d \right) M_{\tilde{q}}^2 \\ & + 2y_u^\dagger M_{\tilde{u}^c} y_u + 2y_d^\dagger M_{\tilde{d}^c} y_d + 2A_u A_u^\dagger + 2A_d A_d^\dagger. \end{aligned} \quad (6.98)$$

The renormalization group equations for the soft masses are given by

$$\begin{aligned}
16\pi^2 \frac{dM_{H_d}^2}{dt} = & -\frac{6}{5}M_1^2 g_1^2 - 6M_2^2 g_2^2 + 2M_{H_d}^2 \left(\text{Tr} h_l h_l^\dagger + 3\text{Tr} y_d y_d^\dagger \right) \\
& + 6\text{Tr} \left(y_d^\dagger M_{\tilde{d}^c}^2 y_d + y_d^\dagger M_{\tilde{q}}^2 y_d \right) + 2\text{Tr} \left(h_l^\dagger M_{\tilde{L}}^2 h_l + h_l^\dagger M_{\tilde{e}^c}^2 h_l \right) \\
& + 2 \left(3\text{Tr} A_d A_d^\dagger + \text{Tr} A_l A_l^\dagger \right), \tag{6.99}
\end{aligned}$$

$$\begin{aligned}
16\pi^2 \frac{dM_{H_u}^2}{dt} = & -\frac{6}{5}M_1^2 g_1^2 - 6M_2^2 g_2^2 + 2M_{H_u}^2 \left(\text{Tr} h_\nu h_\nu^\dagger + 3\text{Tr} y_u y_u^\dagger \right) \\
& + 6\text{Tr} \left(y_u^\dagger M_{\tilde{u}^c}^2 y_u + y_u^\dagger M_{\tilde{q}}^2 y_u \right) + 2\text{Tr} \left(h_\nu^\dagger M_{\tilde{L}}^2 h_\nu + h_\nu^\dagger M_{\tilde{\nu}^c}^2 h_\nu \right) \\
& + 2 \left(3\text{Tr} A_u A_u^\dagger + \text{Tr} A_\nu A_\nu^\dagger \right). \tag{6.100}
\end{aligned}$$

The renormalization group equation for the soft-breaking trilinear coupling are given by,

$$\begin{aligned}
16\pi^2 \frac{dA_l}{dt} = & 2h_l \left[-\frac{9}{5}M_1 g_1^2 - 3M_2 g_2^2 + 2h_l^\dagger A_l + h_\nu^\dagger A_\nu + \text{Tr} \left(A_l h_l^\dagger + 3A_d Y_d^\dagger \right) \right] \\
& + A_l \left[-\frac{9}{5}g_1^2 - 3g_2^2 + 5h_l^\dagger h_l + h_\nu^\dagger h_\nu + \text{Tr} \left(h_l h_l^\dagger + 3y_d y_d^\dagger \right) \right], \tag{6.101}
\end{aligned}$$

$$\begin{aligned}
16\pi^2 \frac{dA_\nu}{dt} = & 2h_\nu \left[-\frac{3}{5}M_1 g_1^2 - 3M_2 g_2^2 + 2h_\nu^\dagger A_\nu + h_l^\dagger A_l + \text{Tr} \left(A_\nu h_\nu^\dagger + 3A_u Y_u^\dagger \right) \right] \\
& + A_h \left[-\frac{3}{5}g_1^2 - 3g_2^2 + 5h_\nu^\dagger h_\nu + h_l^\dagger h_l + \text{Tr} \left(h_\nu h_\nu^\dagger + 3y_u y_u^\dagger \right) \right], \tag{6.102}
\end{aligned}$$

$$\begin{aligned}
16\pi^2 \frac{dA_d}{dt} = & 2y_d \left[-\frac{7}{15}M_1 g_1^2 - 3M_2 g_2^2 - \frac{16}{3}M_3 g_3^2 + 2y_d^\dagger A_d + y_u^\dagger A_u + \text{Tr} \left(A_l h_l^\dagger + 3A_d Y_d^\dagger \right) \right] \\
& + A_d \left[-\frac{7}{15}g_1^2 - 3g_2^2 - \frac{16}{3}g_3^2 + 5y_d^\dagger y_d + y_u^\dagger y_u + \text{Tr} \left(h_l h_l^\dagger + 3y_d y_d^\dagger \right) \right], \tag{6.103}
\end{aligned}$$

$$\begin{aligned}
16\pi^2 \frac{dA_u}{dt} = & 2y_u \left[-\frac{13}{15}M_1 g_1^2 - 3M_2 g_2^2 - \frac{16}{3}M_3 g_3^2 + 2y_u^\dagger A_u + y_d^\dagger A_d + \text{Tr} \left(A_\nu h_\nu^\dagger + 3A_u Y_u^\dagger \right) \right] \\
& + A_u \left[-\frac{13}{15}g_1^2 - 3g_2^2 - \frac{16}{3}g_3^2 + 5y_u^\dagger y_u + y_d^\dagger y_d + \text{Tr} \left(h_\nu h_\nu^\dagger + 3y_u y_u^\dagger \right) \right]. \tag{6.104}
\end{aligned}$$

For $\mu < M_N$, the right-handed neutrino decouples from the massless spectrum, hence, the dimension five operator $\kappa LLH_u H_u / M_N$ is derived. The renormalization group equation for κ are given by [65]

$$16\pi^2 \frac{d\kappa}{dt} = h_\nu \left[-\frac{6}{5}g_1^2 - 6g_2^2 + \text{Tr} y_u^\dagger y_u \right] + h_l^\dagger h_l \kappa + \kappa (h_l^\dagger h_l)^T. \tag{6.105}$$

We can solve these renormalization group equations with certain boundary conditions. However, we consider a simple approximation to estimate the lepton flavor violation in the slepton mass matrix. The renormalization group equation for the slepton mass can

be reduced to

$$16\pi^2 \frac{dM_{\tilde{L}}^2}{dt} = \left(16\pi^2 \frac{dM_{\tilde{L}}^2}{dt} \right)_{MSSM} + M_{\tilde{L}}^2 h_{\nu}^{\dagger} h_{\nu} + h_{\nu}^{\dagger} h_{\nu} M_{\tilde{L}}^2 2 \left(h_{\nu}^{\dagger} M_{\tilde{\nu}}^2 h_{\nu} + M_{H_u}^2 h_{\nu}^{\dagger} h_{\nu} + A_{\nu}^{\dagger} A_{\nu} \right), \quad (6.106)$$

where $(16\pi^2 d/dt M_{\tilde{L}}^2)_{MSSM}$ represents the renormalization group equation in MSSM. This renormalization group equation gives an approximate solution for the slepton mass

$$\Delta_{\nu}(M_{\tilde{L}}^2)_{ij}|_{i \neq j} \simeq -m_0^2(3 + a_0^2)(h_{\nu}^{\dagger} h_{\nu})_{ij} t_N, \quad (6.107)$$

where t_N is given by

$$t_N \equiv \frac{1}{8\pi^2} \ln M_G/M_N. \quad (6.108)$$

We do not know the neutrino Yukawa couplings h_{ν} at M_G , hence, the definite prediction of the slepton mass matrix can not be derived. However, if we assume the CP violating phase in the Yukawa coupling h_{ν} is small, $(h_{\nu}^{\dagger} h_{\nu})_{ij}$ is linked directly to the neutrino mass matrix as the Higgs triplet case. Then, $(h_{\nu}^{\dagger} h_{\nu})_{ij} t_N$ is given in terms of three neutrino masses and three mixing angles by Eq. (6.85),

$$(h_{\nu}^{\dagger} h_{\nu})_{ij} = \frac{(m_{\nu})_{ij}}{m_{\text{atm}}} |h|^2 \quad (6.109)$$

where

$$|h|^2 = \frac{M_N m_{\text{atm}}}{\langle H_u \rangle^2}. \quad (6.110)$$

Also, renormalization effects for $(h_{\nu}^{\dagger} h_{\nu})_{ij}$ is not so large, hence, the estimate of $(h_{\nu}^{\dagger} h_{\nu})_{ij}$ by the value of $(m_{\nu})_{ij}$ at M_W is good approximation for the estimate of the lepton flavor violation. Here, all component of $(h_{\nu}^{\dagger} h_{\nu})_{ij}$ are proportional to the universal right-handed neutrino mass M_N , hence, the magnitude of lepton flavor violation is directly related to M_N .

6.2.2 $\mu \rightarrow e\gamma$ and $\tau \rightarrow \mu\gamma$

The flavor changing radiative decays such as $\mu \rightarrow e\gamma$ and $\tau \rightarrow \mu\gamma$ are induced by the one-loop diagrams as shown in Fig. 6.3. The flavor violation in the slepton mass matrices

also provides the supersymmetric contributions of the $\tilde{l}-\tilde{\chi}^0$ (neutralino) loop and the $\tilde{\nu}-\tilde{\chi}^-$ (chargino) loop, in the supersymmetric seesaw model.

We now estimate the branching ratio of $l_j \rightarrow l_i \gamma$ decay. The decay amplitude is generally given by

$$T(l_j \rightarrow l_i \gamma) = e \epsilon^{\alpha\beta} \bar{l}_i [i \sigma_{\alpha\beta} q^\beta (A_L P_L + A_R P_R)] l_j. \quad (6.111)$$

Then, the decay rate is given by

$$\Gamma(l_j \rightarrow l_i \gamma) = \frac{e^2}{16\pi} m_{l_j}^3 (|A_L|^2 + |A_R|^2), \quad (6.112)$$

and the branching ratio is calculated by

$$\text{Br}(l_j \rightarrow l_i \gamma) = \frac{\Gamma(l_j \rightarrow l_i \gamma)}{G_F^2 m_{l_j}^5 / 192 \pi^3} \text{Br}(l_j \rightarrow l_i \nu_j \bar{\nu}_i). \quad (6.113)$$

The left-handed and right-handed decay amplitudes are calculated in the leading order by combining the one-loop contributions:

$$A_{L,R} = A_{L,R}^{\tilde{\chi}^0} + A_{L,R}^{\tilde{\chi}^-}. \quad (6.114)$$

The interaction Lagrangian of lepton doublet is given by

$$\mathcal{L} = \bar{l}_i \left(C_{ima}^{N,R} P_R + C_{ima}^{N,L} P_L \right) \tilde{\chi}_m^0 \tilde{l}_a + \bar{l}_i \left(C_{inb}^{C,R} P_R + C_{inb}^{C,L} P_L \right) \tilde{\chi}_n^- \tilde{\nu}_b + \text{H.c.} \quad (6.115)$$

By these couplings, we can calculate the neutralino-loop contributions as

$$A_L^{\tilde{\chi}^0} = \frac{1}{32\pi^2} \frac{m_{l_j}}{M_{\tilde{l}_a}} \left(C_{ima}^{N,L} C_{jma}^{N,L*} F_1(x_{ma}) + \frac{M_{\tilde{\chi}_m^0}}{m_{l_j}} C_{ima}^{N,L} C_{jma}^{N,R*} F_2(x_{ma}) \right) \quad (6.116)$$

$$A_R^{\tilde{\chi}^0} = A_L^{\tilde{\chi}^0} \Big|_{L \rightarrow R} \quad (6.117)$$

and chargino-loop as

$$A_L^{\tilde{\chi}^-} = -\frac{1}{32\pi^2} \frac{m_{l_i}}{M_{\tilde{\nu}_b}} \left(C_{inb}^{C,L} C_{jnb}^{C,L*} F_3(x_{nb}) + \frac{M_{\tilde{\chi}_n^-}}{m_{l_i}} C_{inb}^{C,L} C_{jnb}^{C,R*} F_4(x_{nb}) \right) \quad (6.118)$$

$$A_R^{\tilde{\chi}^-} = A_L^{\tilde{\chi}^-} \Big|_{L \rightarrow R} \quad (6.119)$$

where $x_{ma} \equiv (M_{\tilde{\chi}_m^0}/M_{\tilde{l}_a})^2$, $x_{nb} \equiv (M_{\tilde{\chi}_n^-}/M_{\tilde{\nu}_b})^2$ and $F_i(x)$ are defined as

$$F_1(x) = \frac{1 - 6x + 3x^2 + 2x^3 - 6x^2 \ln x}{6(1-x)^4} \quad (6.120)$$

$$F_2(x) = \frac{1 - x^2 + 2x \ln x}{(1-x)^3} \quad (6.121)$$

$$F_3(x) = \frac{2 + 3x - 6x^2 + x^3 + 6x \ln x}{6(1-x)^4} \quad (6.122)$$

$$F_4(x) = \frac{-3 + 4x - x^2 - 2 \ln x}{(1-x)^3} \quad (6.123)$$

The explicit formulas for the couplings $C_{ima}^{N,R(L)}$ and $C_{inb}^{C,R(L)}$ are presented in the literature [56].

Then, the decay amplitudes are given specifically as

$$A_{L,R} = \frac{m_{l_i}}{32\pi^2} (h_\nu^\dagger h_\nu)_{ij} t_N \frac{G_{L,R}}{m_0^2}, \quad (6.124)$$

where the sum is not taken over i . These leading contributions to the decay amplitudes are proportional to the flavor changing factor $(h_\nu^\dagger h_\nu)_{ij} t_N$. This is realized for the $\tilde{l}-\tilde{\chi}^0$ and $\tilde{\nu}-\tilde{\chi}^-$ loops by using the mass-insertion method with the flavor changing elements of slepton mass matrix in Eq. (6.107). The factors $G_{L,R} \sim 1$ are numerically calculated.

Here, $(h_\nu^\dagger h_\nu)_{ij}$ is proportional to M_N as seen in Eq. (6.109). Then, the constraint on $(h_\nu^\dagger h_\nu)_{ij}$ by lepton flavor violating processes is that on M_N . Hence, by the $\mu \rightarrow e\gamma$ and $\tau \rightarrow \mu\gamma$, we can constrain the parameter region of the leptogenesis model discussed in Chap. 4.

Since all right-handed neutrino mass are $M_N < H_{\text{inf}}$, the leptogenesis coupling $h_{\nu LG}$ corresponds to the coupling relevant for the atmospheric neutrino mass. Hence, $h_{\nu LG}$ can be written in terms of M_N as

$$h_{\nu LG}^2 = \frac{m_{\text{atm}} M_N}{\langle H_u \rangle^2} \simeq 2 \times 10^{-3} \left(\frac{M_N}{10^{12} \text{GeV}} \right). \quad (6.125)$$

Since the leptogenesis should generate the sufficient amount of lepton number asymmetry, $n_L/s \sim M T_R / (10^{37} \text{GeV}^2) \sim 10^{-10}$. Hence, the free parameter M can be written in terms of T_R as

$$M = 10^{19} \text{GeV} \left(\frac{T_R}{10^8 \text{GeV}} \right)^{-1}. \quad (6.126)$$

Here, by Eqs. (6.125) and (6.126), the large $h_{\nu LG}$ scenario is realized,

$$h_{\nu LG}^2 > \frac{H_{\text{inf}}}{M} = 10^{-6} \left(\frac{H_{\text{inf}}}{10^{13} \text{GeV}} \right) \left(\frac{T_R}{10^8 \text{GeV}} \right). \quad (6.127)$$

In the large $h_{\nu LG}$ scenario, the condition that thermal masses do not take over the effective negative mass at $H = H_{\text{tr}}$, is $M_N > T_p$. This condition cuts off some region in $M_N - T_R$ plane with $T_p = (T_R^2 H M_P)^{1/4}$.

The plains are shown in Fig. 6.5 ($\tan \beta = 30$) and Fig. 6.6 ($\tan \beta = 10$) for $\mu \rightarrow e\gamma$ process. The gray region is allowed by $\mu \rightarrow e\gamma$ experiments, the thick line represents the

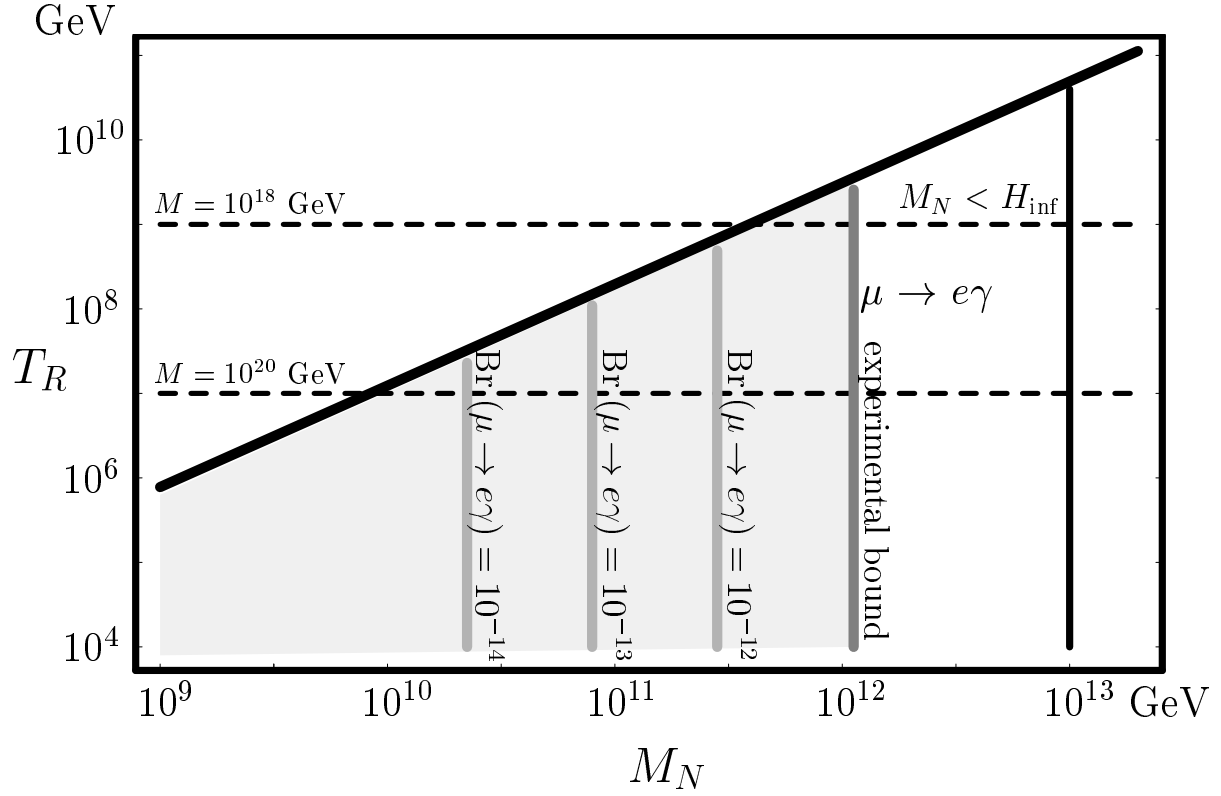


Figure 6.5: The M_N - T_R plain for leptogenesis discussed in Chap. 4 is shown for $\tan \beta = 30$. The gray region is allowed by $\mu \rightarrow e\gamma$ experiments, the thick line represents the condition that thermal masses do not dominate the negative mass. The condition $M_N < H_{\text{inf}}$ is required for the nontrivial evolution of \tilde{N} . Two horizontal dashed lines represent the mass of nonrenormalizable terms (4.4).

condition that thermal masses do not dominate the negative mass. We take typical values of the neutrino masses and mixings are taken in the hierarchical case as

$$(m_1, m_2, m_3) = (10^{-3}\text{eV}, 8 \times 10^{-3}\text{eV}, 5 \times 10^{-2}\text{eV}),$$

$$(\sin \theta_{12}, \sin \theta_{23}, \sin \theta_{13}) = (1/2, 1/\sqrt{2}, 0.1),$$

and the zero CP violating phases. Other parameters are taken as $m_0 = 200\text{GeV}$, $a_0 = 1$, $\mu = 300\text{GeV}$, $M_1 = 100\text{GeV}$ and $M_2 = 200\text{GeV}$ (M_1 and M_2 are the gaugino masses of $U(1)_Y$ and $SU(2)_L$, respectively). The prediction of the $\text{Br}\tau \rightarrow \mu\gamma$ is smaller than the experimental bound. For large $\tan \beta \sim 30$, future lepton flavor violating decay experiments $\text{Br}(\mu \rightarrow e\gamma) \sim 10^{-14}$ [64] can judge our leptogenesis with some assumption.

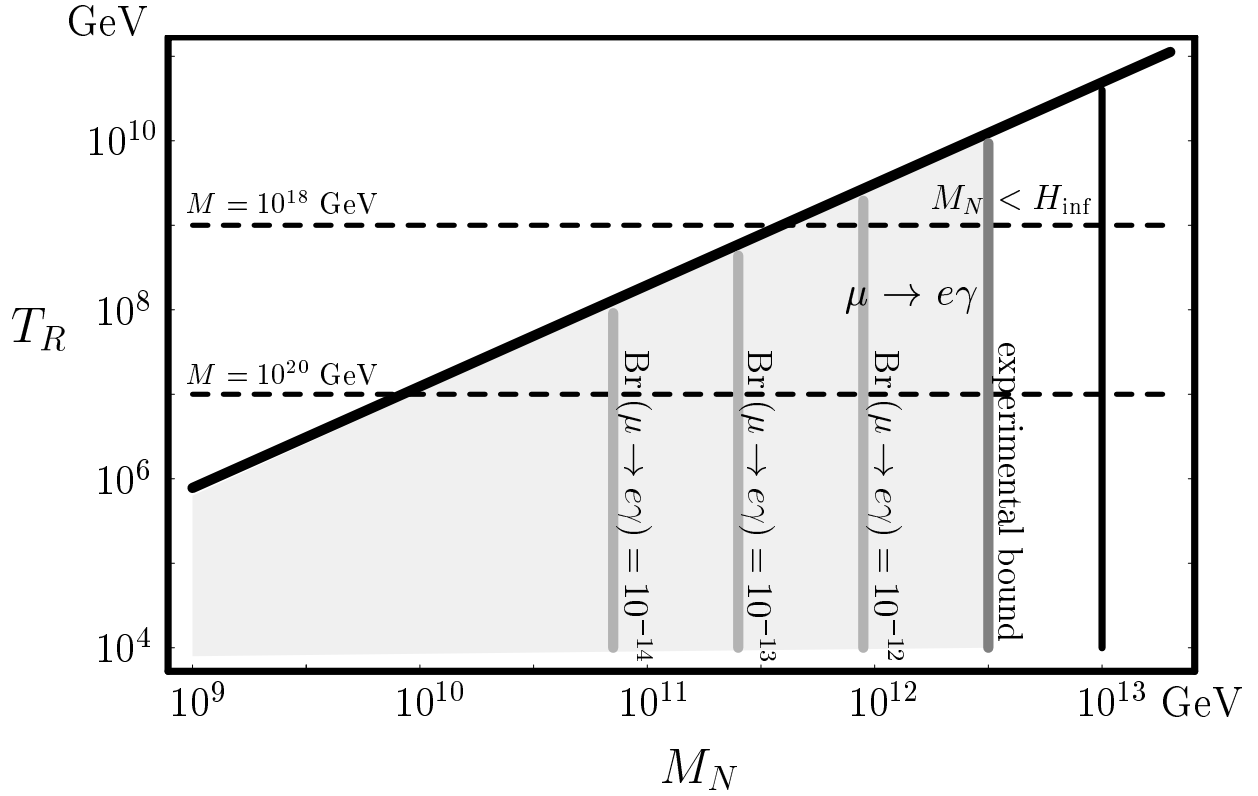


Figure 6.6: The M_N - T_R plain for leptogenesis discussed in Chap. 4 is shown for $\tan \beta = 10$. The gray region is allowed by $\mu \rightarrow e\gamma$ experiments, the thick line represents the condition that thermal masses do not dominate the negative mass. The condition $M_N < H_{\text{inf}}$ is required for the nontrivial evolution of \tilde{N} . Two horizontal dashed lines represent the mass of nonrenormalizable terms (4.4).

6.3 summary

We have investigated the lepton flavor violating processes such as $\mu \rightarrow e\gamma$ and $\tau \rightarrow \mu\gamma$ with the supersymmetric Higgs triplets and the supersymmetric seesaw model in the light of neutrino masses and experimentally verifiable leptogenesis. The Higgs triplet mass M_Δ is expected to be in the range of 1 – 100 TeV. The branching ratios of these charged lepton decays are evaluated in terms of M_Δ and the coupling $fL\Delta L$ of Higgs triplet Δ with lepton doublet pairs LL , which is proportional to the neutrino mass matrix. They may be reached in the future collider experiments. In particular, the $\mu \rightarrow 3e$ decay would be observed indicating the existence of Higgs triplets with $M_\Delta \sim 1\text{--}100\text{ TeV}$ for $|f| \sim 0.1\text{--}1$, while $\text{Br}(\mu \rightarrow e\gamma)$ can be significant irrespective of M_Δ in the supersymmetric model due

to the flavor violation in the slepton mass matrices induced by the renormalization effects. On the other hand, the right-handed neutrino is very heavy as $M_N = 10^9 - 10^{13}$ GeV in the supersymmetric seesaw model for leptogenesis. Hence, the flavor violation is induced in the slepton mass matrices by the renormalization effects. With degenerate right-handed neutrino mass and negligibly small CP phases, the lepton flavor violating coupling ($h^\dagger h$) is proportional to the neutrino mass matrix. The branching ratio of $\mu \rightarrow e\gamma$ constrains the parameter region for the leptogenesis, while the prediction of the $\text{Br}\tau \rightarrow \mu\gamma$ is smaller than the experimental bound. The leptogenesis via $\tilde{N}, \tilde{L}, H_u$ manifold may be judged in the future collider experiments.

Chapter 7

Conclusion

We have investigated the lepton-number asymmetry generation via multiscalar evolution in supersymmetric electroweak models. These models are some extensions of the supersymmetric standard model to generate the neutrino masses. We have clarified characteristic aspects of this flat manifold leptogenesis scenario in these models. The leptogenesis via multiscalar evolution has been found much more efficient than the conventional Affleck-Dine mechanism along the one-dimensional flat direction. In particular, the thermal effect, which suppresses the leptogenesis in Affleck-Dine mechanism, may rather plays a cooperative role in the present multiscalar leptogenesis mechanism. We have also shown possible experimental signatures of these models in the lepton flavor violation processes related to the neutrino mass generation.

In the Higgs triplet model, the neutrino mass matrix is generated by the exchange of Higgs triplet. The lepton number asymmetry is generated sufficiently for the wide range of Higgs triplet mass, $10^3 \text{ GeV} \lesssim M_\Delta \lesssim 10^{13} \text{ GeV}$ on manifold spanned by the flat directions of scalar fields $\Delta\bar{\Delta}$ and $\bar{\Delta}\bar{\Delta}\tilde{e}^c\tilde{e}^c$ manifold. The thermal effects do not disturb the leptogenesis. In particular, the thermal log-term acting as the effective scalar mass term may dominate in some epoch, so that the lepton-number asymmetry can be enhanced significantly.

In the supersymmetric seesaw model, the leptogenesis takes place via the coherent evolution of the scalar fields \tilde{N} , \tilde{L} and H_u . The \tilde{N} asymmetry disappears later through the incoherent decays $\tilde{N} \rightarrow \bar{L}\tilde{H}_u, \tilde{L}H_u$ with almost the same rate but opposite final lepton numbers. The sufficient amount of \tilde{L} asymmetry for baryogenesis can be obtained with the lightest neutrino mass $m_\nu \lesssim 10^{-3} \text{ eV}$ for the reasonable Yukawa coupling of right-handed

neutrino and the right-handed neutrino mass $M_N = 10^{10} - 10^{13}$ GeV.

In the supersymmetric standard model, the multi-dimensional motion of the scalar fields \tilde{L} , H_u , H_d is investigated for leptogenesis with the nonrenormalizable term for neutrino masses. The thermal effects or the quartic coupling from the superpotential term $\bar{h}_e L H_d e^c$ can fix the lepton-number asymmetry to complete the leptogenesis. The lightest neutrino mass can be $m_{\nu_1} \sim 10^{-4}$ eV with the reheating temperature $T_R \sim 10^{10}$ GeV, while it must be extremely small as $m_{\nu_1} \sim 10^{-8}$ eV for the conventional Affleck-Dine mechanism.

We have also investigated the lepton flavor violating processes such as $\mu \rightarrow e\gamma$ and $\tau \rightarrow \mu\gamma$ with the supersymmetric Higgs triplets and the supersymmetric seesaw model in the light of neutrino masses and experimentally verifiable leptogenesis. The branching ratios of these charged lepton decays are evaluated in terms of the Higgs triplet mass M_Δ and the coupling $fL\Delta L$ of Higgs triplet Δ with lepton doublet pairs LL , which is proportional to the neutrino mass matrix. In the future collider experiments, these processes can be discovered as the evidence of the Higgs triplet for the leptogenesis and neutrino mass generation. In particular, the $\mu \rightarrow 3e$ decay is promising to test the existence of Higgs triplets with $M_\Delta \sim 1 - 100$ TeV for $|f| \sim 0.1 - 1$. The $\mu \rightarrow e\gamma$ decay is also interesting, and its branching ratio can be significant irrespective of M_Δ in the supersymmetric model due to the flavor violation in the slepton mass matrices induced by the renormalization effects.

On the other hand, in the supersymmetric seesaw model for leptogenesis, the flavor violation is induced only in the slepton mass matrices by the renormalization effects. This lepton flavor violation can be described in terms of the neutrino mass matrix under some reasonable assumption. Then, the parameter range for leptogenesis is constrained by the present upper bound on the branching ratio of $\mu \rightarrow e\gamma$ decay. This model for leptogenesis via \tilde{N} - \tilde{L} - H_u manifold may also be tested by the lepton flavor violating decays in the future collider experiments.

Acknowledgements

I would like to greatly thank Prof. Katsuji Yamamoto for various instructive suggestions, fruitful discussions and his patience to wait for my very slow writing of manuscripts. Without his encouragement, this work would not be completed.

I thank all the members of quantum physics group of department of nuclear engineering at Kyoto University for hospitality.

I wish to thank my parents Marehito Senami and Shuko Senami for their unfailing support for a long time.

References

- [1] Super-Kamiokande Collaboration, S. Fukuda et al., Phys. Rev. Lett. **81**, 1562 (1998).
- [2] Super-Kamiokande Collaboration, S. Fukuda et al., Phys. Rev. Lett. **86**, 5651 (2001); *ibid.* **86**, 5656 (2001); Phys. Lett. B **539**, 179 (2002).
- [3] SNO Collaboration, Q. R. Ahmad et al., Phys. Rev. Lett. **87** (2001) 071301; *ibid.* **89**, 011301 (2002); *ibid.* **89**, 011302 (2002).
- [4] KamLAND Collaboration, K. Eguchi et al., Phys. Rev. Lett. **90**, 021802 (2003).
- [5] K2K Collaboration, S. H. Ahn et al., Phys. Lett. B **511**, 178 (2001); M. H. Ahn et al., Phys. Rev. Lett. **90**, 041801 (2001).
- [6] For a review, see H. P. Nilles, Phys. Rept. **110**, 1 (1984).
- [7] T. Yanagida, in Proceedings of *Workshop on Unified Theory and Baryon Number in the Universe*, eds. O. Sawada and A. Sugamoto (KEK 1979); M. Gell-Mann, P. Ramond and R. Slansky, in *Supergravity*, eds. P. van Nieuwenhuizen and D. Z. Freedman (North Holland 1979).
- [8] J. Schechter and J. W. F. Valle, Phys. Rev. D **22**, 2227 (1980); R. N. Mohapatra and G. Senjanović, Phys. Rev. Lett. **44**, 912 (1980); Phys. Rev. D **23**, 165 (1981); E. Ma and U. Sarkar, Phys. Rev. Lett. **80**, 5716 (1998);
- [9] M. Senami and K. Yamamoto, hep-ph/0305203.
- [10] M. Senami and K. Yamamoto, Phys. Rev. D **66**, 035006 (2002).
- [11] K. Hagiwara et al., Particle Data Group, Phys. Rev. **D 66**, 010001 (2002), <http://pdg.lbl.gov/>.

- [12] For a review see, E. Kolb and M. Turner, *The Early Universe* (Addison-Wisley, 1990).
- [13] A. T. Lee et al, *Astrophys. J.* **561**, L1 (2001).
- [14] Boomerang Collaboration, C. B. Netterfield et al, *Astrophys. J.* **571**, 604 (2002).
- [15] C. Pryke et al., *Astrophys. J.* **568**, 46 (2002).
- [16] D. N. Spergel et al., astro-ph/0302209.
- [17] V. A. Kuzmin, V. A. Rubakov and M. E. Shaposhnikov, *Phys. Lett. B* **155**, 36 (1985).
- [18] M. Fukugita and T. Yanagida, *Phys. Lett. B* **174**, 45 (1986).
- [19] W. Buchmüller and M. Plümacher, *Phys. Rept.* **320** (1999) 329; M. Plümacher, *Nucl. Phys. B* **530** (1998) 207 and references therein.
- [20] J. Ellis and M. Raidal, *Nucl. Phys. B* **643**, 229 (2002).
- [21] J. Ellis, J. E. Kim and D. V. Nanopoulos, *Phys. Lett. B* **145**, 181 (1984); E. Holtmann, M. Kawasaki, K. Kohri and T. Moroi, *Phys. Rev. D* **60**, 023506 (1999); M. Kawasaki, K. Kohri and T. Moroi, *ibid.* **63**, 103502 (2001).
- [22] K. Kohri, *Phys. Rev. D* **64**, 043515 (2001).
- [23] G.F. Giudice, I. Tkachev, and A. Riotto, *JHEP* **08**, 009 (1999); **11**, 036 (1999); R. Kallosh, L. Kofman, A. Linde, and A. Van Proeyen, *Phys. Rev. D* **61**, 103503 (2000); A. L. Maroto and A. Mazumdar, *Phys. Rev. Lett.* **84**, 1655 (2000); R. Allahverdi, M. Bastero-Gil, and A. Mazumdar, *Phys. Rev. D* **64**, 023516 (2001); H. P. Nilles, M. Peloso, and L. Sorbo, *Phys. Rev. Lett* **87**, 051302 (2001).
- [24] T. Hambye, E. Ma and U. Sarkar, *Nucl. Phys. B* **602**, 21 (2001).
- [25] I. Affleck and M. Dine, *Nucl. Phys. B* **249**, 361 (1985).
- [26] M. Dine, L. Randall and S. Thomas, *Phys. Rev. Lett.* **75**, 398 (1995); *Nucl. Phys. B* **458**, 291 (1996).
- [27] M. Senami and K. Yamamoto, *Phys. Lett. B* **524**, 332 (2002).

- [28] M. Senami and K. Yamamoto, hep-ph/0305202.
- [29] M. Senami and K. Yamamoto, Phys. Rev. D **67**, 095005 (2003).
- [30] G. Jungman, M. Kamionkowski, A. Kosowsky and D. N. Spergel, Phys. Rev. D **54**, 1332 (1996).
- [31] T. J. Pearson et. al., Astrophys. J **591**, 556 (2003).
- [32] ACBAR Collaboration, C. L. Kuo et al., astro-ph/0212289.
- [33] W. J. Percival et. al., Mon. Not. Roy. Astron. Soc. **327**, 1297 (2001). L. Verde et. al., Mon. Not. Roy. Astron. Soc. **335**, 432 (2002).
- [34] R. A. C. Croft, et. al., Astrophys. J **581**, 20 (2002); N. Y. Gnedin and A. J. S. Hamilton, Mon. Not. Roy. Astron. Soc. **334**, 107 (2002).
- [35] M. Yoshimura, Phys. Rev. Lett. **41**, 281 (1978); *Erratum-ibid.* **42**, 746 (1978).
- [36] H. Pagels and J. R. Primack, Phys. Rev. Lett. **48**, 223 (1982).
- [37] Fore reviews see, A. G. Cohen, D. B. Kaplan and A. E. Nelson, Ann. Rev. Nucl. Part. Sci. **43**, 27 (1993); M. Trodden, Rev. Mod. Phys. **71**, 1463 (1999).
- [38] M. Kobayashi and T. Maskawa, Prog. Theor. Phys. **49**, 652 (1973).
- [39] J. A. Harvey and M. S. Turner, Phys. Rev. D **42**, 3344 (1990).
- [40] L. Covi, E. Roulet and F. Vissani, Phys. Lett. B **384**, 169 (1996).
- [41] S. Davidson and A. Ibarra, Phys. Lett. B **535**, 25 (2002).
- [42] H. Murayama and T. Yanagida, Phys. Lett. B. **322**, 349 (1994).
- [43] T. Moroi and H. Murayama, JHEP **0007**, 009 (2000).
- [44] T. Asaka, M. Fujii, K. Hamaguchi and T. Yanagida, Phys. Rev. D **62** (2000) 123514.
- [45] M. Fujii, K. Hamaguchi and T. Yanagida, Phys. Rev. D **63**, 123513 (2001).
- [46] R. Allahverdi, B. A. Campbell and J. Ellis, Nucl. Phys. **B579**, 355 (2000).

- [47] A. Anisimov and M. Dine, *ibid.* **619**, 729 (2001).
- [48] CHOOZ Collaboration, M. Apollonio et al., Phys. Lett. B **466**, 415 (1999).
- [49] K. Yamamoto, Phys. Lett. **B 161**, 289 (1985); *ibid.* **B 168**, 341 (1986).
- [50] D. H. Lyth and E. D. Stewart, Phys. Rev. D **53**, 1784 (1996).
- [51] K. Hamaguchi, H. Murayama and T. Yanagida, Phys. Rev. D **65**, 043512 (2002).
- [52] A. Rossi, Phys. Rev. D **66**, 075003 (2002).
- [53] E. Ma and M. Raidal, Phys. Rev. Lett. **87**, 011802 (2001); *Erratum-ibid.* **87**, 159901 (2001).
- [54] E. J. Chun, K. Y. Lee, and S. C. Park, hep-ph/0304069; M. Kakizaki, Y. Ogura, and F. Shima, hep-ph/0304254.
- [55] Z. Maki, M. Nakagawa and S. Sakata, Prog. Theor. Phys. **28**, 870 (1962).
- [56] J. Hisano, T. Moroi, K. Tobe, M. Yamaguchi and T. Yanagida, Phys. Lett. B **357**, 579 (1995).
- [57] M. L. Swartz, Phys. Rev. D **40**, 1521 (1989).
- [58] SINDRUM Collaboration, U. Bellgardt et al., Nucl. Phys. B. **299**, 1 (1988).
- [59] Y. Kuno and Y. Okada, Rev. Mod. Phys. **73**, 151 (2001).
- [60] Belle Collaboration, Y. Yusa et al., e-print hep-ex/0211017.
- [61] Belle Collaboration, K. Abe et al., e-print hep-ex/0310029.
- [62] L. Willmann et al., Phys. Rev. Lett. **82**, 49 (1999).
- [63] M. Aoki, Nucl. Instrum. Meth. A **503**, 258 (2003).
- [64] L. M. Barkov et al., research proposal for an experiment at PSI (1999).
- [65] P. Chankowski and Z. Pluciennik, Phys. Lett. B **316**, 312 (1993); C. N. Leung, K. S. Babu and J. Pantaleone, *ibid.* **319**, 191 (1993).